

**Antibiotic Resistance Characteristics of *Mycobacterium Abscessus* Rely on Specific
Outer Membrane Porins and Surface-Associated Glycopeptidolipids**

Dissertation

zur

**Erlangung der naturwissenschaftlichen Doktorwürde
(Dr. sc. nat.)**

vorgelegt der

Mathematisch-naturwissenschaftlichen Fakultät

der

Universität Zürich

von

Sakshi Luthra

aus

Indien

Promotionskommission

Prof. Dr. Peter Sander (Vorsitz, Leitung der Dissertation)

Prof. Dr. Markus Seeger

Prof. Dr. Angelika Lehner

Zürich, 2024

~ for my family

ACKNOWLEDGEMENTS

I would like to express my sincere gratitude and respect for my direct supervisor, **Prof. Dr. Peter Sander**, who has been a source of wisdom, guidance and support over the years and whose boundless encouragement and excellent feedback have contributed so substantially to the development and success of this Ph.D. thesis. I learned a tremendous amount — about both research and life — from you, Peter. Thank you, sincerely, for being my teacher.

I am immensely grateful to **Prof. Dr. Markus Seeger** and **Prof. Dr. Angelika Lehner**, members of my Ph.D. committee; their insight and help in finishing this project has been truly invaluable.

Many, many thanks to all my colleagues from the Institute of Medical Microbiology for creating a friendly workspace. Enormous thanks to the current and former members of the “FoSa” group, especially to Petra, Michael, Tizian, Harshitha, Aron, Daniel, Klara, and Aline — for crucial early help with experiments and kindness to always offer materials that I needed. It has been a delight to work with all of you.

Thanks are also due to the Swiss National Science Foundation, Lungenliga Schweiz, the Institute of Medical Microbiology, and the University of Zurich for their financial support in the project.

Finally, my heartfelt thanks to my family and friends, who have been a much-needed voice of love and encouragement along the way. I am immensely grateful to my mother, Anjala, for being a continual source of support. Without her prayers, this thesis would not have been possible. Special thanks to Ms. Judith Zingg for supporting me at every stage in the writing of this dissertation. Extra helpings of thanks to all my friends from the Max — Andreas, Sofia, Marta, Laura, Peider, Moira, Victor, and Alice — for cheering me on.

TABLE OF CONTENTS

SUMMARY		7
INTRODUCTION		9
CHAPTER 1	Antibiotic resistance characteristics of <i>Mycobacterium abscessus</i> rely on specific outer membrane porins and surface-associated glycopeptidolipids	27
CHAPTER 2	The role of antibiotic-target-modifying and antibiotic-modifying enzymes in <i>Mycobacterium abscessus</i> drug resistance	94
CONCLUSION AND OUTLOOK		124
PUBLICATION		127
CURRICULUM VITAE		128

SUMMARY

“*Mycobacterium abscessus* is an opportunistic pathogen, ubiquitous in the environment, that often causes infections in humans with compromised natural defences such as patients with cystic fibrosis or other chronic lung diseases. A current taxonomic classification suggests separation of *M. abscessus* into three distinct subspecies: *M. abscessus* subsp. *abscessus*, *M. abscessus* subsp. *bolletii*, and *M. abscessus* subsp. *massiliense*. Although a saprophyte in water and soil, following lung infection *M. abscessus* can swiftly grow and survive intra-cellularly within macrophages as well as in extra-cellular caseous lesions and airway mucus. Several factors contribute to the success of this rapidly growing mycobacterium. A plethora of intrinsic resistance mechanisms renders almost all clinically used antibiotics ineffective against *M. abscessus*. In addition, the presence of a highly dynamic open pan-genome in *M. abscessus* might explain the ease with which the bacterium evolves and adapts to a wide-spectrum of stressful environmental conditions encountered in diverse habitats. Importantly, the respiratory habitat of *M. abscessus* brings it in close proximity to highly virulent pathogens (for example, *Pseudomonas aeruginosa* in cystic fibrosis lung) which can serve as donors of novel drug resistance or virulence genes” (Luthra, S. et al.).

“Mechanisms underpinning intrinsic drug resistance of *M. abscessus* are multi-fold and fall into two main groups: first, the presence of a highly impermeable cell envelope and/or multi-drug efflux pumps might reduce the effective concentration of antibiotics within the bacterial cells; second, the genome of *M. abscessus* encodes several putative enzymes which can inactivate antibiotics by modification and/or degradation or lower the affinity of the drug for its target by modifying the target. For long, molecular investigations aimed at elucidating antibiotic resistance mechanisms of *M. abscessus* were limited, however, significant progress has been made in recent years owing to the development of efficient tools for genetic manipulation of this bacterium” (Luthra, S. et al.).

We examined, in this study, the role of limiting factors [i.e. β -barrel proteins that function as porins and surface-exposed glycopeptidolipids (GPL)] in regulating β -lactam transport across the mycomembrane and the impact of changes in cell envelope composition with or without the presence of a specific mechanism involved in β -lactam removal (i.e. deactivation by periplasmic β -lactamase) on the antibacterial susceptibility of *M. abscessus* toward a representative set of compounds from three different β -lactam subclasses (i.e. cephalosporins, carbapenems and a penem). This was accomplished through a series of gene knockouts (obtained via two-step homologous recombination) and by the determination of minimal inhibitory concentrations of antibiotics for all *M. abscessus* strains.

SUMMARY

Here, we reveal that in *M. abscessus*, β -lactam susceptibility is linked to the presence of the general porin MapA and that the chromosomally encoded β -lactamase Bla_{Mab} can confer a higher level of β -lactam resistance in a *mapA* mutant than in wildtype *M. abscessus*. Additionally, the results suggest that the GPL environment can affect the levels of susceptibility to drugs that mainly diffuse across the membrane barrier through non-specific porins. This work has yielded new insights into the types and numbers of factors that influence susceptibility to β -lactam antibiotics in *M. abscessus* and how sets of genes act in concert, rather than in isolation, to elicit bacterial resistance to antibiotics.

Through a better understanding of how the modification of cell envelope permeability elicits bacterial resistance, we might be able to develop new, effective means to overcome the ‘impermeability’ resistance strategy in an effort to fight *M. abscessus* infections.

Reference

Reproduced from Luthra, S. et al. The role of antibiotic-target-modifying and antibiotic-modifying enzymes in *Mycobacterium abscessus* drug resistance. *Front. Microbiol.* **9**, 1–13 (2018) (see chapter 2).

INTRODUCTION

Introduction

Mycobacterium abscessus is the major non-tuberculous mycobacterium (NTM) infecting people with cystic fibrosis (CF), with increasing incidence of infections reported within the CF community globally¹. This rapidly growing environmental mycobacterium is separated into three clearly divergent subspecies: *M. abscessus* subsp. *abscessus*, *M. abscessus* subsp. *massiliense* and *M. abscessus* subsp. *bolletii*². Treatment of CF patients that become infected with *M. abscessus*, in whom this intrinsically multidrug-resistant species causes rapid decline in lung function³, is often unsuccessful despite extended combinatorial drug therapy⁴⁻⁶, which leads to increased morbidity and mortality. Initially, infections in CF patients were thought to result from independent environmental acquisition of *M. abscessus*. However, multinational, population-level whole-genome sequencing of clinical isolates from infected CF individuals showed that a greater number of infections were driven by indirect transmission between patients (probably via an environmental intermediary), of a few virulent *M. abscessus* clones that have recently emerged and have rapidly become globally dispersed². These clones displayed increased virulence in *in vitro* and *in vivo* infection models, were more tolerant of antimicrobial agents and correlated with worse clinical outcomes², indicating that the ongoing evolution of infecting *M. abscessus* clones has promoted increased pathogenicity. This observation emphasizes the urgent need for effective therapeutic strategies and control of cross-infection to restrict the evolution of *M. abscessus* from an environmental saprophyte to a true lung pathogen.

An unusual mechanism of cell growth in rough *M. abscessus* promotes virulence and immune evasion during infection

Cell growth in *Mycobacterium tuberculosis*, an ancient and deadly human pathogen, is characterized by a ‘cording’ phenotype⁷, as reported by Robert Koch in 1882. In *M. tuberculosis*, aggregation occurs pole to pole and side to side in bacilli aligned in parallel to generate large serpentine cords, which are key players in the virulence of this bacterium. Large and complex cell wall lipids, particularly the production of trehalose dimycolate (which is referred to as cord factor), contribute to this growth property of mycobacteria. More recently, the ability to grow as cords has been reported for non-tuberculous mycobacteria⁸, including in rough *M. abscessus* variant⁹. Studies that have used zebrafish have modelled how extracellular replication of rough *M. abscessus* generates cords in infected embryos¹⁰. Cording is a key mechanism that rough *M. abscessus* uses to evade the immune system during infection by

INTRODUCTION

forming massive extracellular cords that cannot be contained by neutrophils and macrophages, thus facilitating bacterial survival *in vivo*¹⁰.

Importantly, this unusual mechanism of growth has a substantial negative effect on zebrafish: cords are inducers of abscess production, which predominantly occurs in the central nervous system in the host and cord-induced blood vessel damage may result in haemorrhage, ultimately promoting acute infection and accelerated larval killing¹⁰. It is worth noting that susceptibility to *M. abscessus* infection and cording are greatly increased in embryos with defects in tumour necrosis factor (TNF) signalling¹¹ or cystic fibrosis transmembrane conductance regulator synthesis¹² or with a lack of macrophages¹⁰ compared with wildtype embryos. It therefore seems reasonable to propose that inhibition of cording may attenuate virulence in *M. abscessus* and promote clearance of the infection. This notion is supported by the finding that a mutant strain of rough *M. abscessus* that exhibits *MAB_4780* gene deletion, has a defect in corded growth and that cord-depleted ΔMAB_4780 bacteria show greatly reduced survival in zebrafish embryos lacking either neutrophils or macrophages as well as in wildtype embryos¹³. Building on this work, the combination of structural and biochemical techniques was useful to show that *MAB_4780* gene product is a dehydratase that is involved in mycolic acid metabolism, which is consistent with a role for these lipids in the generation of cords¹³.

The cell envelope of mycobacteria

The hallmark of mycobacteria is their protective cell envelope, which is composed of surface lipids, cell wall and the cytoplasmic membrane, and contains many proteins. The mycobacterial cell wall core consists of peptidoglycan, arabinogalactan and very long chain fatty acids, the mycolic acids as inferred from biochemical¹⁴ and microscopic studies^{15,16}. The defining feature of this envelope is a unique outer membrane (the mycomembrane) that is a supported asymmetric lipid bilayer in which the inner leaflet is composed of mycolic acids connected by covalent interactions to the underlying arabinogalactan of the arabinogalactan-peptidoglycan co-polymer¹⁷. Its outer leaflet consists of free lipids that include long chain lipids such as trehalose dimycolates as well as smaller lipids (16-18 carbons long) such as the diacyl and triacyl trehaloses^{18,19}. Mycolic acids are composed of 2-alkyl, 3-hydroxy fatty acids that are more than 70 carbons long with only a few double bonds. In mycolic acid, the α -chain, which is the lipid at the 2 position, is saturated and consists of 22-26 carbon atoms, while the meromycolate, which is the lipid on the 3-hydroxyl, contains 42-62 carbon atoms^{18,19}. An x-

INTRODUCTION

ray diffraction study confirmed the existence of an outer membrane in mycobacteria and revealed a quasi-crystalline packing of cell wall lipids²⁰. The inner layer of covalently linked mycolic acids showed an extremely low fluidity, while the outer leaflet was moderately fluid as observed by analysis using electron paramagnetic resonance of spin-labeled fatty acids in isolated cell walls of *Mycobacterium chelonae*^{21,22}. Due to its physical properties, the mycomembrane poses a significant permeation barrier, providing mycobacteria with intrinsic resistance to most antibiotics. The permeability of the mycobacterial cell envelope toward β -lactams is 100–1000 times less than that provided by the cell envelope of Gram-negative bacteria²³.

Surface-associated glycopeptidolipids (GPL) are free lipids found in the mycomembrane outer leaflet of several NTM-species, including opportunistic pathogens such as *M. abscessus*, *M. chelonae* and *Mycobacterium avium* and saprophytic mycobacteria such as *Mycobacterium smegmatis*. Similarly to other NTM-species, *M. abscessus* displays both smooth and rough colony morphotypes with clear differences in surface properties and physiopathological aspects and importantly, this morphological heterogeneity is dictated by the GPL composition of the cell envelope. The presence of hydrophilic GPL in smooth *M. abscessus* promotes sliding motility whereas the rough variant, in which these lipids are lacking or present at extremely low levels, is characterized by increased surface hydrophobicity and displays aggregative properties with a propensity to form massive cord-like structures and biofilms^{24,25}. The *gpl* locus, highly conserved in *M. abscessus*, *M. avium* and *M. smegmatis*, encompasses a large collection of genes that encode factors responsible for the biosynthesis, modification and translocation of GPL. Within the *gpl* cluster, *mps1* and *mps2* encode non-ribosomal peptide synthases involved in assembly of the tripeptide-amino-alcohol moiety²⁶ and *gap* encodes an integral membrane protein required for GPL translocation across the cell membrane in *M. smegmatis*²⁷. The *mmpS4-mmpL4a-mmpL4b* system of *M. abscessus* codes not only for two resistance-nodulation-division (RND)-type transporters, MmpL4a and MmpL4b, that are involved in GPL transport across the cell membrane²⁸, but also for MmpS4, a membrane protein that is proposed to facilitate the assembly of the GPL biogenesis and export machinery megacomplex²⁹. It has been suggested that the role of MmpS4 is to function as an accessory protein (similarly to the periplasmic adaptor protein found in tripartite efflux systems of Gram-negative bacteria) that likely forms a complex with a channel protein in the mycomembrane^{25,29}. The transport pathway of GPL across the periplasm to the outer mycomembrane remains elusive. Transitioning from a smooth to a rough variant in *M.*

INTRODUCTION

abscessus, which usually occurs during infection, implicates genetic changes such as single-nucleotide polymorphisms and small insertions or deletions within genes involved in GPL production including *mps1* and *mps2* or those required for transport of GPL such as *mmpS4*, *mmpL4a* and *mmpL4b*^{30,31}.

GPL are major contributors to pathogenesis of *M. abscessus*

Differences in cell wall GPL composition and the resulting heterogeneity in colony morphology affect interactions between *M. abscessus* and the host, its ability to withstand host defences and confer distinct survival advantages to the pathogen during infection. In addition, this morphological heterogeneity has a central role in virulence of *M. abscessus*. GPL-depleted rough *M. abscessus* found as small clusters are taken up by macrophages and localized within social phagosomes that accommodate many bacilli in a phagosome³². In contrast, huge clumps of rough bacilli are not phagocytosed by macrophages and remain associated with phagocytic cups on the surface of the macrophage. The high GPL producing smooth *M. abscessus* are engulfed by macrophages, which ensure their localization in loner phagosomes, which enclose individual bacteria in a phagosome³². Rough and smooth variants within macrophages have been reported to vary considerably in their lifestyles inside the phagosome, which results in discrete host responses to the two variants. Inside macrophages, rough variants found within social phagosomes rapidly encounter phagosome acidification that results from phagosome–lysosome fusion and leads to induction of autophagy and apoptosis³². In contrast, the presence of a close apposition between the cell wall of smooth variant and the phagosome membrane inhibits activation of apoptosis and autophagy by blocking phagosome maturation. Notably, this close proximity of smooth variant to the phagosome membrane generates an electron transparent zone³³ around the bacterial cell.

Depending on the *M. abscessus* variant that is present, the ability of the granuloma to contain the infection differs; for instance, inside macrophages, smooth *M. abscessus* can persist for a long time, eventually inducing a local pro-inflammatory response and recruitment of additional neutrophils and dendritic cells that assemble around infected macrophages to generate a granuloma^{10,34}. Rough *M. abscessus* can also trigger formation of the granuloma; although, the depletion of GPL in the rough variant triggers increased macrophage apoptosis, thereby releasing bacteria, which then undergo extracellular replication in the form of serpentine cords. While enabling the bacterium to withstand phagocytosis and contributing to immune evasion, the formation of massive serpentine cords results in intense inflammation and extensive tissue

INTRODUCTION

damage. Furthermore, the reported ability of the smooth variant to induce phagosome-to-cytosol communication through disruption of the phagosome membrane, may have a major influence on macrophage autophagy and apoptosis³². The ESX-4 secretion system³⁵ and MmpL8_{MAB} (REF.³⁶) are thought to play a part in phagosome escape.

A model for the mechanisms by which these variants induce distinct host responses has been formulated and involves unmasking of underlying immunomodulatory lipoproteins³⁸ and phosphatidyl-*myo*-inositol mannosides³⁷, which are Toll-like receptor 2 (TLR2) agonists, by depletion of surface-associated GPL in rough bacteria. This results in stimulation of TNF expression and strong inflammation. This model also accounts for the phenomenon that GPL synthesis may facilitate host colonization of the smooth variant during early infection stages by shielding the immunostimulatory cell wall components, thereby possibly delaying immune activation through blockage of TLR2 signalling in respiratory epithelial cells³⁹.

Mycobacterial general porins

Most solutes diffuse through the mycomembrane via β -barrel protein channels, termed porins, that allow the passive uptake of small, water-soluble molecules⁴⁰⁻⁴². The mycobacterial outer membrane contains very small amounts of porin, whose channel allows the penetration of small molecules only at a very slow rate⁴³. The pore-containing β -barrel protein, MspA, which was observed in chloroform/ methanol extracts of *M. smegmatis* cells⁴⁴, is the best studied mycobacterial porin, both structurally and functionally. It was reported that the disruption of *mspA* in *M. smegmatis* led to decreased outer membrane permeability to glucose (4-fold) and cephaloridine (9-fold)⁴⁵, showing that this non-specific porin is the main entry point for hydrophilic small molecules in *M. smegmatis*. The x-ray crystal structure of MspA was the first structure of a mycobacterial outer membrane protein to be solved⁴⁶. The structure revealed the existence of two consecutive 16-stranded β -barrels and a globular rim domain in an octameric goblet-shaped protein that contains a single 9.6-nm-long central channel⁴⁶. The atomic structure of this porin has unique properties that were not observed in Gram-negative bacterial porins, which are ~4 nm long and consist of trimers of 16-stranded β -barrels, each of which is a pore itself^{47,48}. The analysis of stained ultrathin sections of mycobacterial cells by electron microscopy suggested outer membrane lipidic layer thicknesses of around 5-12 nm⁴⁹⁻⁵¹, which seemingly conflicts with the length of the hydrophobic β -barrel domain of MspA, which is only 3.7 nm⁴⁶. This inconsistency was reconciled by a cysteine scanning study that described the native topology of MspA and suggested that part of the hydrophilic rim domain as well as loops

INTRODUCTION

are inserted into the *M. smegmatis* outer membrane⁵². This study provided the first indication that a β -barrel outer membrane protein spans the outer membrane with elements other than amphipathic antiparallel β -strands.

Inhibition of cell wall biosynthesis

β -Lactam antibiotics are efficacious, well tolerated and display a very wide spectrum of activity and have become the most frequently prescribed antibiotics in the clinic in recent time⁵³ (FIG. 1). Initially, it was thought that inhibition of peptidoglycan synthesis by β -lactams was caused by inactivation of only the penicillin-binding proteins (also known as D, D-transpeptidases) that facilitate the cross-linking of immature peptidoglycan units by catalysing peptide bond formation between the fourth and third residues of adjacent peptide strands (designated 4 \rightarrow 3 linkages)⁵⁴. Notably, in the peptidoglycan of *M. abscessus*, the major degree of cross-linking occurs between the third residues of the peptide side chains (designated 3 \rightarrow 3 linkages)⁵⁵, which is accomplished by nonclassical transpeptidases, known as, L, D-transpeptidases, by contrast, the classical 4 \rightarrow 3 linkages are fewer in number. Recent evidence suggests that *M. abscessus* may exhibit higher susceptibility to carbapenems⁵⁶; this is attributed to the unique ability of this β -lactam subclass to block L, D-transpeptidase activity⁵⁷. It is worth noting that only two β -lactams, including imipenem (a carbapenem) and cefoxitin (a cephalosporin) are currently in use in combinatorial therapies (comprising the use of several antibiotic classes, aminoglycosides and macrolides in particular) against *M. abscessus*⁵⁸ (TABLE 1).

A study determined the relative inhibition of activities of two L, D-transpeptidases (namely, Ldt_{Mab1} and Ldt_{Mab2}) from *M. abscessus* by a wide variety of β -lactams (including penicillins, cephalosporins, carbapenems and a penem) and found that some compounds (doripenem, biapenem and faropenem) possessed excellent abilities to inactivate both enzymes and that the combination of cefdinir (a cephalosporin) and doripenem (a carbapenem), two β -lactam subtypes that showed distinct affinities for Ldt_{Mab1} and Ldt_{Mab2}, was synergistic against both susceptible *M. abscessus* and multidrug resistant clinical isolates⁵⁹. The study authors suggest that dual combinations of β -lactams can be more effective against *M. abscessus*, displaying a synergistic effect (as noted above for doripenem and cefdinir drug combination) that could be attributed to different levels of inhibition of nonredundant targets which include both D, D-transpeptidases and L, D-transpeptidases. As the naturally occurring broad-spectrum β -lactamase Bla_{Mab} is the highest contributor to β -lactam resistance in *M. abscessus*^{60,61}, the concept has emerged of adding a β -lactamase inhibitor such as the non- β -lactam inhibitor

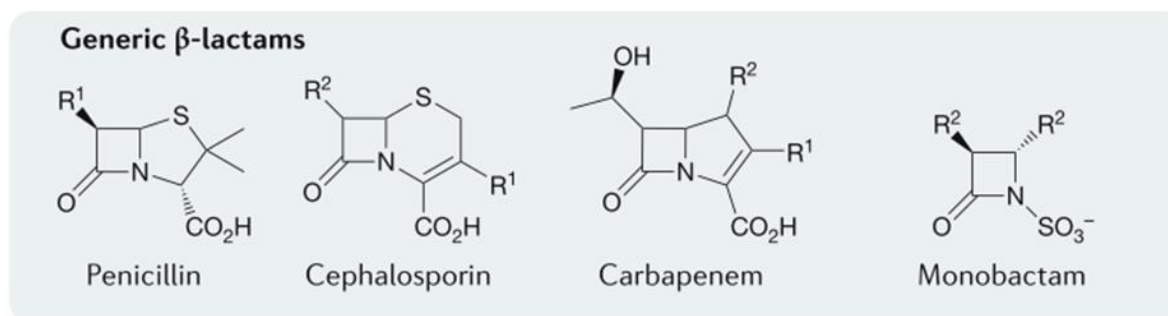
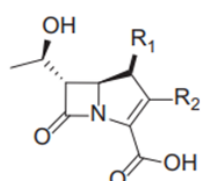
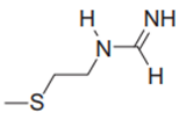
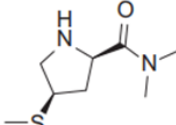
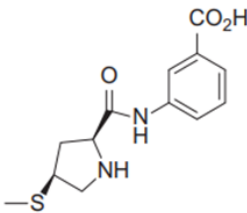
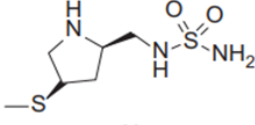
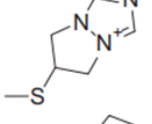
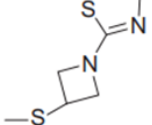


Fig. 1 | **Structures of β -lactams.** Shown are the generic structures of the β -lactams penicillin, cephalosporin, carbapenem and monobactam.

Table 1. Carbapenems of current clinical utility



Name	R ₁	R ₂	Approval date ^{a,b}	Status
Imipenem	H		1985	Widely available
Meropenem	CH ₃		1996	Widely available
Ertapenem	CH ₃		2001	Widely available
Doripenem	CH ₃		2007	Widely available
Biapenem	CH ₃		2001 (Japan)	Available in Japan
Tebipenem ^c	CH ₃		2009 (Japan)	Available in Japan

^aFDA approved unless otherwise noted.

^bDates were updated from Medeiros (1997) (www.accessdata.fda.gov/scripts/cder/drugsatfda; www.drugs.com; adisin.sight.springer.com/drugs/800010812).

^cFormulated as the pivoxil ester.

Table reproduced from Bush & Bradford (2016) (REF.⁵³).

INTRODUCTION

avibactam, which provides excellent protection against Bla_{Mab}^{61,62}, to a dual- β -lactam combination to possibly further enhance the lethality of combinatorial antibiotic treatment.

Porins and β -lactam susceptibility

It is generally accepted that the journey that a β -lactam must take to reach its site of action in Gram-negative bacteria begins with translocation through a porin channel. Recent clinical evidence points towards three major mechanisms for the change in membrane permeability through porin modification by Gram-negative bacteria, which causes multidrug resistance. These include: a substitution of the expressed porin; a mutation that decreases porin function; and an alteration in the porin production level⁶³. The clinical data that we discuss here emphasize the association between outer membrane permeability and β -lactam susceptibility and provide an understanding of the adaptive response of bacteria to antibiotic stress.

Porin replacement

Several studies describe a change in porin balance in clinical *Klebsiella pneumoniae* strains isolated during patient antibiotherapy⁶³. A study observed that there was a shift in the type of porin produced (OmpK35, producing a large channel, was substituted by the smaller OmpK36 channel) in most of the *K. pneumoniae* isolates collected from patients undergoing treatment⁶⁴. In terms of β -lactam susceptibility, there is a clear difference between these *K. pneumoniae* porins. The susceptibility conferred by OmpK35 to β -lactams, including ceftazidime, cefotaxime, cefotetan and cefepime is 4-8 times higher compared with the susceptibility that is observed in OmpK36 producing strains⁶⁵. Altered permeability combined with overproduction of an AcrAB efflux pump that transports drugs from the periplasm across the outer membrane was detected in strains isolated after patient antibiotherapy. These mechanisms acting together severely restrict the intracellular accumulation of antibiotics⁶⁴.

Similarly, in *Salmonella enterica* subsp. *enterica* serovar Typhimurium (*S. typhi*), β -lactam susceptibility has been found to be associated with the balance of porin expression in clinical isolates. Cephalosporin (cephalexin, cefoxitin and cefazolin) susceptibility was observed in all *S. typhi* isolates collected from a patient before antibiotic treatment⁶⁶. However, a cephalosporin-resistant isolate was recovered from a wound drain sample only days after cephalexin therapy was started. No significant increase in β -lactamase activity was detected in this isolate that evolved from a susceptible pre-therapy strain. The expression of the genes encoding OmpC and OmpF is modulated by distinct genetic control systems, such as small regulatory RNAs (MicC and MicF) and the two-component system EnvZ – OmpR^{40,41,67-69}. In

INTRODUCTION

the susceptible parental strain, the EnvZ – OmpR-mediated control of OmpC-OmpF balance by osmolarity was normal *in vitro*: at low osmolarity, both OmpF- and OmpC-type porins were expressed and at high osmolarity, only OmpC-type porins were synthesized. By contrast, the resistant strain was found to be fully repressed in the synthesis of OmpF- and OmpC-type porins under high osmolarity conditions, and produced only OmpF-type porins at low osmolarity⁶⁶.

These findings emphasize a generalizable step in the porin adaptive response – high osmolarity conditions found *in vivo* favour the production of the more restricted OmpC channel, which naturally reduces the permeation of polar large molecules. Liposome swelling assays were useful to show that cephalosporins diffuse through OmpF and OmpC channels at different rates⁷⁰. The acquisition of sequential adaptive modifications in porin synthesis under continuous antibiotic pressure, to which the pathogen is exposed *in vivo*, further decreases antibiotic influx at every step⁷¹. Clinical isolates lacking OmpC show complete impermeability to β -lactams. The loss of both major porins can cause a significant reduction in growth rate in resistant isolates, while enabling survival during intensive antibiotic treatment⁷².

Following the loss of general porins, Enterobacteriaceae isolates can deploy alternative porins to restore their fitness. A possible porin substitution involves deployment of a quiescent porin⁷³. Examples include OmpN from *Escherichia coli*, OmpK37 of *K. pneumoniae* and OmpS2 from *S. typhi*. A narrow pore caused by the existence of a bulky tyrosine residue in the constriction region of OmpN, might function to block the transport of large β -lactams, such as ceftaxime or cefotaxime, while allowing passage of small nutrients much more readily⁷⁴. Notably, the OmpN-encoding gene is transcribed divergently to the MicC sRNA, which is known to post-transcriptionally repress OmpC expression, on the *ompN – micC* operon, and it has recently been reported that β -lactam compounds increase the transcription of *ompN* and *micC* genes⁷⁵. An association was reported between the expression of the quiescent porin OmpK37 (OmpN homologue) and β -lactam resistance in a strain of *K. pneumoniae* that lacks OmpK35 and OmpK36. In contrast to OmpK35 or OmpK36 expression, the expression of OmpK37 provided a strong decrease in β -lactam susceptibility in *K. pneumoniae in vitro*⁷⁴.

Synthesis of mutated porins

In enterobacterial porins, the 35-residue internal loop L3, sitting in a bent conformation inside the pore, allows the formation of a constriction region (also called eyelet), giving rise to a narrow pore^{41,42}. The amino-acid residues on L3 loop that point towards the lumen are

INTRODUCTION

negatively charged residues (Asp105 and Glu109 in *E. coli* OmpC) that lie opposite a positive cluster (Lys16, Arg37, Arg74 and Arg124 in OmpC) on the barrel wall, causing a strong (transverse) electrostatic field across the constriction zone that governs the permeation of small polar molecules^{40,41}. The constriction region exerts considerable influence on antibiotic diffusion and therefore represents a critical region of the porin⁷⁶. Consequently, the type of mutation that changes the electrostatic properties of a porin will be found in L3 loop at or close to the eyelet.

A variant of Omp36, exhibiting the G112D substitution in L3 internal loop, was detected in β -lactam-resistant isolates of *Enterobacter aerogenes*^{77,78}. An *ompF* mutant carrying the G119D substitution, previously obtained using targeted mutagenesis, resembles this Omp36 porin mutation. The presence of a major protrusion in the lumen of OmpF caused by the G119D mutation, produces strong steric hindrance inside the pore that leads to high-level β -lactam resistance^{79,80}. In *E. aerogenes*, β -lactam translocation through the Omp36 porin is severely reduced in isolates that carry the G112D mutation (cefepime diffusion through the G112D Omp36 porin is strongly decreased)^{81,82}. The *E. aerogenes* Omp36 G112D mutation causes similar electrophysiological changes in the porin channel as that caused by the G119D mutation of *E. coli* OmpF^{78,79}.

Clinical *E. coli* strains synthesize OmpC variants that carry diverse mutations of amino acids positioned in the pore eyelet, which lead to alterations of the shape but not the size of the transverse electric field. This traps the drug in an unfavourable orientation and makes permeation through the constriction zone difficult^{83,84}. Thus, the level of drug diffusion through the porin is reduced, causing a reduction in intracellular concentration, and leading to β -lactam resistance, independent of the number of channels produced⁶³. Furthermore, this decreased susceptibility to β -lactams also correlates with β -lactamase expression⁸⁵.

Decreased porin production

A study observed that there was a close connection between imipenem therapy and the isolation of resistant strains of *E. aerogenes* that were altered in the levels of the major Omp36 porin⁸⁶. These *E. aerogenes* isolates with reduced imipenem susceptibility, that were obtained only days after the start of antibiotic treatment, were descendants of an original susceptible infecting strain, as indicated by epidemiological typing⁸⁷. Notably, the isolates collected a few days after the cessation of treatment were susceptible to imipenem. This observation is suggestive of the involvement of a mechanism that regulates porin synthesis. There was a good correlation

INTRODUCTION

between the absence of Omp36 porin and the β -lactam (imipenem and cephalosporin) resistance of the isolates⁸⁶. Furthermore, this Omp36 repression was accompanied by the expression of an efflux transporter in resistant *E. aerogenes* strains, suggesting a coordinated regulation of porin and transporter synthesis^{86,88}.

Similarly, in *Enterobacter cloacae*, reduced synthesis of the major porins, together with the overproduction of an efflux system, was detected in a resistant clinical strain that was isolated after antibiotherapy (imipenem and amikacin)⁸⁹. This suggests that the synthesis of porins is regulated by an efficient mechanism, most likely involving the Mar regulon that functions primarily in the enterobacterial response following external stresses such as antibiotics, disinfectants and detergents. The Mar regulon consists of an activator encoded by *marA* that is in an operon with *marR*, which encodes a repressor that is able to repress the transcription of *marA*^{67,90,91}. A regulatory cascade is triggered by the de-repression of *marA* under antibiotic stress conditions that downregulates the levels of porins and upregulates the levels of multidrug efflux pumps, and leads to global control of envelope permeability^{67,90-94}.

Objectives of the study

1. To investigate the relationship between the presence of general diffusion porins that belong to the MspA porin family and β -lactam susceptibility in *M. abscessus*.
2. To explore the association between an altered porin phenotype and β -lactamase expression during resistance.
3. Given that specific interactions between membrane proteins and lipids are increasingly prominent in cell biology, we sought to explore whether the total loss of GPL (a change that enables *M. abscessus* to transition from a smooth to a rough variant) has an impact upon the integral membrane proteins embedded in the mycomembrane, especially those involved in antibiotic transport (i.e. general porins).

References

1. Floto, R. A. et al. US Cystic Fibrosis Foundation and European Cystic Fibrosis Society consensus recommendations for the management of non-tuberculous mycobacteria in individuals with cystic fibrosis. *Thorax* **71**, i1–i22 (2016).
2. Bryant, J. M. et al. Emergence and spread of a human-transmissible multidrug-resistant nontuberculous mycobacterium. *Science* **354**, 751–757 (2016).
3. Esther, C. R., Esserman, D. A., Gilligan, P., Kerr, A. & Noone, P. G. Chronic *Mycobacterium abscessus* infection and lung function decline in cystic fibrosis. *J. Cyst. Fibros.* **9**, 117–123 (2010).
4. Jarand, J. et al. Clinical and microbiologic outcomes in patients receiving treatment for *Mycobacterium abscessus* pulmonary disease. *Clin. Infect. Dis.* **52**, 565–571 (2011).
5. Nessar, R., Cambau, E., Reyrat, J. M., Murray, A. & Gicquel, B. *Mycobacterium abscessus*: a new antibiotic nightmare. *J. Antimicrob. Chemother.* **67**, 810–818 (2012).
6. Kwak, N. et al. *Mycobacterium abscessus* pulmonary disease: individual patient data meta-analysis. *Eur. Resp. J.* <https://doi.org/10.1183/13993003.01991-2018> (2019).
7. Koch, R. Die Aetiologie der Tuberkulose. *Berl. Klin. Wochenschr.* **15**, 221–230 (1882).
8. Julián, E. et al. Microscopic cords, a virulence-related characteristic of *Mycobacterium tuberculosis*, are also present in nonpathogenic mycobacteria. *J. Bacteriol.* **192**, 1751–1760 (2010).
9. Sánchez-Chardi, A. et al. Demonstration of cord formation by rough *Mycobacterium abscessus* variants: implications for the clinical microbiology laboratory. *J. Clin. Microbiol.* **49**, 2293–2295 (2011).
10. Bernut, A. et al. *Mycobacterium abscessus* cording prevents phagocytosis and promotes abscess formation. *Proc. Natl Acad. Sci. USA* **111**, E943–E952 (2014).
11. Bernut, A. et al. *Mycobacterium abscessus*-induced granuloma formation is strictly dependent on TNF signaling and neutrophil trafficking. *PLoS Pathog.* **12**, e1005986 (2016).
12. Bernut, A. et al. CFTR protects against *Mycobacterium abscessus* infection by fine-tuning host oxidative defenses. *Cell Rep.* **26**, 1828–1840.e4 (2019).
13. Halloum, I. et al. Deletion of a dehydratase important for intracellular growth and cording renders rough *Mycobacterium abscessus* avirulent. *Proc. Natl Acad. Sci. USA* **113**, E4228–E4237 (2016).

14. Chiaradia, L. et al. Dissecting the mycobacterial cell envelope and defining the composition of the native mycomembrane. *Sci. Rep.* **7**, 12807 (2017).
15. Hoffmann, C., Leis, A., Niederweis, M., Pitzko, J. M. & Engelhardt, H. Disclosure of the mycobacterial outer membrane: cryo-electron tomography and vitreous sections reveal the lipid bilayer structure. *Proc. Natl Acad. Sci. USA* **105**, 3963–3967 (2008).
16. Zuber, B. et al. Direct visualization of the outer membrane of mycobacteria and corynebacteria in their native state. *J. Bacteriol.* **190**, 5672–5680 (2008).
17. Minnikin, D. E. et al. Pathophysiological implications of cell envelope structure in *Mycobacterium tuberculosis* and related taxa. in *Tuberculosis - Expanding Knowl.* (ed. Ribon, W.) (InTech, 2015). <https://doi.org/10.5772/59585>
18. Marrakchi, H., Lanéelle, M.-A. & Daffé, M. Mycolic acids: structures, biosynthesis, and beyond. *Chem. & Biol.* **21**, 67–85 (2014).
19. Dulberger, C. L., Rubin, E. J. & Boutte, C. C. The mycobacterial cell envelope — a moving target. *Nat. Rev. Microbiol.* **18**, 47–59 (2020).
20. Nikaido, H., Kim, S. H. & Rosenberg, E. Y. Physical organization of lipids in the cell wall of *Mycobacterium chelonae*. *Mol. Microbiol.* **8**, 1025–1030 (1993).
21. Liu, J., Rosenberg, E. Y. & Nikaido, H. Fluidity of the lipid domain of cell wall from *Mycobacterium chelonae*. *Proc. Natl Acad. Sci. USA* **92**, 11254–11258 (1995).
22. Liu, J., Barry, C. E., Besra, G. S. & Nikaido, H. Mycolic acid structure determines the fluidity of the mycobacterial cell wall. *J. Biol. Chem.* **271**, 29545–29551 (1996).
23. Jarlier, V. & Nikaido, H. Permeability barrier to hydrophilic solutes in *Mycobacterium chelonae*. *J. Bacteriol.* **172**, 1418–1423 (1990).
24. Gutiérrez, A. V., Viljoen, A., Ghigo, E., Herrmann, J.-L. & Kremer, L. Glycopeptidolipids, a double-edged sword of the *Mycobacterium abscessus* complex. *Front. Microbiol.* **9**, 1145 (2018).
25. Johansen, M. D., Herrmann, J. L. & Kremer, L. Non-tuberculous mycobacteria and the rise of *Mycobacterium abscessus*. *Nat. Rev. Microbiol.* **18**, 392–407 (2020).
26. Billman-Jacobe, H., McConville, M. J., Haites, R. E., Kovacevic, S. & Coppel, R. L. Identification of a peptide synthetase involved in the biosynthesis of glycopeptidolipids of *Mycobacterium smegmatis*. *Mol. Microbiol.* **33**, 1244–1253 (1999).
27. Sondén, B. et al. Gap, a mycobacterial specific integral membrane protein, is required for glycolipid transport to the cell surface. *Mol. Microbiol.* **58**, 426–440 (2005).

28. Bernut, A. et al. Insights into the smooth-to-rough transitioning in *Mycobacterium boletii* unravels a functional Tyr residue conserved in all mycobacterial MmpL family members. *Mol. Microbiol.* **99**, 866–883 (2016).
29. Deshayes, C. et al. MmpS4 promotes glycopeptidolipids biosynthesis and export in *Mycobacterium smegmatis*. *Mol. Microbiol.* **78**, 989–1003 (2010).
30. Pawlik, A. et al. Identification and characterization of the genetic changes responsible for the characteristic smooth-to-rough morphotype alterations of clinically persistent *Mycobacterium abscessus*. *Mol. Microbiol.* **90**, 612–629 (2013).
31. Park, I. K. et al. Clonal diversification and changes in lipid traits and colony morphology in *Mycobacterium abscessus* clinical isolates. *J. Clin. Microbiol.* **53**, 3438–3447 (2015).
32. Roux, A.-L. et al. The distinct fate of smooth and rough *Mycobacterium abscessus* variants inside macrophages. *Open Biol.* **6**, 160185 (2016).
33. Frehel, C., Ryter, A., Rastogi, N. & David, H. The electron-transparent zone in phagocytized *Mycobacterium avium* and other mycobacteria: formation, persistence and role in bacterial survival. *Ann. Inst. Pasteur Microbiol.* **137B**, 239–257 (1986).
34. Ramakrishnan, L. Revisiting the role of the granuloma in tuberculosis. *Nat. Rev. Immunol.* **12**, 352–366 (2012).
35. Laencina, L. et al. Identification of genes required for *Mycobacterium abscessus* growth *in vivo* with a prominent role of the ESX-4 locus. *Proc. Natl Acad. Sci. USA* **115**, E1002–E1011 (2018).
36. Dubois, V. et al. MmpL8_{MAB} controls *Mycobacterium abscessus* virulence and production of a previously unknown glycolipid family. *Proc. Natl Acad. Sci. USA* **115**, E10147–E10156 (2018).
37. Rhoades, E. R. et al. *Mycobacterium abscessus* glycopeptidolipids mask underlying cell wall phosphatidyl-*myo*-inositol mannosides blocking induction of human macrophage TNF- α by preventing interaction with TLR2. *J. Immunol.* **183**, 1997–2007 (2009).
38. Roux, A.-L. et al. Overexpression of proinflammatory TLR-2-signalling lipoproteins in hypervirulent mycobacterial variants. *Cell. Microbiol.* **13**, 692–704 (2011).
39. Davidson, L. B., Nessar, R., Kempaiah, P., Perkins, D. J. & Byrd, T. F. *Mycobacterium abscessus* glycopeptidolipid prevents respiratory epithelial TLR2 signaling as measured by H β D2 gene expression and IL-8 release. *PLoS One* **6**, e29148 (2011).

40. Nikaido, H. Molecular basis of bacterial outer membrane permeability revisited. *Microbiol. Mol. Biol. Rev.* **67**, 593–656 (2003).
41. Delcour, A. H. Solute uptake through general porins. *Front. Biosci.* **8**, D1055–D1071 (2003).
42. Schulz, G. E. The structure of bacterial outer membrane proteins. *Biochim. Biophys. Acta* **1565**, 308–317 (2002).
43. Nikaido, H. Prevention of drug access to bacterial targets: permeability barriers and active efflux. *Science* **264**, 382–388 (1994).
44. Niederweis, M. et al. Cloning of the *mspA* gene encoding a porin from *Mycobacterium smegmatis*. *Mol. Microbiol.* **33**, 933–945 (1999).
45. Stahl, C. et al. MspA provides the main hydrophilic pathway through the cell wall of *Mycobacterium smegmatis*. *Mol. Microbiol.* **40**, 451–464 (2001).
46. Faller, M., Niederweis, M. & Schulz, G. E. The Structure of a Mycobacterial Outer-Membrane Channel. *Science* **303**, 1189–1192 (2004).
47. Cowan, S. W. et al. Crystal structures explain functional properties of two *E. coli* porins. *Nature* **358**, 727–733 (1992).
48. Baslé, A., Rummel, G., Storici, P., Rosenbusch, J. P. & Schirmer, T. Crystal structure of osmoporin OmpC from *E. coli* at 2.0 Å. *J. Mol. Biol.* **362**, 933–942 (2006).
49. Paul, T. R. & Beveridge, T. J. Reevaluation of envelope profiles and cytoplasmic ultrastructure of mycobacteria processed by conventional embedding and freeze-substitution protocols. *J. Bacteriol.* **174**, 6508–6517 (1992).
50. Paul, T. R. & Beveridge, T. J. Ultrastructure of mycobacterial surfaces by freeze-substitution. *Zentbl. Bakteriologie* **279**, 450–457 (1993).
51. Paul, T. R. & Beveridge, T. J. Preservation of surface lipids and determination of ultrastructure of *Mycobacterium kansasii* by freeze-substitution. *Infect. Immun.* **62**, 1542–1550 (1994).
52. Mahfoud, M., Sukumaran, S., Hülsmann, P., Grieger, K. & Niederweis, M. Topology of the porin MspA in the outer membrane of *Mycobacterium smegmatis*. *J. Biol. Chem.* **281**, 5908–5915 (2006).
53. Bush, K. & Bradford, P. A. in *Antibiotics and Antibiotic Resistance* (eds Silver, L. L. & Bush, K.) 23–44 (Cold Spring Harbor Laboratory Press, 2016).
54. Kohanski, M. A., Dwyer, D. J. & Collins, J. J. How antibiotics kill bacteria: from targets to networks. *Nat. Rev. Microbiol.* **8**, 423–435 (2010).

55. Lavollay, M. et al. The peptidoglycan of *Mycobacterium abscessus* is predominantly cross-linked by L,D-transpeptidases. *J. Bacteriol.* **193**, 778–782 (2011).
56. Kaushik, A. et al. Carbapenems and Rifampin Exhibit Synergy against *Mycobacterium tuberculosis* and *Mycobacterium abscessus*. *Antimicrob. Agents Chemother.* **59**, 6561–6567 (2015).
57. Kumar, P. et al. Non-classical transpeptidases yield insight into new antibacterials. *Nat. Chem. Biol.* **13**, 54–61 (2017).
58. Lefebvre, A.-L. et al. Bactericidal and intracellular activity of β -lactams against *Mycobacterium abscessus*. *J. Antimicrob. Chemother.* **71**, 1556–1563 (2016).
59. Kumar, P. et al. *Mycobacterium abscessus* L,D-transpeptidases are susceptible to inactivation by carbapenems and cephalosporins but not penicillins. *Antimicrob. Agents Chemother.* <https://doi.org/10.1128/AAC.00866-17> (2017).
60. Soroka, D. et al. Characterization of broad-spectrum *Mycobacterium abscessus* class A β -lactamase. *J. Antimicrob. Chemother.* **69**, 691–696 (2014).
61. Luthra, S., Rominski, A. & Sander, P. The role of antibiotic-target-modifying and antibiotic-modifying enzymes in *Mycobacterium abscessus* drug resistance. *Front. Microbiol.* **9**, 1–13 (2018).
62. Soroka, D. et al. Inhibition of β -lactamases of mycobacteria by avibactam and clavulanate. *J. Antimicrob. Chemother.* **72**, 1081–1088 (2017).
63. Pagès, J. M., James, C. E. & Winterhalter, M. The porin and the permeating antibiotic: a selective diffusion barrier in Gram-negative bacteria. *Nat. Rev. Microbiol.* **6**, 893–903 (2008).
64. Hasdemir, U. O., Chevalier, J., Nordmann, P. & Pagès, J.-M. Detection and prevalence of active drug efflux mechanism in various multidrug-resistant *Klebsiella pneumoniae* strains from Turkey. *J. Clin. Microbiol.* **42**, 2701–2706 (2004).
65. Doménech-Sánchez, A. et al. Role of *Klebsiella pneumoniae* OmpK35 porin in antimicrobial resistance. *Antimicrob. Agents Chemother.* **47**, 3332–3335 (2003).
66. Medeiros, A. A., O'Brien, T. F., Rosenberg, E. Y. & Nikaido, H. Loss of OmpC porin in a strain of *Salmonella typhimurium* causes increased resistance to cephalosporins during therapy. *J. Infect. Dis.* **156**, 751–757 (1987).
67. Davin-Regli, A. et al. Membrane permeability and regulation of drug “influx and efflux” in enterobacterial pathogens. *Curr. Drug Targets* **9**, 750–759 (2008).
68. Koebnik, R., Locher, K. P. & Van Gelder, P. Structure and function of bacterial outer membrane proteins: barrels in a nutshell. *Mol. Microbiol.* **37**, 239–253 (2000).

69. Guillier, M., Gottesman, S. & Storz, G. Modulating the outer membrane with small RNAs. *Genes Dev.* **20**, 2338–2348 (2006).
70. Yoshimura, F. & Nikaido, H. Diffusion of β -lactam antibiotics through the porin channels of *Escherichia coli* K-12. *Antimicrob. Agents Chemother.* **27**, 84–92 (1985).
71. Pagès, J.-M. Role of bacterial porins in antibiotic susceptibility of Gram-negative bacteria in *Bacterial and Eukaryotic Porins* (ed. Benz, R.) 41–59 (Wiley-VCH, Weinheim, 2004).
72. Ferenci, T. Maintaining a healthy SPANC balance through regulatory and mutational adaptation. *Mol. Microbiol.* **57**, 1–8 (2005).
73. Prilipov, A., Phale, P. S., Koebnik, R., Widmer, C. & Rosenbusch, J. P. Identification and characterization of two quiescent porin genes, *nmpC* and *ompN*, in *Escherichia coli* BE. *J. Bacteriol.* **180**, 3388–3392 (1998).
74. Doménech-Sánchez, A., Hernández-Allés, S., Martínez-Martínez, L., Benedí, V. J. & Albertí, S. Identification and characterization of a new porin gene of *Klebsiella pneumoniae*: its role in β -lactam antibiotic resistance. *J. Bacteriol.* **181**, 2726–2732 (1999).
75. Vergalli, J. et al. Porins and small-molecule translocation across the outer membrane of Gram-negative bacteria. *Nat. Rev. Microbiol.* **18**, 164–176 (2020).
76. Simonet, V., Malléa, M., Fourel, D., Bolla, J. M. & Pagès, J.-M. Crucial domains are conserved in *Enterobacteriaceae* porins. *FEMS Microbiol. Lett.* **136**, 91–97 (1996).
77. Malléa, M. et al. Porin alteration and active efflux: two *in vivo* drug resistance strategies used by *Enterobacter aerogenes*. *Microbiology* **144**, 3003–3009 (1998).
78. Dé, E. et al. A new mechanism of antibiotic resistance in *Enterobacteriaceae* induced by a structural modification of the major porin. *Mol. Microbiol.* **41**, 189–198 (2001).
79. Jeanteur, D. et al. Structural and functional alterations of a colicin-resistant mutant of OmpF porin from *Escherichia coli*. *Proc. Natl Acad. Sci. USA* **91**, 10675–10679 (1994).
80. Simonet, V., Malléa, M. & Pagès, J.-M. Substitutions in the eyelet region disrupt cefepime diffusion through the *Escherichia coli* OmpF channel. *Antimicrob. Agents Chemother.* **44**, 311–315 (2000).
81. Thiolas, A., Bornet, C., Davin-Régli, A., Pagès, J.-M. & Bollet, C. Resistance to imipenem, cefepime, and cefpirome associated with mutation in Omp36 osmoporin of *Enterobacter aerogenes*. *Biochem. Biophys. Res. Commun.* **317**, 851–856 (2004).

82. Chevalier, J., Pagès, J.-M. & Malléa, M. *In vivo* modification of porin activity conferring antibiotic resistance to *Enterobacter aerogenes*. *Biochem. Biophys. Res. Commun.* **266**, 248–251 (1999).
83. Lou, H. et al. Altered antibiotic transport in OmpC mutants isolated from a series of clinical strains of multi-drug resistant *E. coli*. *PLOS ONE* **6**, e25825 (2011).
84. Bajaj, H. et al. Molecular basis of filtering carbapenems by porins from β -lactam-resistant clinical strains of *Escherichia coli*. *J. Biol. Chem.* **291**, 2837–2847 (2016).
85. Sun, D., Rubio-Aparicio, D., Nelson, K., Dudley, M. N. & Lomovskaya, O. Meropenem-vaborbactam resistance selection, resistance prevention, and molecular mechanisms in mutants of KPC-producing *Klebsiella pneumoniae*. *Antimicrob. Agents Chemother.* **61**, e01694-17 (2017).
86. Bornet, C., Davin-Régli, A., Bosi, C., Pagès, J.-M. & Bollet, C. Imipenem resistance of *Enterobacter aerogenes* mediated by outer membrane permeability. *J. Clin. Microbiol.* **38**, 1048–1052 (2000).
87. Bosi, C. et al. Most *Enterobacter aerogenes* strains in France belong to a prevalent clone. *Clin. Microbiol.* **37**, 2165–2169 (1999).
88. Bornet, C. et al. Imipenem and expression of multidrug efflux pump in *Enterobacter aerogenes*. *Biochem. Biophys. Res. Commun.* **301**, 985–990 (2003).
89. Szabó, D. et al. Outer membrane protein changes and efflux pump expression together may confer resistance to ertapenem in *Enterobacter cloacae*. *Antimicrob. Agents Chemother.* **50**, 2833–2835 (2006).
90. Li, X. Z. & Nikaido, H. Efflux-mediated drug resistance in bacteria. *Drugs* **64**, 159–204 (2004).
91. Piddock, L. J. Multidrug-resistance efflux pumps — not just for resistance. *Nature Rev. Microbiol.* **4**, 629–636 (2006).
92. Poole, K. Efflux-mediated antimicrobial resistance. *J. Antimicrob. Chemother.* **56**, 20–51 (2005).
93. Davin-Régli, A. & Pagès, J.-M. in *Antimicrobial Resistance in Bacteria* (ed. Zmabiles-Cuevos, C. F.) 55–75 (Horizon Biosciences, Norfolk, 2006).
94. Randall, L. P. & Woodward, M. J. The multiple antibiotic resistance (*mar*) locus and its significance. *Res. Vet. Sci.* **72**, 87–93 (2002).

Antibiotic resistance characteristics of *Mycobacterium abscessus* rely on specific outer membrane porins and surface-associated glycopeptidolipids

Sakshi Luthra and Peter Sander

In preparation

Abstract

Infections with *Mycobacterium abscessus*, which is a multidrug-resistant species of nontuberculous mycobacteria, are effectively untreatable and are becoming more prevalent globally. The impermeability of the mycobacterial cell envelope represents a key drug-resistance mechanism that *M. abscessus* uses to decrease the internal accumulation of antibiotics. Through a better understanding of how the modification of cell envelope permeability elicits bacterial resistance, we might be able to develop new, effective means to overcome the ‘impermeability’ resistance strategy in an effort to fight *M. abscessus* infections. Here, by determination of susceptibility of an extensive collection of gene knockout strains to a series of β -lactams, we reveal that in *M. abscessus*, β -lactam susceptibility is linked to the presence of the general porin MapA and that the chromosomally encoded β -lactamase Bla_{Mab} can confer a higher level of β -lactam resistance in a *mapA* mutant than in wildtype *M. abscessus*. Additionally, the results suggest that the glycopeptidolipid (GPL) environment can affect the levels of susceptibility to drugs that mainly diffuse across the membrane barrier through non-specific porins. This work has yielded new insights into the types and numbers of factors that influence susceptibility to β -lactam compounds in *M. abscessus* and how sets of genes act in concert, rather than in isolation, to elicit bacterial resistance to antibiotics.

Introduction

Mycobacterium abscessus is the major non-tuberculous mycobacterium (NTM) infecting people with cystic fibrosis (CF), with increasing incidence of infections reported within the CF community globally¹. This rapidly growing environmental mycobacterium is separated into three clearly divergent subspecies: *M. abscessus* subsp. *abscessus*, *M. abscessus* subsp. *massiliense* and *M. abscessus* subsp. *bolletii*². Treatment of CF patients that become infected with *M. abscessus*, in whom this intrinsically multidrug-resistant species causes rapid decline in lung function³, is often unsuccessful despite extended combinatorial drug therapy⁴⁻⁶, which leads to increased morbidity and mortality. Initially, infections in CF patients were thought to result from independent environmental acquisition of *M. abscessus*. However, multinational, population-level whole-genome sequencing of clinical isolates from infected CF individuals showed that a greater number of infections were driven by indirect transmission between patients (probably via an environmental intermediary), of a few virulent *M. abscessus* clones that have recently emerged and have rapidly become globally dispersed². These clones displayed increased virulence in *in vitro* and *in vivo* infection models, were more tolerant of antimicrobial agents and correlated with worse clinical outcomes², indicating that the ongoing evolution of infecting *M. abscessus* clones has promoted increased pathogenicity. This observation emphasizes the urgent need for effective therapeutic strategies and control of cross-infection to restrict the evolution of *M. abscessus* from an environmental saprophyte to a true lung pathogen.

The hallmark of mycobacteria is their protective cell envelope, which is composed of surface lipids, cell wall and the cytoplasmic membrane, and contains many proteins. The mycobacterial cell wall core consists of peptidoglycan, arabinogalactan and very long chain fatty acids, the mycolic acids as inferred from biochemical⁷ and microscopic studies^{8,9}. The defining feature of this envelope is a unique outer membrane (the mycomembrane) that is a supported asymmetric lipid bilayer in which the inner leaflet is composed of mycolic acids connected by covalent interactions to the underlying arabinogalactan of the arabinogalactan-peptidoglycan co-polymer¹⁰. Its outer leaflet consists of free lipids that include long chain lipids such as trehalose dimycolates as well as smaller lipids (16-18 carbons long) such as the diacyl and triacyl trehaloses^{11,12}. Mycolic acids are composed of 2-alkyl, 3-hydroxy fatty acids that are more than 70 carbons long with only a few double bonds. In mycolic acid, the α -chain, which is the lipid at the 2 position, is saturated and consists of 22-26 carbon atoms, while the meromycolate, which is the lipid on the 3-hydroxyl, contains 42-62 carbon atoms^{11,12}. An x-

ray diffraction study confirmed the existence of an outer membrane in mycobacteria and revealed a quasi-crystalline packing of cell wall lipids¹³. The inner layer of covalently linked mycolic acids showed an extremely low fluidity, while the outer leaflet was moderately fluid as observed by analysis using electron paramagnetic resonance of spin-labeled fatty acids in isolated cell walls of *Mycobacterium chelonae*^{14,15}. Due to its physical properties, the mycomembrane poses a significant permeation barrier, providing mycobacteria with intrinsic resistance to most antibiotics. The permeability of the mycobacterial cell envelope toward β -lactams is 100–1000 times less than that provided by the cell envelope of Gram-negative bacteria¹⁶.

Most solutes diffuse through the mycomembrane via β -barrel protein channels, termed porins, that allow the passive uptake of small, water-soluble molecules¹⁷⁻¹⁹. The mycobacterial outer membrane contains very small amounts of porin, whose channel allows the penetration of small molecules only at a very slow rate²⁰. The pore-containing β -barrel protein, MspA, which was observed in chloroform/ methanol extracts of *Mycobacterium smegmatis* cells²¹, is the best studied mycobacterial porin, both structurally and functionally. It was reported that the disruption of *mspA* in *M. smegmatis* led to decreased outer membrane permeability to glucose (4-fold) and cephaloridine (9-fold)²², showing that this non-specific porin is the main entry point for hydrophilic small molecules in *M. smegmatis*. The x-ray crystal structure of MspA was the first structure of a mycobacterial outer membrane protein to be solved²³. The structure revealed the existence of two consecutive 16-stranded β -barrels and a globular rim domain in an octameric goblet-shaped protein that contains a single 9.6-nm-long central channel²³. The atomic structure of this porin has unique properties that were not observed in Gram-negative bacterial porins, which are ~4 nm long and consist of trimers of 16-stranded β -barrels, each of which is a pore itself^{24,25}. The analysis of stained ultrathin sections of mycobacterial cells by electron microscopy suggested outer membrane lipidic layer thicknesses of around 5-12 nm²⁶⁻²⁸, which seemingly conflicts with the length of the hydrophobic β -barrel domain of MspA, which is only 3.7 nm²³. This inconsistency was reconciled by a cysteine scanning study that described the native topology of MspA and suggested that part of the hydrophilic rim domain as well as loops are inserted into the *M. smegmatis* outer membrane²⁹. This study provided the first indication that a β -barrel outer membrane protein spans the outer membrane with elements other than amphipathic antiparallel β -strands.

β -Lactam antibiotics are efficacious, well tolerated and display a very wide spectrum of activity and have become the most frequently prescribed antibiotics in the clinic in recent time³⁰.

Initially, it was thought that inhibition of peptidoglycan synthesis by β -lactams was caused by inactivation of only the penicillin-binding proteins (also known as D, D-transpeptidases) that facilitate the cross-linking of immature peptidoglycan units by catalysing peptide bond formation between the fourth and third residues of adjacent peptide strands (designated 4 \rightarrow 3 linkages)³¹. Notably, in the peptidoglycan of *M. abscessus*, the major degree of cross-linking occurs between the third residues of the peptide side chains (designated 3 \rightarrow 3 linkages)³², which is accomplished by nonclassical transpeptidases, known as, L, D-transpeptidases, by contrast, the classical 4 \rightarrow 3 linkages are fewer in number. Recent evidence suggests that *M. abscessus* may exhibit higher susceptibility to carbapenems³³; this is attributed to the unique ability of this β -lactam subclass to block L, D-transpeptidase activity³⁴. It is worth noting that only two β -lactams, including imipenem (a carbapenem) and ceftazidime (a cephalosporin) are currently in use in combinatorial therapies against *M. abscessus*³⁵. A study determined the relative inhibition of activities of two L, D-transpeptidases (namely, Ldt_{Mab1} and Ldt_{Mab2}) from *M. abscessus* by a wide variety of β -lactams (including penicillins, cephalosporins, carbapenems and a penem) and found that some compounds (doripenem, biapenem and faropenem) possessed excellent abilities to inactivate both enzymes and that the combination of ceftazidime (a cephalosporin) and doripenem (a carbapenem), two β -lactam subtypes that showed distinct affinities for Ldt_{Mab1} and Ldt_{Mab2}, was synergistic against both susceptible *M. abscessus* and multidrug resistant clinical isolates³⁶. The study authors suggest that dual combinations of β -lactams can be more effective against *M. abscessus*, displaying a synergistic effect (as noted above for doripenem and ceftazidime drug combination) that could be attributed to different levels of inhibition of nonredundant targets which include both D, D-transpeptidases and L, D-transpeptidases. As the naturally occurring broad-spectrum β -lactamase Bla_{Mab} is the highest contributor to β -lactam resistance in *M. abscessus*^{37,38}, the concept has emerged of adding a β -lactamase inhibitor such as the non- β -lactam inhibitor avibactam, which provides excellent protection against Bla_{Mab}^{38,39}, to a dual- β -lactam combination to possibly further enhance the lethality of combinatorial antibiotic treatment.

Surface-associated GPL are free lipids found in the mycomembrane outer leaflet of several NTM-species, including opportunistic pathogens such as *M. abscessus*, *M. chelonae* and *Mycobacterium avium* and saprophytic mycobacteria such as *M. smegmatis*. Similarly to other NTM-species, *M. abscessus* displays both smooth and rough colony morphotypes with clear differences in surface properties and physiopathological aspects and importantly, this morphological heterogeneity is dictated by the GPL composition of the cell envelope. The

presence of hydrophilic GPL in smooth *M. abscessus* promotes sliding motility whereas the rough variant, in which these lipids are lacking or present at extremely low levels, is characterized by increased surface hydrophobicity and displays aggregative properties with a propensity to form massive cord-like structures and biofilms^{40,41}. The *gpl* locus, highly conserved in *M. abscessus*, *M. avium* and *M. smegmatis*, encompasses a large collection of genes that encode factors responsible for the biosynthesis, modification and translocation of GPL. Within the *gpl* cluster, *mps1* and *mps2* encode non-ribosomal peptide synthases involved in assembly of the tripeptide-amino-alcohol moiety⁴² and *gap* encodes an integral membrane protein required for GPL translocation across the cell membrane in *M. smegmatis*⁴³. Transitioning from a smooth to a rough variant in *M. abscessus*, which usually occurs during infection, implicates genetic changes such as single-nucleotide polymorphisms and small insertions or deletions within genes involved in GPL production including *mps1* and *mps2* or those required for transport of GPL such as *mmpS4*, *mmpL4a* and *mmpL4b*^{44,45}.

By the determination of susceptibility of an extensive collection of gene knockout strains to a series of β -lactams, here, we show that in *M. abscessus*, β -lactam susceptibility is linked to the presence of the general porin MapA and that the chromosomally encoded β -lactamase Bla_{Mab} can confer a higher level of β -lactam resistance in a *mapA* mutant than in the wildtype strain of *M. abscessus*. In addition, the results suggest that the GPL environment can affect the levels of susceptibility to drugs that mainly diffuse across the membrane barrier through non-specific porins. These results uncover the transport pathway of a prominent class of antibiotics through the mycobacterial outer membrane and allow the understanding of membrane-associated resistance mechanisms in an intrinsically multidrug-resistant species of NTM.

Results

Construction of porin and glycopeptidolipid mutants in *M. abscessus*

The genome of *M. abscessus* encodes three orthologues of MspA, the prototype of a family of four known octameric general diffusion porins found in *M. smegmatis*²⁹. The MspA channel is the main entry pathway for hydrophilic molecules in *M. smegmatis*²². The MapA and MapB proteins from *M. abscessus*, encoded by two adjacent genes MAB_1080 & MAB_1081, respectively, have sequences that share high similarity with the MspA polypeptide sequence. The *mapC* (MAB_2800) gene, spatially distinct from *mapA* and *mapB* genes in the *M. abscessus* genome, encodes a protein showing a structural relationship to MspA. To investigate the relationship between the presence of general diffusion porins that belong to the MspA porin family and β -lactam susceptibility in *M. abscessus* and to explore the association between an altered porin phenotype and β -lactamase expression during resistance, unmarked gene deletions for all three porin-encoding genes were generated in both β -lactamase-producing *M. abscessus* ATCC 19977 strain and β -lactamase-null *M. abscessus* Δbla strain. To generate unmarked gene deletions in *M. abscessus* by homologous recombination, flanking regions of porin-encoding genes, *mapA*, *mapB* and *mapC*, were cloned into the mycobacterial suicide vector pKH-*apr-dsred2-katG*, yielding the knockout vectors pKH- $\Delta mapA$, pKH- $\Delta mapB$ and pKH- $\Delta mapC$, respectively.

The knockout vector harbors an apramycin resistance marker required for selection of single crossover transformants resulting from chromosomal integration of plasmid by intermolecular homologous recombination. The plasmid also carries the *katG* gene that serves as a counterselection marker. Expression of *katG*, encoding a drug activating enzyme, renders *M. abscessus* sensitive to the prodrug isoniazid and facilitates selection of gene deletion mutants resulting from the loss of vector caused by a second intramolecular homologous recombination⁴⁶. Following transformation of knockout plasmid into *M. abscessus* by electroporation, single crossover transformants were first selected on apramycin plates and distinguished from background growth by colony fluorescence of red fluorescent protein DsRed2 (present on the vector backbone as a fusion gene with apramycin resistance marker) and confirmed by colony PCR. Positive single crossover clones were then subjected to isoniazid counterselection and non-fluorescent colonies corresponding to clones in which the second recombination event had occurred, were screened for gene deletion by PCR amplifying the deleted region. The genotype of each *M. abscessus* porin gene deletion mutant was confirmed by Southern blot analysis (FIG. 2a, b, c).

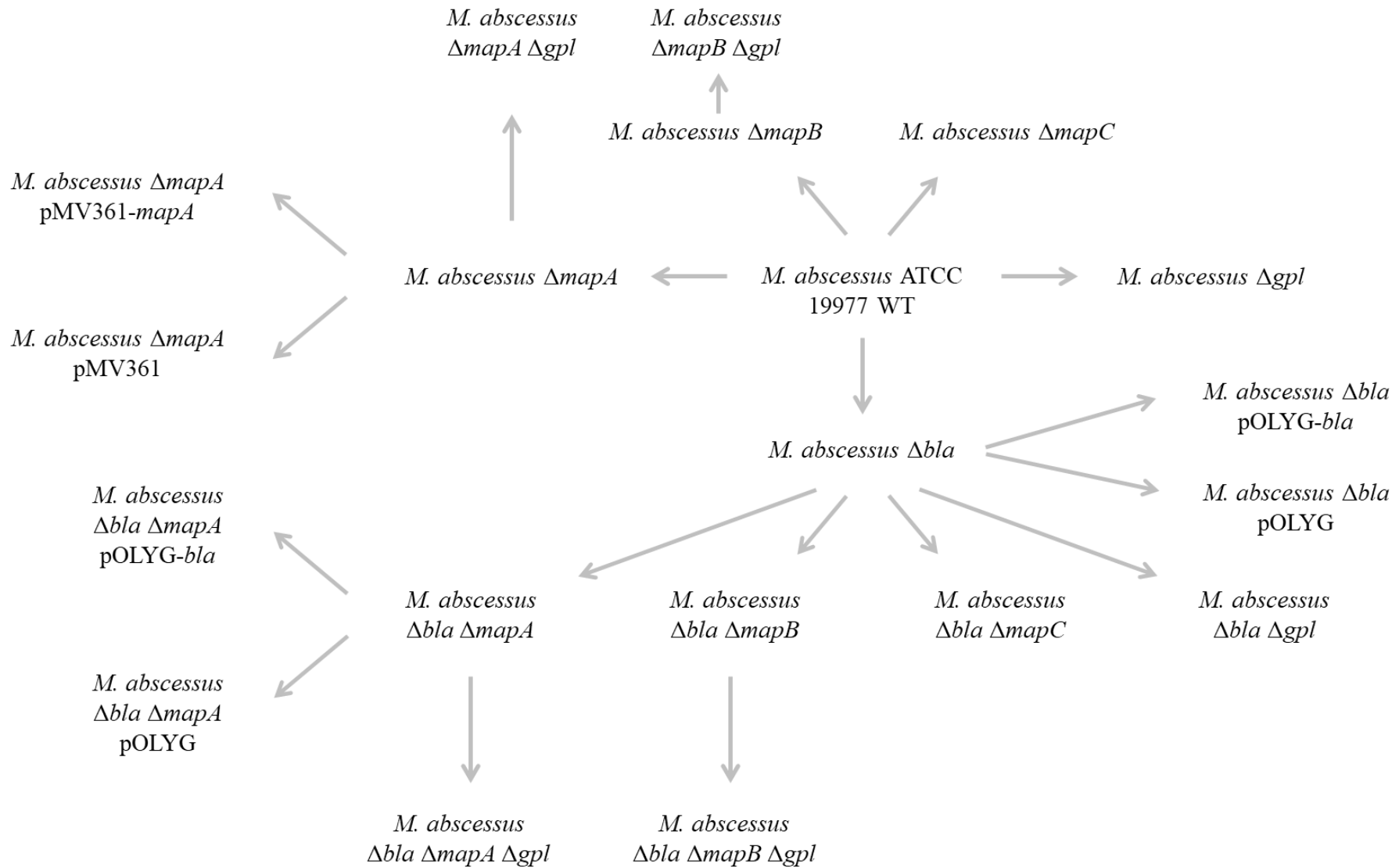


Figure 1 | Genealogy of *M. abscessus* strains used for the generation of single, double and triple knockout strains in this study.

For functional complementation of *M. abscessus* $\Delta mapA$ strain carrying *mapA* gene disruption conferring a carbapenem resistance phenotype, the single copy pMV361 integrative vector that integrates into the mycobacterial chromosome via *attP/attB* recombination⁴⁶, was used. The complementation vector pMV361-*mapA* or the control vector pMV361-*apr* was transformed into *M. abscessus* $\Delta mapA$ strain and integrants were obtained by positive selection on apramycin plates. The presence of *mapA* or *apr* gene in the resulting strains was confirmed by colony PCR. Furthermore, to confirm if the observed correlation between the absence of MapA porin and the level of β -lactam susceptibility in *M. abscessus* was associated with β -lactamase expression, the operon containing Bla_{Mab}-encoding gene (MAB_2875) was expressed in β -lactamase-null *M. abscessus* strains that either show normal expression of wildtype MapA (i.e. *M. abscessus* Δbla) or exhibit MapA loss (i.e. *M. abscessus* $\Delta bla \Delta mapA$), using the replicative multicopy pOLYG vector. Following electroporation of pOLYG-*bla* complementation vector or pOLYG-*apr* control vector into *M. abscessus* Δbla and *M. abscessus* $\Delta bla \Delta mapA$ mutants, respectively, transformants were selected on agar plates containing apramycin and confirmed by colony PCR.

Table 1. Strains used in this study

Strain	Description	Source
<i>E. coli</i> XL1-Blue MRF'	Cloning and propagation of plasmids	Stratagene
<i>M. abscessus</i> ATCC 19977	<i>M. abscessus</i> type strain	(Ripoll <i>et al.</i> , 2009)
<i>M. abscessus</i> Δbla	<i>M. abscessus</i> <i>bla</i> deletion mutant; derivative of <i>M. abscessus</i> ATCC 19977	(Rominski <i>et al.</i> , 2017)
<i>M. abscessus</i> $\Delta mapA$	<i>M. abscessus</i> <i>mapA</i> deletion mutant; derivative of <i>M. abscessus</i> ATCC 19977	This study
<i>M. abscessus</i> $\Delta mapB$	<i>M. abscessus</i> <i>mapB</i> deletion mutant; derivative of <i>M. abscessus</i> ATCC 19977	This study
<i>M. abscessus</i> $\Delta mapC$	<i>M. abscessus</i> <i>mapC</i> deletion mutant; derivative of <i>M. abscessus</i> ATCC 19977	This study
<i>M. abscessus</i> Δgpl	<i>M. abscessus</i> <i>gpl</i> deletion mutant; derivative of <i>M. abscessus</i> ATCC 19977	This study
<i>M. abscessus</i> $\Delta bla \Delta mapA$	<i>M. abscessus</i> <i>bla mapA</i> double deletion mutant; derivative of <i>M. abscessus</i> Δbla	This study

CHAPTER 1

<i>M. abscessus</i> Δbla $\Delta mapB$	<i>M. abscessus bla mapB</i> double deletion mutant; derivative of <i>M. abscessus</i> Δbla	This study
<i>M. abscessus</i> Δbla $\Delta mapC$	<i>M. abscessus bla mapC</i> double deletion mutant; derivative of <i>M. abscessus</i> Δbla	This study
<i>M. abscessus</i> Δbla Δgpl	<i>M. abscessus bla gpl</i> double deletion mutant; derivative of <i>M. abscessus</i> Δbla	This study
<i>M. abscessus</i> $\Delta mapA$ Δgpl	<i>M. abscessus mapA gpl</i> double deletion mutant; derivative of <i>M. abscessus</i> $\Delta mapA$	This study
<i>M. abscessus</i> $\Delta mapB$ Δgpl	<i>M. abscessus mapB gpl</i> double deletion mutant; derivative of <i>M. abscessus</i> $\Delta mapB$	This study
<i>M. abscessus</i> Δbla $\Delta mapA$ Δgpl	<i>M. abscessus bla mapA gpl</i> triple deletion mutant; derivative of <i>M. abscessus</i> Δbla $\Delta mapA$	This study
<i>M. abscessus</i> Δbla $\Delta mapB$ Δgpl	<i>M. abscessus bla mapB gpl</i> triple deletion mutant; derivative of <i>M. abscessus</i> Δbla $\Delta mapB$	This study
<i>M. abscessus</i> Δbla pOLYG- <i>bla</i>	<i>M. abscessus bla</i> null mutant transformed with pOLYG- <i>bla</i> complementation vector	This study
<i>M. abscessus</i> Δbla pOLYG	<i>M. abscessus bla</i> null mutant transformed with control vector pOLYG	This study
<i>M. abscessus</i> $\Delta mapA$ pMV361- <i>mapA</i>	<i>M. abscessus mapA</i> null mutant transformed with complementation vector pMV361- <i>mapA</i>	This study
<i>M. abscessus</i> $\Delta mapA$ pMV361	<i>M. abscessus mapA</i> null mutant transformed with pMV361 control vector	This study
<i>M. abscessus</i> Δbla $\Delta mapA$ pOLYG- <i>bla</i>	<i>M. abscessus bla mapA</i> double mutant transformed with complementation vector pOLYG- <i>bla</i>	This study
<i>M. abscessus</i> Δbla $\Delta mapA$ pOLYG	<i>M. abscessus bla mapA</i> double mutant transformed with pOLYG control vector	This study

Table 2. Plasmids used in this study

Plasmid	Purpose and description; selection marker	Source
pKH- <i>apr-dsred2-katG</i>	Suicide vector for generation of gene deletions in <i>M. abscessus</i> . Contains an <i>apr-dsred2</i> fusion gene for positive selection and a <i>katG</i> gene for negative selection; Apr ^R , INH ^S	(Rominski <i>et al.</i> , 2017)
pKH- Δ <i>mapA</i>	Suicide vector for gene deletion. A derivative of pKH- <i>apr-dsred2-katG</i> containing <i>mapA</i> flanking regions; Apr ^R , INH ^S	This study
pKH- Δ <i>mapB</i>	Suicide vector for gene deletion. A derivative of pKH- <i>apr-dsred2-katG</i> containing <i>mapB</i> flanking regions; Apr ^R , INH ^S	This study
pKH- Δ <i>mapA</i> - Δ <i>mapB</i>	Suicide vector for gene deletion. A derivative of pKH- <i>apr-dsred2-katG</i> carrying the Δ <i>mapA</i> Δ <i>mapB</i> allele; Apr ^R , INH ^S	This study
pKH- Δ <i>mapA</i> _N	Suicide vector for gene deletion. Analogous to pKH- Δ <i>mapA</i> but meant for <i>mapA</i> deletion in <i>M. abscessus</i> Δ <i>mapB</i> and Δ <i>bla</i> Δ <i>mapB</i> strains; Apr ^R , INH ^S	This study
pKH- Δ <i>mapB</i> _N	Suicide vector for gene deletion. Analogous to pKH- Δ <i>mapB</i> but meant for <i>mapB</i> deletion in <i>M. abscessus</i> Δ <i>mapA</i> and Δ <i>bla</i> Δ <i>mapA</i> strains; Apr ^R , INH ^S	This study
pKH- Δ <i>mapC</i>	Suicide vector for gene deletion. A derivative of pKH- <i>apr-dsred2-katG</i> containing <i>mapC</i> flanking regions; Apr ^R , INH ^S	This study
pKH- Δ <i>gpl</i>	Suicide vector for gene deletion. A derivative of pKH- <i>apr-dsred2-katG</i> carrying the Δ <i>gpl</i> allele; Apr ^R , INH ^S	This study
pMV361- <i>apr</i>	<i>E. coli</i> replicative vector that contains the mycobacteriophage integrase <i>int</i> and <i>attP</i> site for integration into the mycobacterial chromosome as a single copy by site-specific recombination with the <i>attB</i> site; Apr ^R , Kan ^R	(Rominski <i>et al.</i> , 2017)
pMV361- <i>mapA</i>	Integrative vector for gene complementation. A derivative of pMV361- <i>apr</i> containing the <i>mapA</i> gene; Apr ^R , Kan ^R	This study

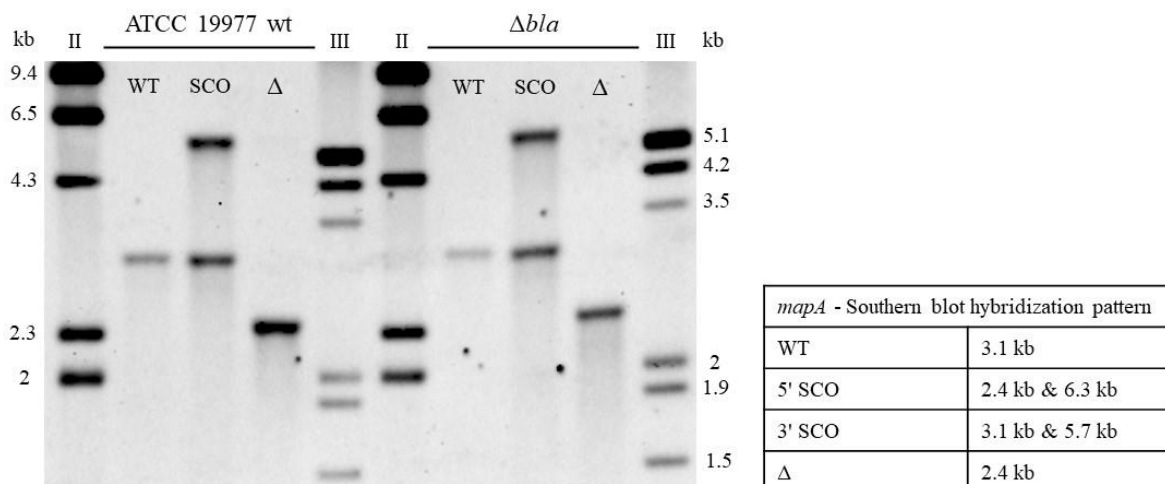
pOLYG- <i>apr</i>	Vector for constitutive expression in mycobacteria. Contains a mycobacterial origin of replication (<i>oriM</i>), thus being a replicative multicopy vector that can confer higher expression levels than the integrative pMV361- <i>apr</i> vector; Apr ^R , Hyg ^R	(Becker <i>et al.</i> , 2017)
pOLYG- <i>bla</i>	Replicative vector for gene complementation. A derivative of pOLYG- <i>apr</i> containing the MAB_2874-MAB_2875 (<i>bla</i>) operon; Apr ^R , Hyg ^R	This study
pMV361-MapA-MapB	Intermediate vector containing ORFs coding for MapA (fused to a C-terminal Strep-tag II) and MapB. A derivative of pMV361- <i>apr</i> ; Apr ^R , Kan ^R	This study
pINIT- <i>cat</i>	Intermediate vector used for initial sequence verification and subsequent subcloning of the ORF to a desired FX cloning compatible expression vector; Cm ^R	(Arnold <i>et al.</i> , 2018)
pACEC3GH- <i>apr</i>	Replicative vector harboring an acetamide inducible promoter for a controlled, high-level expression in mycobacteria. Compatible with FX cloning and fuses a 3C cleavage site, a GFP tag (for detection of protein production) and a His ₁₀ -tag (for protein purification) to the C-terminus of the target ORF; Apr ^R	(Arnold <i>et al.</i> , 2018)
pACE-MapA-MapB	Replicative expression vector based on the acetamide promoter. A derivative of pACEC3GH- <i>apr</i> containing ORFs coding for MapA (with a C-terminal Strep-tag II fusion) and MapB (with a C-terminal His ₁₀ -tag fusion). Lacks the GFP tag; Apr ^R	This study
pACE-MspA	Replicative expression vector based on the acetamide promoter. A derivative of pACEC3GH- <i>apr</i> containing the ORF coding for MspA (with a C-terminal His ₁₀ -tag fusion). Is devoid of GFP tag; Apr ^R	This study

Apr^R, apramycin resistance marker; Kan^R, kanamycin resistance marker; Hyg^R, hygromycin resistance marker; Cm^R, chloramphenicol resistance marker; INH^S, isoniazid susceptibility cassette

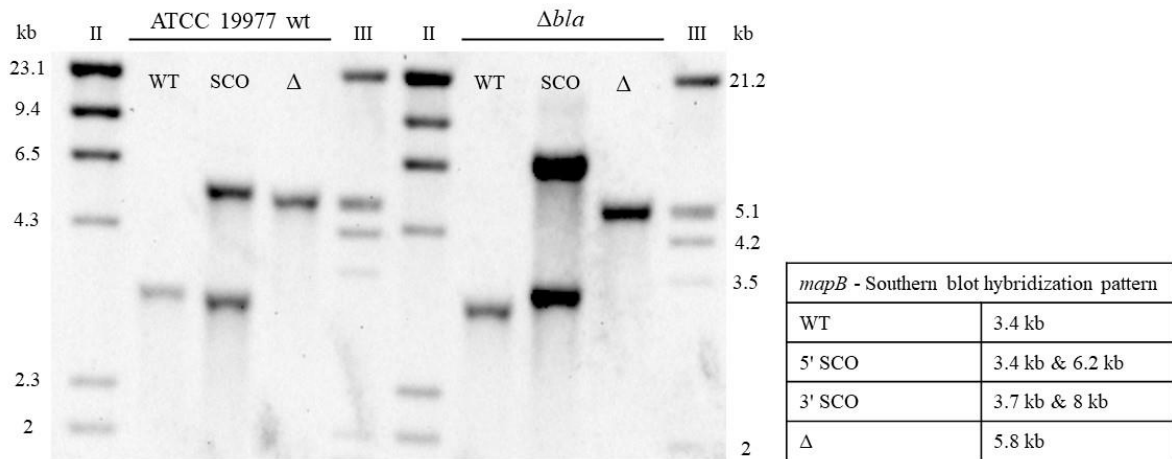
CHAPTER 1

In the mycomembrane of smooth *M. abscessus*, a high-GPL producer⁴¹, GPL form the environment into which outer membrane proteins are inserted. Hence, it seems very likely that outer membrane porins interact with GPL and such interactions may have a role in the formation of stable channels in the mycomembrane. To investigate the influence of the total loss of GPL on resistance to hydrophilic β -lactams in *M. abscessus*, a collection of rough *M. abscessus* strains showing an arrest of GPL production was generated by the deletion of three adjacent genes, *mps1* (MAB_4099c), *mps2* (MAB_4098c) and *gap* (MAB_4097c), of the *gpl* locus using the knockout plasmid pKH- Δgpl . These include (i) rough variants of *M. abscessus* strains that exhibit normal porin expression with or without basal production of periplasmic β -lactamase (i.e. *M. abscessus* Δgpl and *M. abscessus* $\Delta bla \Delta gpl$ strains); (ii) GPL-null *M. abscessus* strains that are devoid of a general porin but exhibit normal β -lactamase expression (i.e. *M. abscessus* $\Delta mapA \Delta gpl$ and *M. abscessus* $\Delta mapB \Delta gpl$ strains); (iii) *M. abscessus* strains that exhibit an altered GPL phenotype together with porin loss and lack of β -lactamase activity (i.e. *M. abscessus* $\Delta bla \Delta mapA \Delta gpl$ and *M. abscessus* $\Delta bla \Delta mapB \Delta gpl$ strains). The double deletion mutants, *M. abscessus* $\Delta bla \Delta gpl$, *M. abscessus* $\Delta mapA \Delta gpl$ and *M. abscessus* $\Delta mapB \Delta gpl$, respectively, were generated by transformation of pKH- Δgpl vector into the following single deletion mutants, *M. abscessus* Δbla , *M. abscessus* $\Delta mapA$ and *M. abscessus* $\Delta mapB$, respectively. Furthermore, transformation of pKH- Δgpl plasmid into *M. abscessus* $\Delta bla \Delta mapA$ and *M. abscessus* $\Delta bla \Delta mapB$ double mutants enabled the construction of *M. abscessus* $\Delta bla \Delta mapA \Delta gpl$ and *M. abscessus* $\Delta bla \Delta mapB \Delta gpl$ triple mutants, respectively (refer Table 1 for list of strains, FIG. 1 for genealogy of strains and Table 2 for list of plasmids). The deletion of *gpl* genes in *M. abscessus* was confirmed by Southern blot analysis (FIG. 2d).

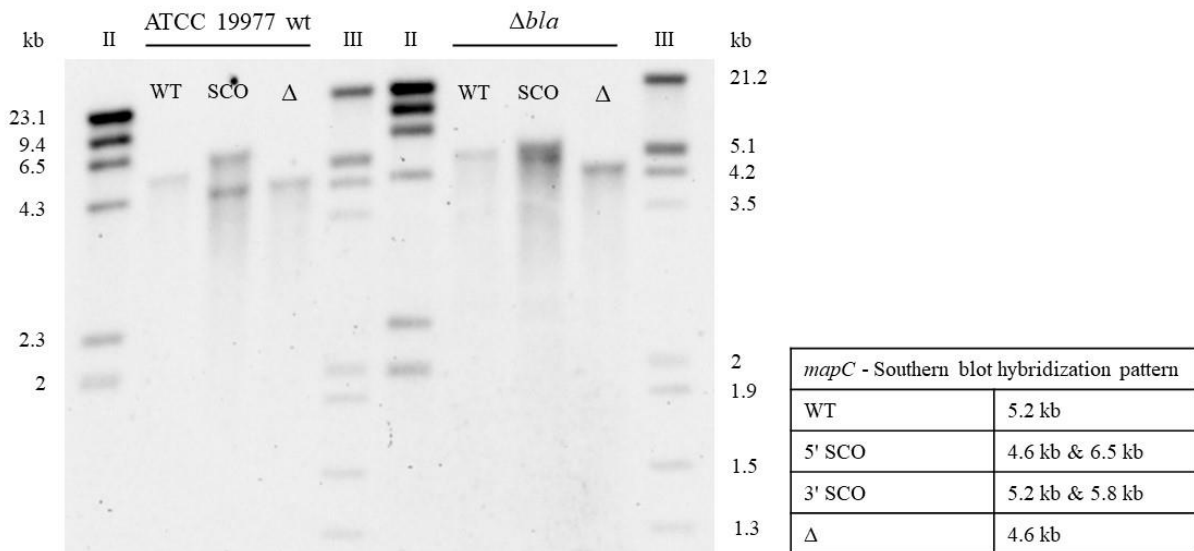
A



B



C



D

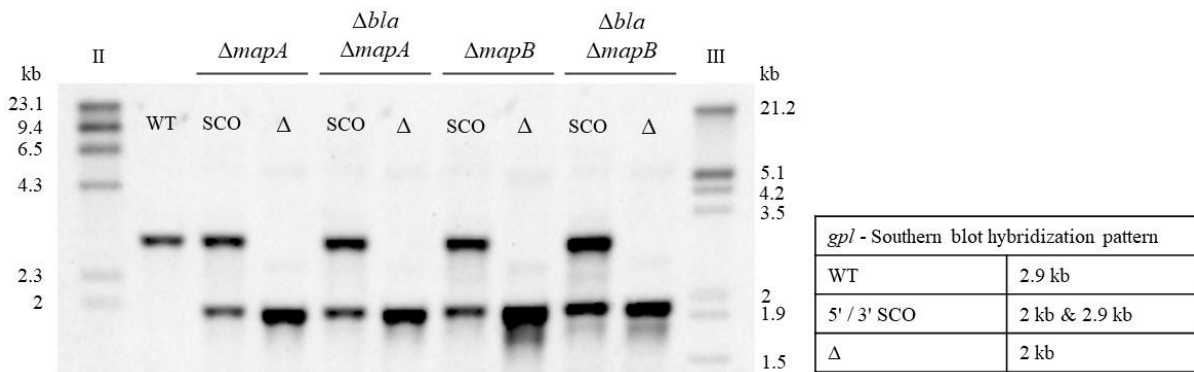


Figure 2 | Genotypic analyses of porin and glycopeptidolipid mutants of *M. abscessus*.

(A) Generation of unmarked gene deletion of the general diffusion porin *mapA* in *M. abscessus* ATCC 19977 strain and *M. abscessus* Δ *bla* mutant. Deletion of *mapA* in *M. abscessus* was confirmed by Southern blot analysis of BamHI digested genomic DNA with a 5' *mapA* probe. The hybridization fragments from the wildtype control (WT, expected size of 3.1 kb), the strain harboring the integrated pKH- Δ *mapA* suicide vector as obtained after site-specific homologous recombination (3' SCO, expected sizes of 3.1 kb and 5.7 kb) and the *mapA* deletion mutant (Δ , expected size of 2.4 kb) for *M. abscessus* ATCC 19977 and *M. abscessus* Δ *bla* strains, are shown. **(B)** Generation of unmarked gene deletion of the general diffusion porin *mapB* in *M. abscessus* ATCC 19977 strain and *M. abscessus* Δ *bla* mutant. Deletion of *mapB* in *M. abscessus* was verified by Southern blot analysis of BamHI digested genomic DNA with a 3' *mapB* probe. The hybridization fragments from the wildtype control, the strain containing the integrated suicide vector pKH- Δ *mapB* and the *mapB* deletion mutant for *M. abscessus* ATCC 19977 and *M. abscessus* Δ *bla* strains, are shown. The expected sizes of the hybridization fragments for wildtype/ 5' or 3' single crossover/ mutant are as follows: 3.4 kb/ 3.4 kb and 6.2 kb or 3.7 kb and 8 kb/ 5.8 kb. The two bands observed in strains containing the integrated suicide vector correspond to the expected sizes of fragments for 5' single crossover in *M. abscessus* ATCC 19977 strain and for 3' single crossover in *M. abscessus* Δ *bla* strain. **(C)** Generation of unmarked gene deletion of the general diffusion porin *mapC* in *M. abscessus* ATCC 19977 strain and *M. abscessus* Δ *bla* mutant. Deletion of *mapC* in *M. abscessus* was confirmed by Southern blot analysis of BamHI digested genomic DNA with a 5' *mapC* probe. For *M. abscessus* ATCC 19977 and *M. abscessus* Δ *bla* strains, the hybridization fragments from the wildtype control, the strain containing the integrated pKH- Δ *mapC* suicide vector and the *mapC* deletion mutant are shown. The expected sizes of the hybridization fragments for wildtype/ 5' or 3' single crossover/ mutant are as follows: 5.2 kb/ 4.6 kb and 6.5 kb or 5.2 kb and 5.8 kb/ 4.6 kb. In strains containing the integrated suicide vector, the observed bands correspond to the expected sizes of fragments for 5' single crossover in *M. abscessus* ATCC 19977 strain and for 3' single crossover in *M. abscessus* Δ *bla* strain. **(D)** Targeted deletion of *mps1*, *mps2* and *gap*, clustered on the distal end of the *gpl* locus and encoding components used for the production and transport of GPL, in *M. abscessus*. Deletion of this cluster in *M. abscessus* mutants including *M. abscessus* Δ *mapA*, *M. abscessus* Δ *bla* Δ *mapA*, *M. abscessus* Δ *mapB* and *M. abscessus* Δ *bla* Δ *mapB*, was confirmed by Southern blot analysis of Van91I digested genomic DNA with a 5' *gpl* probe. The hybridization fragments from the strain containing the integrated pKH- Δ *gpl* suicide vector (expected sizes of 2 kb and 2.9 kb) and the *gpl* deletion mutant (expected size of 2 kb) for *M. abscessus* Δ *mapA*, *M. abscessus* Δ *bla* Δ *mapA*, *M. abscessus* Δ *mapB* and *M. abscessus* Δ *bla* Δ *mapB* strains and from the *M. abscessus* ATCC 19977 wildtype control (expected size of 2.9 kb) are shown.

Starting with wildtype *M. abscessus* or a strain lacking either *mapA* or *mapB* gene, our efforts to generate *mapA mapB* double mutant using this genetic approach (see the methods section) were unsuccessful. This suggests that the loss of both porins likely leads to severe loss of bacterial fitness.

MapA and MapB porins from *M. abscessus* form hetero-oligomers in *M. smegmatis*

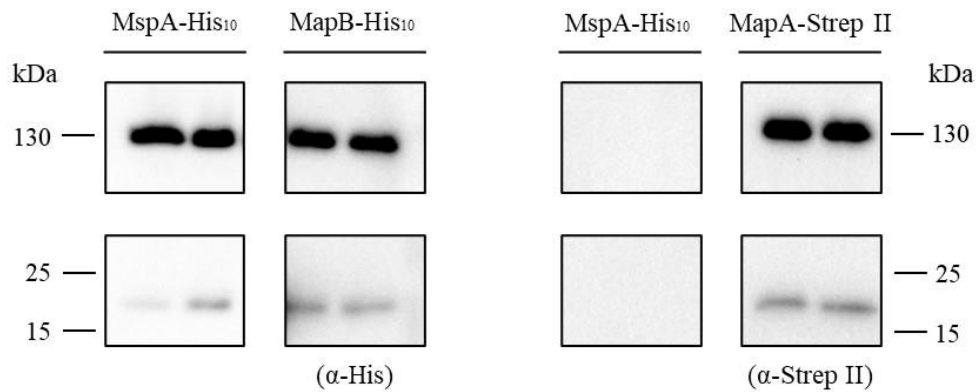
In Gram-negative bacteria, the β -barrel assembly machinery complex is responsible for the final assembly of porins as functional trimers into the outer membrane⁴⁷ and a stable interaction with LPS is also required for porin biogenesis⁴⁸, in contrast, how β -barrel transmembrane proteins are assembled into the outer membrane of mycobacteria remains to be understood.

The major porin MspA from *M. smegmatis* contains eight polypeptide subunits that constitute a tightly interconnected homo-octamer with a goblet-like conformation and a single channel²³. Moreover, *M. smegmatis* also contains two other very closely related isomers, MspB and MspC, that differ in only 2 and 4 positions, respectively, from MspA²³ and this observation renders the natural existence of hetero-oligomeric Msp porins in *M. smegmatis* very likely. In fact, the formation of hetero-oligomers of MspA was demonstrated in *M. smegmatis* strain ML16 that lacks the three porin genes *mspA*, *mspC* and *mspD*, respectively, by expression of MspA proteins with different affinity tags⁴⁹. Like in *M. smegmatis*, the MspA orthologues MapA and MapB of *M. abscessus* are two very closely related proteins with only three exchange positions and can possibly form hetero-oligomeric porins.

To address this, the *mapA* gene fused to a C-terminal Strep-tag II and the *mapB* gene fused to a His₁₀-tag at its C-terminus, were expressed in *M. smegmatis* mc² 155 strain using a single expression vector harboring a mycobacterial origin of replication and the strong acetamide inducible promoter to allow a controlled, high-level expression of proteins⁵⁰. In addition, the wildtype *mspA* gene with a C-terminal His₁₀-tag was expressed in *M. smegmatis* using the pACE vector⁵⁰. To examine the expression of tagged porins in the outer membrane of *M. smegmatis*, we employed a selective extraction procedure for Msp-type porins which mainly yields MspA when *M. smegmatis* whole cells are heated to 100 °C in the presence of 0.5% octyl-POE²⁹. The detection of tagged proteins in these selective extracts by Western blot experiments using anti-His-tag and anti-Strep-tag II antibodies demonstrated that all three proteins were produced in *M. smegmatis*, although at levels not detectable in Coomassie Brilliant Blue-stained polyacrylamide gels (not shown). The oligomer was clearly observed in detergent extracts for both MapA and MapB proteins, as the major band in Western blot experiments indicating that these *M. abscessus* proteins were mainly produced as oligomers that were stable enough to resist dissociation and denaturation at 100 °C for 30 min during extraction out of *M. smegmatis* (FIG. 3a). As expected, the major part of the tagged MspA protein in selective extracts of *M. smegmatis* was observed as oligomer in these experiments (FIG. 3a). The MapB protein was selectively purified from these detergent extracts using Ni²⁺-NTA chromatography via the C-terminal His₁₀-tag. After purification, both the oligomer and the monomer of MapB protein were observed as clear bands in a Western blot experiment using anti-His-tag antibody (FIG. 3b). Furthermore, the detection of the oligomer but not the monomer of purified MapB protein by Western blot analysis using anti-Strep-tag II antibody demonstrated that MapA (with a C-terminal Strep-tag II) was copurified with MapB (FIG. 3b). This observation indicates that

the oligomers formed by *M. abscessus* MapA and MapB in the mycomembrane of *M. smegmatis* are heterogeneous in composition.

A



B

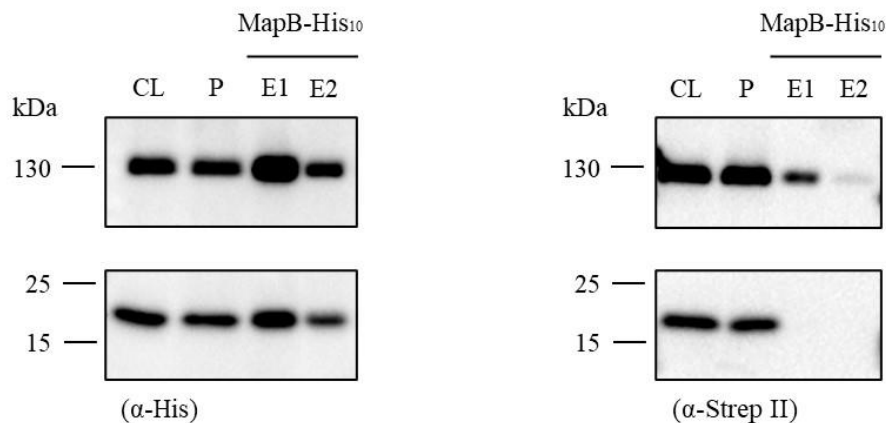


Figure 3 | Expression and preparation of *M. abscessus* general porins in *M. smegmatis*.

(A) Detection of the *M. smegmatis* general porin MspA and the MapA and MapB porins from *M. abscessus*, expressed as tagged proteins with a C-terminally fused His₁₀-tag or Strep-tag II, from the replicative pACE expression vector in *M. smegmatis* mc²155 strain. The MspA-like porins were selectively extracted by heating *M. smegmatis* whole cells to 100 °C in a buffer containing 0.5% octyl-POE. The detergent extracts were separated on a 10% polyacrylamide gel and MspA-His₁₀ and MapB-His₁₀ proteins were detected by Western blotting using anti-His-tag antibody (shown in left panel). The right panel shows the production of MapA-Strep II protein in selective extracts of *M. smegmatis*, visualized by Western blot analysis using anti-Strep-tag II antibody. The two bands observed for MspA-His₁₀, MapB-His₁₀ (left panel) and MapA-Strep II (right panel) correspond to oligomer (upper band at around 130 kDa) and monomer (lower band between 15 and 25 kDa). The expression vector pACE-MspA served as a positive control. (B) Production of hetero-oligomers of *M. abscessus* MapA and MapB in *M. smegmatis*. The MapB-His₁₀ protein was selectively purified from detergent extracts using Ni²⁺-NTA chromatography via the C-terminally fused His₁₀-tag. Samples from *M. smegmatis* whole cell extract (CL), the buffer containing total protein after precipitation with acetone (P) and the two fractions eluting from Ni²⁺-NTA chromatography (E1 and E2) were separated by SDS-PAGE and MapB-His₁₀ was detected by Western blotting using anti-His-tag antibody (shown in left panel). The two bands

observed for MapB-His₁₀ in fractions eluting from Ni²⁺-NTA chromatography, correspond to oligomer (upper band at around 130 kDa) and monomer (lower band between 15 and 25 kDa). The right panel shows the same series of protein samples separated by SDS-PAGE and analysed by Western blotting using anti-Strep-tag II antibody for detection of hetero-oligomer production. The single band observed for MapA-Strep II in fractions obtained after Ni²⁺-NTA purification of MapB-His₁₀, corresponds to the expected size of the MapB-His₁₀ oligomer. Samples from *M. smegmatis* detergent extracts and the buffer containing total protein after precipitation with acetone included in the analysis, served as positive controls.

β-Lactam susceptibility of *M. abscessus* strains

To decipher the influence of distinct mechanisms of mycomembrane modification (i.e. a lack of general diffusion porins and/ or an altered glycopeptidolipid phenotype) on the antibiotic influx process and to discern the contribution of reduced mycomembrane permeability alone or in combination with enzymatic degradation (i.e. basal or overexpression of periplasmic β-lactamase) on the antibacterial susceptibility of *M. abscessus* towards β-lactams, we determined the susceptibilities of *M. abscessus* strains toward a variety of β-lactams, including a cephalosporin (cefotaxime), carbapenems (imipenem, meropenem, doripenem, biapenem and ertapenem) and a penem (faropenem) in minimal inhibitory concentration (MIC) assays. The MICs were determined in Cation-Adjusted Müller-Hinton Broth by visual inspection of bacterial growth after 3, 5, 7 and 12 days of incubation. The median MIC values read on day 5 are shown in Tables 3 and 4. The median MIC values determined at all time points are listed in Table S2.

The Bla_{Mab} enzyme is able to hydrolyse, at least to some extent, all tested β-lactams as inferred from drug MIC values for β-lactamase-null and β-lactamase-overexpressing strains of *M. abscessus* (*M. abscessus* Δ*bla* and *M. abscessus* Δ*bla* pOLYG-*bla* strains; see Table 4) and from the data available concerning Bla_{Mab} kinetic parameters for most of these antibiotics³⁷.

The disruption of the *mapA* gene, which encodes a MspA-type general diffusion porin, in *M. abscessus* ATCC 19977 strain showing constitutive expression of the chromosomal Ambler class A β-lactamase Bla_{Mab} at a low level, provided a decrease in carbapenem susceptibility (FIG. 4a). For *M. abscessus* Δ*mapA* strain, small increases (up to 2- to 4-fold) in MICs were observed for all carbapenems while the level of susceptibility to cefotaxime and faropenem was unaltered compared with *M. abscessus* wildtype strain. In contrast, *M. abscessus* showing a lack of either MapB or MapC porin (other orthologues of *M. smegmatis* MspA) was unaltered in its susceptibility to all β-lactam compounds (no observed change in MICs compared with *M. abscessus* wildtype strain). These observations suggest that there is a differential β-lactam susceptibility among these *M. abscessus* porins.

Table 3. MIC values of deletion mutants that exhibit porin loss and/or an altered glycopeptidolipid phenotype compared to wildtype *M. abscessus* (median, day 5) ^{a,b}

Compound	<i>M. abscessus</i> strain						
	Wildtype	$\Delta mapA$	$\Delta mapB$	$\Delta mapC$	Δgpl	$\Delta mapA \Delta gpl$	$\Delta mapB \Delta gpl$
	Day 5 MIC (mg/L)						
Cefotaxime	32	32	32	32	128	512	256
Imipenem	16	64	16	16	16	64	16
Meropenem	32	64	32	32	32	128	64
Doripenem	16	64	16	16	16	128	32
Biapenem	64	128	64	64	64	256	128
Ertapenem	128	512	128	128	128	512	256
Faropenem	32	32	32	32	64	256	128

^a A complete overview of MIC results evaluated on days 3, 5, 7 and 12 is provided in Table S2

^b Carbapenem susceptibility phenotype of *mapA*-null strain carrying the complementation vector pMV361-*mapA* or the empty vector pMV361 as a control is also reported in Table S2

Table 4. MIC values of deletion mutants that exhibit porin loss together with lack of β -lactamase activity compared to *M. abscessus* Δbla strain (median, day 5) ^{a,b,c}

Compound	<i>M. abscessus</i> strain							
	Δbla	Δbla pOLYG- <i>bla</i>	Δbla pOLYG	$\Delta bla \Delta mapA$	$\Delta bla \Delta mapA$ pOLYG- <i>bla</i>	$\Delta bla \Delta mapA$ pOLYG	$\Delta bla \Delta mapB$	$\Delta bla \Delta mapC$
	Day 5 MIC (mg/L)							
Cefotaxime	16	128	16	16	128	16	16	16
Imipenem	4	32	8	4	256	8	4	4
Meropenem	4	256	4	4	256	8	4	4
Doripenem	4	128	4	4	512	8	4	4
Biapenem	8	128	16	8	256	16	8	8
Ertapenem	8	512	16	32	1024	32	16	8
Faropenem	8	64	16	8	256	16	8	8

^a MIC data of *M. abscessus bla* mutant and *M. abscessus bla mapA* double mutant carrying the complementation plasmid pOLYG-*bla* or the empty plasmid pOLYG as a control is also reported in Table 4

^b A complete overview of MIC results evaluated on days 3, 5, 7 and 12 is provided in Table S2

^c β -Lactam susceptibility phenotype of rough variants of β -lactamase-null strains that either exhibit normal porin expression (*M. abscessus* $\Delta bla \Delta gpl$) or show an altered porin phenotype (*M. abscessus* $\Delta bla \Delta mapA \Delta gpl$ and *M. abscessus* $\Delta bla \Delta mapB \Delta gpl$) is also reported in Table S2

Notably, no change in susceptibility to various β -lactams, including imipenem, meropenem, doripenem, biapenem, cefotaxime and faropenem, was observed following the loss of MapA in *M. abscessus* Δbla strain showing a lack of β -lactamase activity (FIG. 4b). Likewise, the β -lactamase-null *M. abscessus* $\Delta bla \Delta mapB$ strain that lacked MapB porin also showed an unaltered susceptibility to these β -lactams (no observed change in MICs compared with *M. abscessus* Δbla strain). The data showed small increases (up to 2- to 4-fold) in MICs for only ertapenem in these two β -lactamase-null *M. abscessus* porin mutants compared with the parental strain *M. abscessus* Δbla . Similarly, no change in β -lactam susceptibility was observed following the disruption of *mapC* gene in *M. abscessus* Δbla strain. These findings suggest that the relationship between an altered porin phenotype (porin loss) and the level of β -lactam susceptibility in *M. abscessus* seems to be associated with β -lactamase expression.

The *M. abscessus* wildtype strain, owing to its constitutive expression of the β -lactamase Bla_{Mab}, displayed high levels of resistance to certain carbapenems including meropenem, biapenem and ertapenem (as evidenced by 8- to 16-fold higher MICs) and low to intermediate resistance to other β -lactams (up to 2- to 4-fold higher MICs) compared with *M. abscessus* Δbla strain. A sequential step that involved a modification of the porin profile of *M. abscessus* wildtype strain by disruption of the MapA-encoding gene resulted in further reduced susceptibility and large increases (up to 16- to 64-fold) in MICs were observed for all carbapenems in the resulting *M. abscessus* $\Delta mapA$ strain compared with the susceptibility that was observed in *M. abscessus* Δbla strain (FIG. 5a). These observations are in agreement with the notion that in porin-deficient strains the effect of hydrolysing β -lactamase activity on the overall susceptibility to a β -lactam is strongly reinforced by reduced outer membrane permeability.

To further support this notion as well as to test an alternative hypothesis that high levels of β -lactamase activity (owing to Bla_{Mab} overproduction) can amplify the effect of porin alteration on β -lactam susceptibility of *M. abscessus*, the *bla* gene was overexpressed in β -lactamase-null *M. abscessus* strains that either exhibit normal expression of wildtype MapA (i.e. *M. abscessus* Δbla) or show an altered porin phenotype (i.e. *M. abscessus* $\Delta bla \Delta mapA$) and β -lactam susceptibilities of the corresponding strains were determined. To achieve constitutive expression of β -lactamase at a high level, the operon containing Bla_{Mab}-encoding gene was expressed in *M. abscessus* Δbla and *M. abscessus* $\Delta bla \Delta mapA$ strains using the mycobacterial replicative vector pOLYG-*apr*⁵¹. Amplification of the *bla* gene with its native promoter on a

replicating plasmid can confer higher production levels than the basal expression level observed in *M. abscessus* wildtype strain.

As expected, a strong decrease in susceptibility to all antibiotics was observed in β -lactamase-overproducing *M. abscessus* Δbla pOLYG-*bla* strain as evidenced by 8- to 64-fold higher MICs for carbapenems and 8-fold higher MICs for both cefotaxime and faropenem compared with *M. abscessus* Δbla strain. Importantly, the level of susceptibility to β -lactams observed in *M. abscessus* wildtype strain showing basal β -lactamase expression, was higher than the susceptibility that was observed in *M. abscessus* Δbla pOLYG-*bla* strain. Furthermore, *M. abscessus* exhibiting β -lactamase overexpression displayed the highest level of resistance after the loss of a general porin. In this regard, significantly large increases (up to 32- to 128-fold) in MICs were observed for certain carbapenems, including biapenem, imipenem, doripenem and ertapenem as well as for the β -lactam faropenem (up to 32-fold) in the *M. abscessus* Δbla $\Delta mapA$ pOLYG-*bla* strain compared with *M. abscessus* Δbla strain (FIG. 5b). These and previous observations suggest that the hydrolytic activity of β -lactamase can cause much higher levels of β -lactam resistance in *M. abscessus* strains that exhibit porin defects (i.e. *M. abscessus* $\Delta mapA$ and *M. abscessus* Δbla $\Delta mapA$ pOLYG-*bla* strains), especially when the enzyme is overexpressed.

Notably, we found that the different levels of resistance to certain β -lactams conferred by the loss of the same porin in *M. abscessus* strains correlate with differences in the levels of β -lactamase expressed by these strains. In this connection, the β -lactamase-overproducing *M. abscessus* Δbla $\Delta mapA$ pOLYG-*bla* strain that lacked MapA porin, exhibited higher resistance to imipenem and faropenem as evidenced by 8- and 4-fold higher MICs compared with *M. abscessus* Δbla pOLYG-*bla* strain (FIG. 6b). In contrast, the loss of MapA in *M. abscessus* wildtype strain showing basal β -lactamase expression, led to a smaller increase in the MIC for imipenem (up to 4-fold) while susceptibility to faropenem was unaltered (FIG. 6a). Taken together, the notion that there exists a cooperativity between the two mechanisms — porin alteration and hydrolytic β -lactamase activity during resistance, is strongly supported by these findings.

Given that specific interactions between membrane proteins and lipids are increasingly prominent in cell biology, we sought to explore whether the total loss of GPL (a change that enables *M. abscessus* to transition from a smooth to a rough variant) has an impact upon the integral membrane proteins embedded in the mycomembrane, especially those involved in

antibiotic transport (i.e. general porins). For this purpose, we determined and analysed the β -lactam susceptibilities of smooth and rough *M. abscessus* variants that harbour an altered porin phenotype with or without Bla_{Mab} enzyme activity. The rough strains exhibit a lack of GPL expression owing to the disruption of three genes of the *gpl* cluster i.e. *mps1*, *mps2* and *gap* that encode protein components of the GPL biosynthesis and transport machinery, respectively. It was observed that for specific β -lactams, the decrease in susceptibility following the loss of a general porin (MapA or MapB) was more pronounced in a GPL-null rough *M. abscessus* strain than in the corresponding smooth strain showing expression of surface-exposed GPL. The MapA-null *M. abscessus* $\Delta mapA \Delta gpl$ strain, devoid of its surface-exposed GPL, was found to be less susceptible to specific carbapenems including meropenem, biapenem and doripenem (as evidenced by 4- to 8-fold higher MICs compared with *M. abscessus* wildtype strain) compared with the susceptibility that was observed for these antibiotics in GPL-expressing *M. abscessus* $\Delta mapA$ strain showing a lack of the same porin (up to 2- to 4-fold higher MICs compared with *M. abscessus* wildtype strain). Moreover, the *M. abscessus* $\Delta mapA \Delta gpl$ strain also displayed increased resistance to faropenem and cefotaxime (up to 8- to 16-fold higher MICs compared with *M. abscessus* wildtype strain) whereas the susceptibility to these antibiotics was unaltered in the *M. abscessus* $\Delta mapA$ strain (no observed change in MICs compared with *M. abscessus* wildtype strain) (FIG. 7b, c). Likewise, a reduced susceptibility to specific compounds, including meropenem, doripenem, biapenem, ertapenem, faropenem and cefotaxime was detected in the GPL-null *M. abscessus* $\Delta mapB \Delta gpl$ strain that lacked MapB porin (as evidenced by 2- to 8-fold higher MICs compared with *M. abscessus* wildtype strain) whereas the MapB-null smooth *M. abscessus* variant i.e. *M. abscessus* $\Delta mapB$ was unaltered in its susceptibility to these antibiotics compared with *M. abscessus* wildtype strain (FIG. 7d, e). Notably, no change in susceptibility to all carbapenems was observed following the loss of only surface-exposed GPL in *M. abscessus* wildtype strain. However, the data showed small increases (up to 2- to 4-fold) in MICs for faropenem and cefotaxime in *M. abscessus* Δgpl strain compared with *M. abscessus* wildtype strain (FIG. 7a).

It is of particular interest that in terms of antibiotic susceptibility, the phenotype conferred by the combined loss of GPL and porin in *M. abscessus* is different from the phenotype that is observed when only one membrane component, either porin or GPL, is missing. Individually, both porin (either MapA or MapB) and GPL loss either decrease or do not alter the susceptibility of *M. abscessus* to specific β -lactams (FIG. 7a, b, d). However, when both factors are missing, the susceptibility of the cells to these antibiotics is reduced further (FIG. 7c, e).

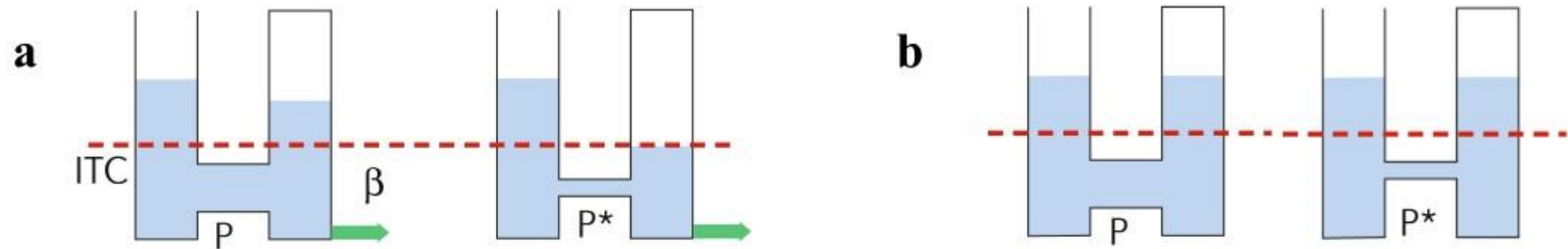
This phenotype can be explained by a proposal that suggests that specific interactions with surface-exposed GPL, the most abundant free lipids in smooth *M. abscessus*, guide the folding and insertion of porins into the mycomembrane and the absence of GPL in a rough variant is associated with a reduced incorporation of porins into the bilayer, a situation that may produce a decrease in susceptibility to small hydrophilic β -lactams (for which non-specific porin channels serve as their main entry pathway into the cell) owing to a decrease in membrane permeability. So, this model, if correct, predicts that owing to the disruption of a porin-encoding gene together with defects in GPL-mediated porin biogenesis, both *M. abscessus* $\Delta mapA$ Δgpl and $\Delta mapB$ Δgpl strains harbour lower levels of porins than found in the corresponding smooth strains in which a general porin is missing (i.e. *M. abscessus* $\Delta mapA$ and $\Delta mapB$) or in a rough strain in which the GPL-dependent porin assembly is defective (i.e. *M. abscessus* Δgpl). This notion may explain the observed effects on susceptibility to specific β -lactams in these mutants. However, direct evidence (for instance, by mutagenesis and structural studies) providing support for a specific molecular interaction between GPL and mycobacterial porin and whether binding to GPL has a direct influence on biogenesis of porins *in vivo*, is currently lacking.

Discussion

The low permeability of the mycobacterial cell envelope plays a major role in the well-known intrinsic resistance of *M. abscessus* to a wide variety of antibiotics. We examined, in this study, the role of limiting factors (i.e. β -barrel proteins that function as porins and surface-exposed GPL) in regulating β -lactam transport across the mycomembrane and the impact of changes in cell envelope composition with or without the presence of a specific mechanism involved in β -lactam removal (i.e. deactivation by periplasmic β -lactamase) on the antibacterial susceptibility of *M. abscessus* toward a representative set of compounds from three different β -lactam subclasses (i.e. cephalosporins, carbapenems and a penem). This was accomplished through a series of gene knockouts (obtained via two-step homologous recombination) and by the determination of minimal inhibitory concentrations of antibiotics for all *M. abscessus* strains.

Three orthologues of MspA, which is the dominant porin in *M. smegmatis*, are encoded on the *M. abscessus* genome. Here, we chose to focus on the closely related MspA homologues from *M. abscessus*, namely, MapA and MapB, which are two very similar proteins that share ~98% amino acid sequence similarity. Interestingly, a differential antibiotic susceptibility was detected in strains of *M. abscessus* lacking either MapA or MapB porin. The level of susceptibility to carbapenems, including imipenem, meropenem, doripenem, biapenem and ertapenem, was decreased in *M. abscessus* $\Delta mapA$ strain that was devoid of the porin MapA (as evidenced by 2- to 4-fold higher MICs compared with *M. abscessus* wildtype strain) (FIG. 4a, lower panel). However, a strain exhibiting MapB loss i.e. *M. abscessus* $\Delta mapB$ was as susceptible to these antibiotics as the *M. abscessus* wildtype strain. The simplest explanation for this observation is that among these two non-specific porins of *M. abscessus*, MapA is likely synthesized at high levels and therefore plays a major role in the transport of most β -lactams. In contrast, the porin MapB seems to have only a minor role in β -lactam resistance presumably due to a reduced level of expression in *M. abscessus*.

Strikingly, the decreased susceptibility to various carbapenems (including imipenem, meropenem, doripenem and biapenem) conferred by the *mapA* mutant, was suppressed by the disruption of the Bla_{Mab} -encoding gene in *M. abscessus*. This observation can be explained by the fact that the transport of hydrophilic toxic molecules such as β -lactams across the outer membrane mainly occurs by passive diffusion through porins. Consequently, the level of antibiotic accumulation in the periplasm will eventually approach the external level regardless of the magnitude of the diffusion rate, in the absence of a mechanism for removal of incoming



Strain	ATCC 19977 wildtype	$\Delta mapA$
β -Lactam	MIC (mg/L) [^a Fold change]	
Imipenem	16	64 (4-fold)
Meropenem	32	64 (2-fold)
Doripenem	16	64 (4-fold)
Biapenem	64	128 (2-fold)
Ertapenem	128	512 (4-fold)

^aFold change in MIC compared to *M. abscessus* wildtype strain

Δbla	$\Delta bla \Delta mapA$
MIC (mg/L) [^b Fold change]	
4	4
4	4
4	4
8	8
8	32 (4-fold)

^bFold change in MIC compared to *M. abscessus* Δbla strain

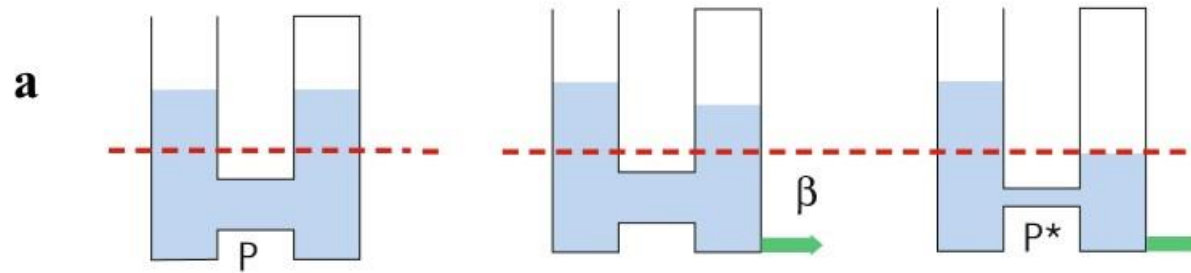
Figure 4 | **Loss of *M. abscessus* MapA porin correlates with carbapenem resistance that is also associated with β -lactamase production.** The transport of β -lactams through the outer membrane via a porin is shown. The larger channel (P) joining the surrounding medium (left column) and the periplasm (right column) represents normal synthesis of wildtype porin while an altered porin phenotype (porin loss) is represented by the smaller channel (P*). A β -lactamase expressed in the periplasm cleaves β -lactams and is represented by the green arrow (β). The critical intracellular concentration required for target inhibition is

CHAPTER 1

denoted by a red dashed line (part **a**, upper panel). The decreased periplasmic accumulation of the drug in porin-deficient cells is closely related to the activity of the β -lactamase enzyme. The two limiting factors cooperate to reduce the intracellular concentration of active β -lactams (part **a**, upper panel). Genetic analysis reveals a functional connection between MapA and Bla_{Mab}, as a *mapA*-null mutant renders *M. abscessus* more resistant to various β -lactams only when the mutant strain carries a functional *bla* gene (part **a**, lower panel). Because the transport of β -lactam molecules through porins is driven by passive diffusion and is a relatively fast event, the accumulation level in the periplasm approaches that in the surrounding medium unless the drug is inactivated by hydrolysing enzymes (or extruded directly into the external medium by tripartite efflux systems) (part **b**, upper panel). This would explain why the loss of Bla_{Mab} reverses a resistance phenotype for many carbapenems caused by the lack of MapA in *M. abscessus* (part **b**, lower panel). In parts **a**, **b** in the figure, the image in the upper panel is reproduced from Vergalli, J. et al. (REF.⁵³).

antibiotic molecules (for instance, by enzymatic degradation and/or an efflux pump activity) from the periplasmic space^{20,52,53}. Importantly, permeation of antibiotics across bacterial membranes through porins occurs relatively rapidly and steady state accumulation levels are generally reached after 5-15 min of incubation as previously reported for antibiotics of different classes⁵⁴. This phenomenon is thought to occur in *M. abscessus* $\Delta bla \Delta mapA$ strain owing to its lack of expression of the chromosomally encoded β -lactamase Bla_{Mab}, a hydrolysing enzyme located in the periplasmic space that facilitates the rapid addition of a water molecule across the common β -lactam bond, leading to the generation of a microbiologically ineffective ring-opened antibiotic⁵³. This would explain why an association between the absence of MapA and reduced carbapenem susceptibility that was observed in *M. abscessus mapA* mutant, was not detected in *M. abscessus bla mapA* double mutant (FIG. 4b).

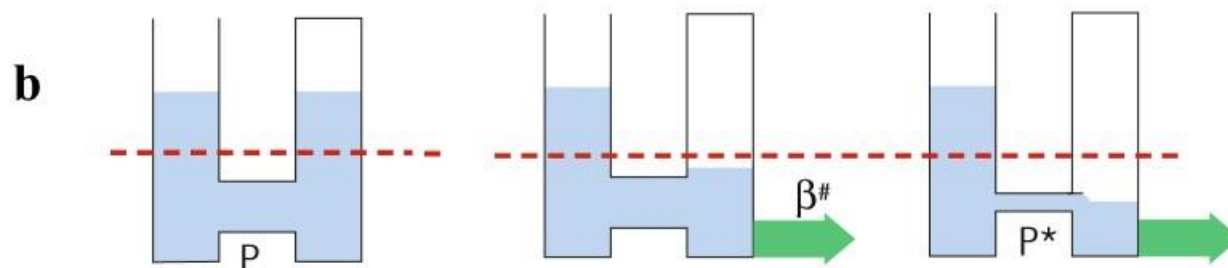
By contrast, we interpret the reduced carbapenem susceptibility of *M. abscessus* $\Delta mapA$ strain to mean that this phenotype results from a functional interaction between two key factors - porin deficiency (owing to *mapA* gene disruption) and hydrolytic β -lactamase activity. The loss of the MapA porin is thought to decrease the permeability of the mycomembrane, leading to reduced periplasmic accumulation of the antibiotic, which correlates with the resistance phenotype. Importantly, this decrease in the periplasmic antibiotic level is also associated with β -lactamase production^{20,52,53}. This simple model may explain the reduced susceptibility conferred by the *mapA* mutant to specific β -lactams in the β -lactamase-expressing *M. abscessus* strain (FIG. 4a). These results leave little doubt that the relationship between an altered porin phenotype (porin loss) and the level of β -lactam susceptibility in *M. abscessus* is associated with β -lactamase expression. This finding is consistent with the mounting recent evidence for the prevalence of these well-combined resistance strategies in key Gram-negative clinical pathogens such as *Escherichia coli*, *Enterobacter cloacae*, *Enterobacter aerogenes*, *Klebsiella pneumoniae*, *Salmonella enterica* subsp. *enterica* serovar Typhimurium and *Pseudomonas aeruginosa*^{52,53}. In various collections of antibiotic-resistant Enterobacteriaceae clinical isolates, an altered porin phenotype [a decrease in porin expression or the mutational loss of the major porins, porin exchange (OmpF, which has a large channel size, is substituted by the smaller OmpC channel) or a mutation that perturbs the transverse electric field at and close to the pore constriction area] is often found to be associated with overexpression of multidrug efflux pumps and the production of various β -lactamases; these mechanisms synergistically contribute to reduce the intracellular accumulation of active β -lactams, which leads to bacterial survival and therapeutic failure^{52,53,55-57}.



Strain	Δbla	$\Delta bla \Delta mapA$	ATCC 19977 wildtype	$\Delta mapA$
β -Lactam	MIC (mg/L) [^a Fold change]			
Imipenem	4	4	16 (4-fold)	64 (16-fold)
Meropenem	4	4	32 (8-fold)	64 (16-fold)
Doripenem	4	4	16 (4-fold)	64 (16-fold)
Biapenem	8	8	64 (8-fold)	128 (16-fold)
Ertapenem	8	32 (4-fold)	128 (16-fold)	512 (64-fold)

^aFold change in MIC compared to *M. abscessus* Δbla strain

MIC



Strain	Δbla	$\Delta bla \Delta mapA$	Δbla pOLYG- <i>bla</i>	$\Delta bla \Delta mapA$ pOLYG- <i>bla</i>
β -Lactam	MIC (mg/L) [^a Fold change]			
Imipenem	4	4	32 (8-fold)	256 (64-fold)
Doripenem	4	4	128 (32-fold)	512 (128-fold)
Biapenem	8	8	128 (16-fold)	256 (32-fold)
Ertapenem	8	32 (4-fold)	512 (64-fold)	1024 (128-fold)
Faropenem	8	8	64 (8-fold)	256 (32-fold)

Δbla pOLYG	$\Delta bla \Delta mapA$ pOLYG
MIC (mg/L)	
8	8
4	8
16	16
16	32
16	16

^aFold change in MIC compared to *M. abscessus* Δbla strain



Figure 5 | The effect of Bla_{Mab} activity on β -lactam susceptibility of *M. abscessus* is enhanced by knocking out *mapA*.

Shows that the activity of the Bla_{Mab} β -lactamase can produce much higher levels of β -lactam resistance in *M. abscessus* strains that exhibit porin defects (i.e. *M. abscessus* Δ mapA and *M. abscessus* Δ bla Δ mapA pOLYG-bla strains), especially when the enzyme is overexpressed. A simple schematic of the mechanistic model that accounts for this phenomenon is shown at the top of the figure. The thickness of the green arrows reflects the level of β -lactamase expression. The thin arrow (β) corresponds to basal expression and the thick arrow ($\beta\#$) represents overproduction of the enzyme (parts **a**, **b**, upper panel). Wildtype *M. abscessus*, owing to its constitutive expression of the β -lactamase Bla_{Mab}, exhibits a decrease in carbapenem susceptibility (up to 4- to 16-fold higher MICs compared with *M. abscessus* Δ bla strain). A sequential step that involves a modification of the porin profile of wildtype *M. abscessus* by disruption of the MapA-encoding gene results in further reduced susceptibility to these antibiotics. Accordingly, large increases (up to 16- to 64-fold) in MICs are observed for all carbapenems in *M. abscessus* Δ mapA strain compared with the susceptibility that is observed in *M. abscessus* Δ bla strain (part **a**, lower panel). Overexpression of bla into a bla-null strain causes a drastic reduction in β -lactam susceptibility. Accordingly, *M. abscessus* Δ bla pOLYG-bla strain shows both reduced faropenem susceptibility (up to 8-fold higher MIC) and carbapenem (imipenem, biapenem, doripenem and ertapenem) resistance (up to 8- to 64-fold higher MICs) compared with *M. abscessus* Δ bla strain. The lack of MapA in a β -lactamase-overexpressing *M. abscessus* strain results in the highest level of resistance. In this regard, significantly large increases (up to 32- to 128-fold) in MICs are observed for carbapenems, including biapenem, imipenem, doripenem and ertapenem as well as for faropenem (up to 32-fold) in *M. abscessus* Δ bla Δ mapA pOLYG-bla strain compared with *M. abscessus* Δ bla strain (part **b**, lower panel). In parts **a**, **b** in the figure, the image in the upper panel is reproduced from Vergalli, J. et al. (REF.⁵³).

The decrease in susceptibility to all carbapenems caused by basal β -lactamase production in *M. abscessus* wildtype strain was less pronounced (up to 4- to 16-fold higher MICs compared with *M. abscessus* Δbla strain) than that conferred by Bla_{Mab} (at basal expression level) in *M. abscessus* $\Delta mapA$ strain (as evidenced by 16- to 64-fold higher MICs compared with *M. abscessus* Δbla strain) (FIG. 5a, lower panel). Similarly, when Bla_{Mab} was overexpressed in a β -lactamase-null *M. abscessus* strain that showed a reduction in outer membrane porin levels caused by total loss of the MapA porin (i.e. *M. abscessus* $\Delta bla \Delta mapA$ pOLYG-*bla* strain), susceptibility to specific β -lactams was severely decreased (as evidenced by 32- to 128-fold higher MICs for carbapenems including biapenem, imipenem, doripenem and ertapenem and 32-fold higher MIC for the β -lactam faropenem compared with *M. abscessus* Δbla strain) (FIG. 5b, lower panel). By contrast, the decrease in susceptibility to these agents conferred by the enzyme, when synthesized at the same level, in a β -lactamase-null *M. abscessus* strain that exhibited normal porin expression (i.e. *M. abscessus* Δbla pOLYG-*bla* strain), was less pronounced (up to 8- to 64-fold higher MICs for carbapenems including imipenem, biapenem, doripenem and ertapenem and 8-fold higher MIC for the β -lactam faropenem compared with *M. abscessus* Δbla strain) (FIG. 5b, lower panel). From these results it can be concluded that the overall effect of *mapA* gene disruption caused the Bla_{Mab} enzyme to become more efficient in hydrolysing certain β -lactams, thereby conferring high levels of resistance to these compounds in the producing *M. abscessus* strains. This finding is consistent with the expectation that since steady-state concentrations of β -lactams in the periplasmic space are determined by antibiotic influx and removal rates, it is likely that in porin-deficient cells the resulting level of antibiotic accumulation in the periplasm is below the saturation level of the enzyme (especially when reduced permeability is combined with high-levels of β -lactamase activity due to increased expression), which increases the efficiency of the enzyme and makes the system far more effective in producing resistance under these conditions^{20,53}.

In this connection, a combination of an effective permeability barrier and multidrug efflux transporters, especially the three component efflux complexes belonging to resistance-nodulation-division (RND) superfamily of H⁺-drug antiporters, which extrude drugs directly into the external medium rather than into the periplasm, results in synergistic enhancement of resistance towards various antibiotics in Gram-negative bacteria^{20,54}. In RND-type tripartite efflux systems, a complex consisting of an inner membrane transporter (such as AcrB of *E. coli* and MexB of *P. aeruginosa*), a periplasmic accessory protein (such as AcrA of *E. coli* and MexA of *P. aeruginosa*) and an outer membrane channel (such as TolC of *E. coli* and OprM of

P. aeruginosa) forms a continuous channel opening into the surrounding medium for extrusion of antibiotic molecules from the periplasm that have either penetrated through the outer membrane or have been pumped out from the cytoplasm by simple transporters^{20,54,58}. Some RND transporters can handle a wide variety of substrates. AcrB transporter from *E. coli* was shown to pump out a wide range of antibiotics (such as macrolides, β -lactams, tetracyclines and chloramphenicol), detergents (such as SDS and Triton X-100), dyes (such as ethidium bromide, acriflavine and crystal violet), bile acids and solvents, substrates that are unrelated not only in physical properties but also in chemical structure^{20,54}.

Notably, in mycobacteria, the transport of a large and diverse repertoire of lipid species to the mycomembrane is mediated by several MmpL transporters that belong to the RND family of proteins. Genes encoding MmpL proteins are diverse and widely distributed in *M. abscessus*⁴¹. For example, the *mmpS4-mmpL4a-mmpL4b* system of *M. abscessus* codes not only for two RND-type transporters, MmpL4a and MmpL4b, that are involved in GPL transport across the inner membrane⁵⁹, but also for MmpS4, a membrane protein that is proposed to facilitate the assembly of the GPL biogenesis and export machinery megacomplex⁶⁰. It has been suggested that the role of MmpS4 is to function as an accessory protein (similarly to the periplasmic adaptor protein found in tripartite efflux systems of Gram-negative bacteria) that likely forms a complex with a channel protein in the mycomembrane^{41,60}. How GPL are transported across the periplasm to the outer mycomembrane remains elusive. Importantly, emerging evidence has indicated that *M. abscessus* deploys MmpL-derived efflux pump systems to transport drugs across the mycomembrane to the extracellular environment^{41,61-63}. Various point mutations in MAB_2299c, encoding a TetR transcriptional regulator that was able to repress the expression of two *M. abscessus* MmpS-MmpL efflux pumps (MAB_2300-2301 and MAB_1135c-1134c), were uncovered by whole-genome sequencing in *in vitro*-selected clofazimine-resistant strains that also showed cross-resistance to bedaquiline. The expression of both efflux systems was upregulated in *M. abscessus* strains that expressed variants of MAB_2299c, owing to loss of DNA-binding activity of this regulatory protein. Consequently, drug efflux was increased, thereby conferring resistance to clofazimine and bedaquiline in these strains^{61,62}. Similarly, mutations in the TetR-encoding gene MAB_4384, a regulatory protein of a MmpS5-MmpL5 complex efflux pump expression, were associated with resistance to thiacetazone analogues in *M. abscessus*⁶³. However, so far, there is no strong evidence to suggest the involvement of this type of efflux activity in β -lactam resistance in *M. abscessus*.

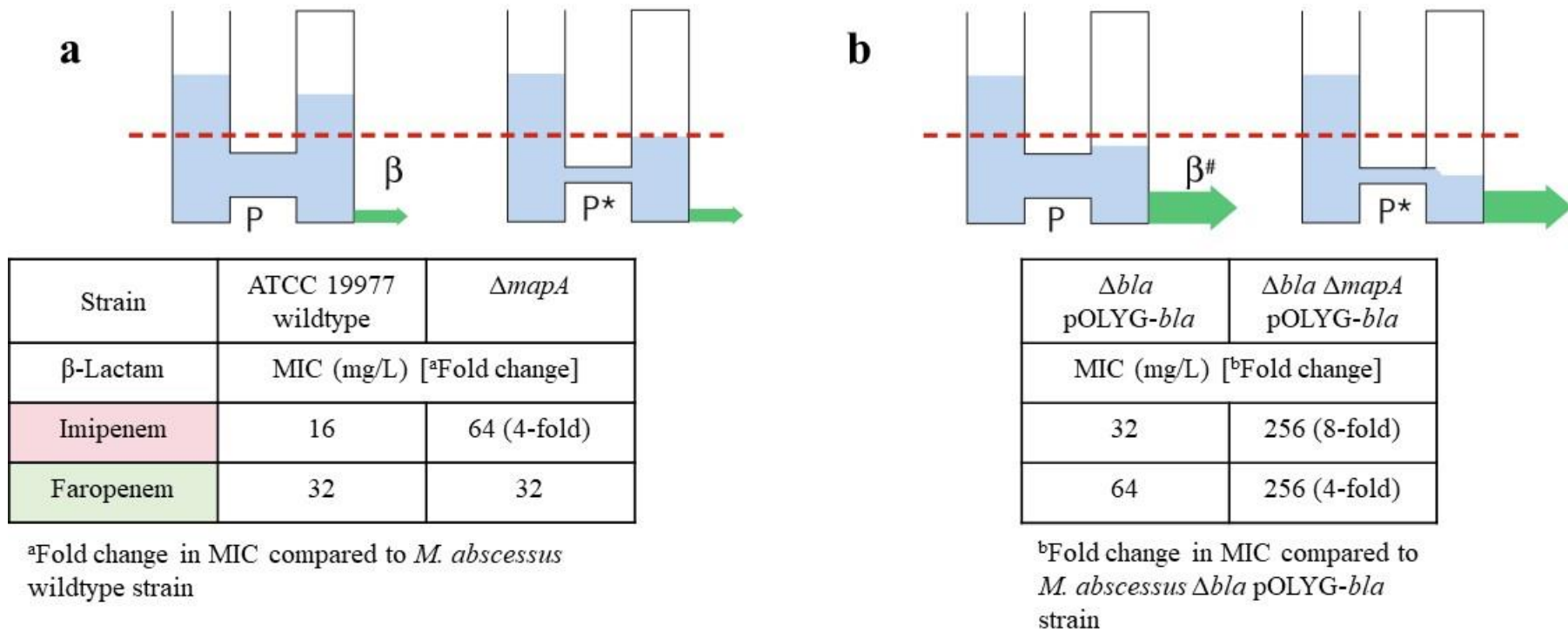


Figure 6 | *M. abscessus* strains that are altered in the levels of Bla_{MapA} , show different levels of resistance to β -lactams following the loss of MapA. In this connection, the β -lactamase-overproducing *M. abscessus* $\Delta bla \Delta mapA$ pOLYG-*bla* strain that is devoid of MapA, exhibits increased levels of resistance to imipenem and faropenem as evidenced by 8- and 4-fold higher MICs compared with *M. abscessus* Δbla pOLYG-*bla* strain (part b, lower panel). By contrast, when *mapA* gene is inactivated in the wildtype strain of *M. abscessus* expressing Bla_{MapA} at a low level, a small increase (up to 4-fold) in MIC for imipenem is observed. Notably, *M. abscessus* $\Delta mapA$ strain is as susceptible as *M. abscessus* wildtype strain to faropenem (part a, lower panel). A simple schematic of the mechanistic model that accounts for this phenomenon is shown at the top of the figure. Shows how the limiting factors (porins and β -lactamases) act in concert, rather than in isolation, to control the antibiotic accumulation level inside bacterial cells (parts a, b, upper panel). In parts a, b in the figure, the image in the upper panel is reproduced from Vergalli, J. et al. (REF.⁵³).

Furthermore, we discovered that *M. abscessus* strains that were altered in the levels of the β -lactamase, showed different levels of resistance to β -lactams following the loss of MapA. In this connection, the β -lactamase-overproducing *M. abscessus* $\Delta bla \Delta mapA$ pOLYG-*bla* strain that lacked MapA, showed increased levels of resistance to imipenem and faropenem as evidenced by 8- and 4-fold higher MICs compared with *M. abscessus* Δbla pOLYG-*bla* strain (FIG. 6b, lower panel). By contrast, when *mapA* gene was inactivated in the wildtype strain of *M. abscessus* that expressed Bla_{Mab} at a low level, a small increase (up to 4-fold) in MIC for imipenem was detected. Notably, *M. abscessus* $\Delta mapA$ strain was as susceptible as *M. abscessus* wildtype strain to faropenem (FIG. 6a, lower panel). The different levels of resistance can be explained by the synergy between the outer membrane barrier and the enzymatic barrier due to β -lactamase. As the concentration of active antibiotic in the periplasm is a consequence of the balance between the rate of influx and the rate of removal, reducing the number of porins in the outer membrane is likely to cause a drastic reduction in the intracellular accumulation of β -lactams when these molecules are removed rapidly from the periplasmic space (as a result of high levels of β -lactamase activity). When hydrolysis occurs rapidly, the outer membrane barrier acts as a limiting factor in the overall deactivation of β -lactams by the periplasmic enzyme, and thus reduced outer membrane permeability has strong effect on MIC. In contrast, the deficiency of porins is unlikely to have a substantial effect on the internal antibiotic level and on MIC when drug removal from the periplasm occurs at a slow rate^{20,64}.

Regarding β -lactam susceptibility, it was observed that the loss of a porin (either MapA or MapB) in a GPL-producing *M. abscessus* strain resulted in milder phenotypes than those caused by the lack of the same porin in a strain that was devoid of GPL (FIG. 7b, c, d and e, lower panel). This observation can be explained by a model which proposes that specific interactions between porins and GPL, the most abundant free lipids that form the outer leaflet of the mycomembrane in smooth *M. abscessus*, possibly help to drive the biogenesis of porins at the mycomembrane and one crucial consequence of the absence of GPL in a rough variant is the decrease in porin incorporation into the bilayer, a scenario that may produce a decrease in susceptibility to small hydrophilic β -lactams (that mainly enter the cell through non-specific porin channels) owing to a decrease in membrane permeability. This concept can be rationalized by the fact that gram-negative bacterial porins contain specific binding sites for lipopolysaccharide (LPS), the main component of the outer membrane barrier function, that allow them to stabilize, rather than perturb, the ordered structure of LPS monolayer and maintain its impermeability⁴⁸. A decrease in porin production was detected in the LPS mutants

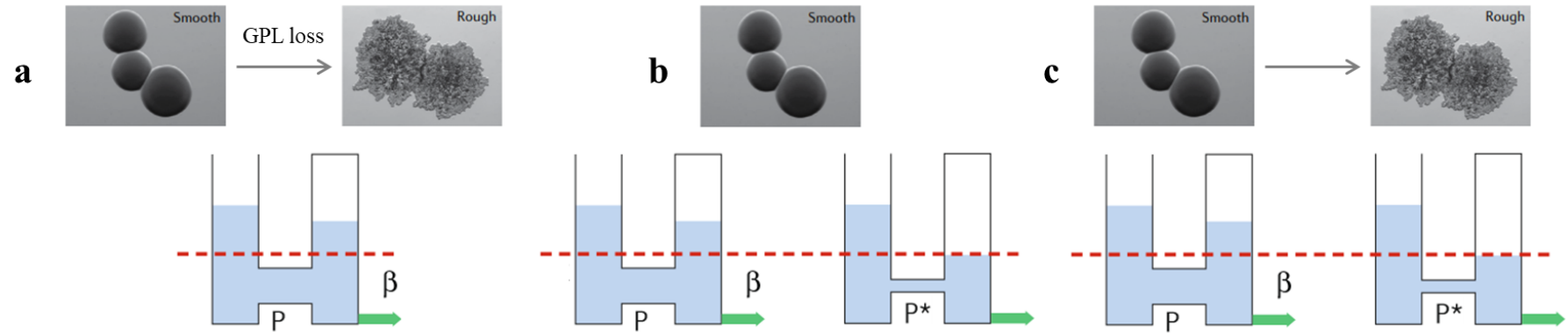
of *Salmonella typhimurium* and *Escherichia coli* (i.e. the so-called ‘deep rough’ mutants) that produce a core oligosaccharide of very incomplete structure containing only KDO (3-deoxy-D-manno-oct-2-ulosonic acid) residues or KDO and one or two heptose residues. The LPS mutants exhibited increased susceptibility to hydrophobic compounds, a characteristic that was associated with increased outer membrane permeability. The reduction in outer membrane protein (OMP) levels caused by LPS alteration in the deep rough mutants, causes a disruption of the bilayer’s asymmetry by allowing phospholipids to flip to the external leaflet of the outer membrane. The presence of phospholipids that were shown to be distributed in patches in the external leaflet of the outer membrane of these mutants (as mixing of phospholipids and LPS is thermodynamically unfavourable), has direct consequences for the translocation of hydrophobic compounds, as such molecules can easily permeate through the phospholipid bilayer regions of this modified outer membrane. This would explain why the susceptibility to lipophilic compounds is increased in these mutants⁶⁵⁻⁷¹.

It has been conclusively demonstrated experimentally by mutagenesis and structural studies (X-ray and neutron scattering) that a stable interaction with LPS is essential for successful assembly of porin trimers *in vivo*⁴⁸. This would explain why a defect in LPS structure results in reduced incorporation of porins into the outer membrane of deep rough mutants, as such porin-LPS interactions could not possibly occur properly with the deep rough LPS owing to its very incomplete structure. Using the solved crystal structure of *Enterobacter cloacae* porin OmpE36 with bound LPS and by mutation of residues in two potential LPS binding sites on OmpF porin of *E. coli* that were predicted using the structure of LPS-OMP complex solved for FhuA, the siderophore transporter from *E. coli*, Arunmanee *et al.*⁴⁸ found that there were two specific LPS binding sites per porin monomer and that the presence of one site (designated LPS B site) was required for the biogenesis of trimers *in vivo* in the outer membrane. In Gram-negative bacteria, the β -barrel assembly machinery (BAM) complex at the outer membrane, is responsible for the assembly of most OMPs. The nascent OMPs are stabilized by periplasmic chaperones such as Skp and SurA and delivered to components of the BAM complex for folding and insertion into the outer membrane via a mechanism that remains poorly understood⁴⁷. As OmpF also binds LPS via the LPS B site on the protein and this binding is required for the maturation of trimer *in vivo*, it has been postulated that the OmpF-LPS B association stabilizes an intermediate during the formation of trimeric OmpF in the outer membrane by the BAM complex, however, this notion remains to be demonstrated experimentally⁴⁸.

Mounting evidence indicates a strong interaction of the nonpolar outer surface of the β -barrels of porin MspA with components of the outer membrane in *M. smegmatis*. The hydrophobic β -barrels of MspA are bound by large amounts of membrane lipids even after extensive purification, as demonstrated by infrared spectroscopy. Addition of 2% SDS did not dissociate the bound lipids from MspA and these lipids were only partially removed by acetone precipitation⁷², implying the presence of a tight association between lipids and the membrane-exposed hydrophobic surface of MspA. A study performed to examine the membrane topology of MspA by cysteine scanning mutagenesis, showed that the residues on the outer surface of the two β -barrels that form the hydrophobic stem domain, were highly protected from modification by a membrane-impermeable compound *in vitro*, although nearly all of these residues were predicted as accessible from the crystal structure²⁹. This suggests that other molecules cover the external surface of the hydrophobic β -barrel domain and protect it from labeling. This notion is supported by the close association of lipids with the membrane-facing hydrophobic stem domain as observed in preparations of native MspA from *M. smegmatis* outer membrane if lipids are not removed intentionally⁷². Furthermore, Heinz *et al.*⁷² found that purified MspA was less protected against thermal denaturation compared to MspA in detergent extracts of *M. smegmatis* (for instance, only MspA octamer was detectable in octyl-POE extracts after heating *M. smegmatis* cells to 100 °C for 30 min, in contrast, the monomer was already observed after incubation of purified MspA at 80 °C for 15 min). This observation may be explained by the existence of a stabilizing molecule that was removed in the course of purification. As the octyl-POE extracts of *M. smegmatis*, contained only small amounts of proteins other than MspA, the associated lipids, that were removed by precipitation with acetone during purification, are thought to increase the stability of MspA.

The important observations made for MspA of *M. smegmatis*, which is the best studied mycobacterial porin and what is known about the role of LPS in the biogenesis of β -barrel membrane proteins in Gram-negative negative bacteria, align with our proposed idea that MspA-like general porins specifically interact with GPL in the external leaflet of the mycomembrane and that the assembly of these OMPs *in vivo* in the mycomembrane requires GPL binding. However, experimental verification is certainly necessary to fully test this model. The proposed model, if correct, predicts that a reduced incorporation of general porins (possibly MapB and MapC) linked to the absence of GPL in rough *M. abscessus* $\Delta mapA \Delta gpl$ strain that is devoid of MapA, results in further decreased influx, which correlates with increased resistance to various carbapenems, including meropenem, biapenem and doripenem

CHAPTER 1

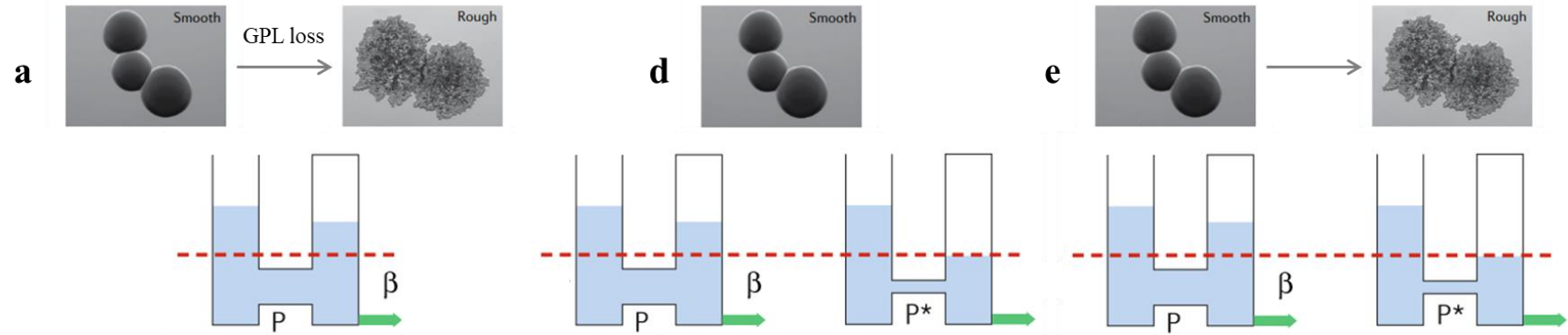


Strain	ATCC 19977 wildtype	Δgpl
β -Lactam	MIC (mg/L) [^a Fold change]	
Cefotaxime	32	128 (4-fold)
Imipenem	16	16
Meropenem	32	32
Doripenem	16	16
Biapenem	64	64
Ertapenem	128	128
Faropenem	32	64 (2-fold)

ATCC 19977 wildtype	$\Delta mapA$
MIC (mg/L) [^b Fold change]	
32	32
16	64 (4-fold)
32	64 (2-fold)
16	64 (4-fold)
64	128 (2-fold)
128	512 (4-fold)
32	32

ATCC 19977 wildtype	$\Delta mapA \Delta gpl$
MIC (mg/L) [^c Fold change]	
32	512 (16-fold)
16	64 (4-fold)
32	128 (4-fold)
16	128 (8-fold)
64	256 (4-fold)
128	512 (4-fold)
32	256 (8-fold)

^{a,b,c}Fold change in MIC compared to *M. abscessus* wildtype strain



Strain	ATCC 19977 wildtype	Δgpl
β -Lactam	MIC (mg/L) [^a Fold change]	
Cefotaxime	32	128 (4-fold)
Imipenem	16	16
Meropenem	32	32
Doripenem	16	16
Biapenem	64	64
Ertapenem	128	128
Faropenem	32	64 (2-fold)

ATCC 19977 wildtype	$\Delta mapB$
MIC (mg/L) [^b Fold change]	
32	32
16	16
32	32
16	16
64	64
128	128
32	32

ATCC 19977 wildtype	$\Delta mapB \Delta gpl$
MIC (mg/L) [^c Fold change]	
32	256 (8-fold)
16	16
32	64 (2-fold)
16	32 (2-fold)
64	128 (2-fold)
128	256 (2-fold)
32	128 (4-fold)

^{a,b,c}Fold change in MIC compared to *M. abscessus* wildtype strain

Figure 7 | Smooth and rough variants of *M. abscessus* lacking the same porin differ in their susceptibility to various β -lactams.

Shows that in terms of antibiotic susceptibility, the phenotype conferred by the combined loss of GPL and porin in *M. abscessus* is different from the phenotype that is observed when only one membrane component, either porin or GPL, is missing. Individually, both porin and GPL loss either decrease or do not alter the

CHAPTER 1

susceptibility of *M. abscessus* to specific β -lactams (**bold**) (parts **a**, **b**, **d**). However, when both factors are missing, the susceptibility of the cells to these antibiotics is reduced further (parts **c**, **e**). In parts **a-e** in the figure, the images in the upper panel are reproduced from REFS^{41, 53}.

(as evidenced by 4- to 8-fold higher MICs) as well as other β -lactams, including faropenem and cefotaxime (up to 8- to 16-fold higher MICs) (FIG. 7c, lower panel). By contrast, the MapA-null smooth *M. abscessus* variant (i.e. *M. abscessus* $\Delta mapA$) that exhibits normal GPL-dependent biogenesis of remaining general porins, is less resistant to carbapenems, including meropenem, biapenem and doripenem (up to 2- to 4-fold higher MICs) and unaltered in its susceptibility to other β -lactams, including faropenem and cefotaxime (FIG. 7b, lower panel). Furthermore, we propose that the low- to intermediate-resistance to various β -lactams, including meropenem, doripenem, biapenem, ertapenem and faropenem (as evidenced by 2- to 4-fold higher MICs) and a strong decrease in susceptibility to cefotaxime (up to 8-fold higher MIC) observed in rough *M. abscessus* $\Delta mapB \Delta gpl$ strain that lacks MapB, is caused by a similar reduction in levels of general porins (possibly MapA and MapC) (FIG. 7e, lower panel). It is conceivable that this decrease is more pronounced in porin species which are more abundant in the mycomembrane than MapB (possibly MapA) given that the MapB-null smooth *M. abscessus* variant (i.e. *M. abscessus* $\Delta mapB$) is unaltered in its susceptibility to these antibiotics (FIG. 7d, lower panel). Moreover, small increases in MICs for faropenem and cefotaxime (up to 2- to 4-fold) and unaltered susceptibility to all carbapenems observed in *M. abscessus* Δgpl strain, favour the hypothesis that the loss of GPL alone causes only mild defects in porin biogenesis and membrane permeability (FIG. 7a, lower panel).

Taken together, the genetic approach that we used in this study, was useful to identify different types of factors related to drug molecule influx or degradation that influence β -lactam susceptibility of *M. abscessus* and to show how sets of genes act in concert, rather than in isolation, to elicit bacterial resistance to antibiotics. Through a better understanding of how the alteration of mycomembrane permeability elicits bacterial resistance, we might be able to develop new means to overcome the ‘impermeability’ resistance mechanism in an effort to fight highly resistant *M. abscessus* infections.

Materials and Methods

Bacterial strains and growth conditions

The *E. coli* XL1-Blue strain was used for cloning of gene deletion and complementation constructs, and of open reading frames (ORFs) into expression vectors. For liquid cultures, Luria Broth (LB) was used, and for plates, Luria Broth Agar (LB-Agar) was used. Antibiotics were used in the following concentrations for *E. coli*: apramycin 50 mg/L, chloramphenicol 25 mg/L. The deletion mutants and complementation strains were generated in the *M. abscessus* ATCC 19977 strain. The *M. smegmatis* strain mc²155 was used for expression and preparation of *M. abscessus* porins in *M. smegmatis*. 7H9 supplemented with OADC was used for liquid cultures, and 7H10 with OADC supplement or LB-Agar was used for plates. Antibiotics were used in the following concentrations for *M. abscessus*: apramycin 50 mg/L, isoniazid 32 mg/L. Apramycin was used in a concentration of 25 mg/L for *M. smegmatis*. Bacteria were grown by incubation at 37 °C.

Electrocompetent cells of *M. abscessus* were prepared as described previously⁴⁶. In brief, 2x 200 ml 7H9 cultures were inoculated 1:100 with precultures of *M. abscessus* and grown at 37 °C. When the cells reached an optical density (A_{600}) of around 0.4-0.8, cultures were cooled for 90 min on ice. All further steps were performed on ice and with ice-cold 10% glycerol. Cells were then harvested, washed repeatedly by resuspending in 10% glycerol while the suspension volume was gradually decreased and, in the end, resuspended in 2 ml of 10% glycerol. Cells were flash-frozen in liquid nitrogen and stored at -80 °C until use.

Cloning of flanking regions into a mycobacterial suicide vector by high-fidelity (HiFi) DNA assembly

For the generation of gene deletions in *M. abscessus* via two-step recombination, the upstream and downstream homology sequences flanking the target gene, each having a length in the range of 1.3 to 1.5 kb, were PCR amplified from *M. abscessus* genomic DNA. To amplify flanking regions, Q5 DNA polymerase (NEB) and PCR primers, each containing at its 5' end a 15-25 nucleotide overlap sequence between the adjacent DNA fragments, designed with the NEBuilder assembly tool (nebuilder.neb.com), were used. The mycobacterial suicide vector pKH-*apr-dsred2-katG* was linearized by digestion with MunI and PvuI and the entire overlap sequence included in the forward primer for the upstream flanking region and the reverse primer for the downstream flanking region originated from the vector sequence. Restriction enzyme digested vector and PCR fragments were gel-purified. The PCR fragments containing

upstream and downstream homology sequences, flanked by 15-25 nt overlaps, were subsequently cloned into MunI and PvuI digested pKH-*apr-dsred2-katG* vector in a single step according to the HiFi DNA assembly protocol recommended for assembly of 2-3 fragments, with a modification⁵⁰. In brief, 50-100 ng of MunI/PvuI cut pKH-*apr-dsred2-katG* vector was mixed with the PCR fragments to a final molar ratio of 1:2 (vector:insert) and the reaction volume was adjusted to 10 μ l with water. The total amount of all DNA fragments in the assembly reaction was 0.03-0.2 pmols. After addition of 10 μ l of 2X NEBuilder HiFi DNA assembly master mix (NEB), the reaction mixture was incubated at 50 °C for 60 minutes. The assembly reaction time was increased to 1 h instead of 15 minutes, recommended when assembling 1 or 2 fragments into a vector. A 1 μ l aliquot of the reaction mixture was transformed into 60 μ l electrocompetent *E. coli* XL1-Blue cells. Aliquots were plated on LB-agar supplemented with 50 mg/L apramycin and colonies were obtained after overnight incubation at 37 °C. Analytical restriction digests were performed to select positive clones carrying the correctly assembled construct resulting in the respective knockout vector and flanking regions were sequenced.

For the deletion of *mapA* (MAB_1080) gene in *M. abscessus* ATCC 19977 strain and Δ *bla* mutant, a 1.5 kb PCR fragment containing the 5' flanking sequence of *mapA* including the first three codons of the ORF was amplified with primers 1080_UP_F (p161) and 1080_UP_R (p162) and a 1.5 kb PCR fragment containing the 3' flanking sequence of *mapA* including the last three codons of the ORF was amplified with primers 1080_DW_F (p163) and 1080_DW_R (p164) using the genomic DNA of *M. abscessus* ATCC 19977 as template. The upstream and downstream flanking regions were subsequently cloned into MunI and PvuI linearized pKH-*apr-dsred2-katG* vector in a single HiFi DNA assembly reaction (for details see above) resulting in the knockout vector pKH- Δ *mapA*.

For the deletion of *mapB* (MAB_1081) gene in *M. abscessus* ATCC 19977 strain and Δ *bla* mutant, a 1.5 kb fragment containing the 5' flanking sequence of *mapB* including the first three codons of the ORF was PCR amplified with primers 1081_UP_F (p165) and 1081_UP_R (p166) and a 1.5 kb fragment containing the 3' flanking sequence of *mapB* including the last three codons of the ORF was PCR amplified with primers 1081_DW_F (p167) and 1081_DW_R (p168) using the genomic DNA of *M. abscessus* ATCC 19977 as template. Subsequent insertion of amplified flanking regions into the pKH-*apr-dsred2-katG* vector digested with MunI and PvuI according to the HiFi DNA assembly protocol, resulted in the knockout vector pKH- Δ *mapB*.

Three different knockout vectors were constructed for the generation of *M. abscessus* $\Delta mapA$ $\Delta mapB$ and Δbla $\Delta mapA$ $\Delta mapB$ mutants. To generate the pKH- $\Delta mapA$ - $\Delta mapB$ vector meant for the deletion of *mapA* and *mapB* genes in *M. abscessus* ATCC 19977 strain and Δbla mutant, the 1.5 kb fragment containing the 5' flanking sequence of *mapA* including the first three codons of the ORF was PCR amplified with primers 1080-1081_UP_F (identical to the forward primer 1080_UP_F, p161) and 1080-1081_UP_R (p169) and the 1.5 kb fragment containing the 3' flanking sequence of *mapB* including the last three codons of the ORF was PCR amplified with primers 1080-1081_DW_F (p170) and 1080-1081_DW_R (identical to the reverse primer 1081_DW_R, p168) using genomic DNA from *M. abscessus* ATCC 19977 strain as template and subsequently cloned into MunI and PvuI digested pKH-*apr-dsred2-katG* vector using the same procedure described above.

To construct the vector pKH- $\Delta mapA$ _N analogous to the pKH- $\Delta mapA$ vector but meant for the deletion of *mapA* in $\Delta mapB$ and Δbla $\Delta mapB$ mutants, the 1.5 kb PCR fragment containing the upstream flanking sequence of *mapA* including the first three codons of the ORF was amplified with primers 1080- Δ 1081_UP_F (p161) and 1080- Δ 1081_UP_R (p162) (identical to the forward and reverse primers 1080_UP_F and 1080_UP_R) from *M. abscessus* ATCC 19977 genomic DNA and a new 1.5 kb PCR fragment containing the downstream flanking sequence of *mapA* including the last three codons of the ORF and encompassing the *mapB* gene knockout region was amplified with primers 1080- Δ 1081_DW_F (p237) and 1080- Δ 1081_DW_R (p238) from the genomic DNA of $\Delta mapB$ mutant. The resulting PCR products were cloned in a single reaction into the pKH-*apr-dsred2-katG* vector digested with MunI and PvuI according to the HiFi DNA assembly protocol to form the knockout vector pKH- $\Delta mapA$ _N.

To delete the *mapB* gene from the genomes of *M. abscessus* $\Delta mapA$ and Δbla $\Delta mapA$ mutants, the vector pKH- $\Delta mapB$ _N was constructed analogously to the vector pKH- $\Delta mapB$ by amplifying a new 1.5 kb PCR fragment containing the 5' flanking sequence of *mapB* including the first three codons of the ORF and encompassing the *mapA* gene deletion region with primers 1081- Δ 1080_UP_F (p239) and 1081- Δ 1080_UP_R (p240) from $\Delta mapA$ genomic DNA and the 1.5 kb PCR fragment containing the 3' flanking sequence of *mapB* including the last three codons of the ORF with primers 1081- Δ 1080_DW_F (p167) and 1081- Δ 1080_DW_R (p168) (identical to the forward and reverse primers 1081_DW_F and 1081_DW_R) using genomic DNA from *M. abscessus* ATCC 19977 strain and subsequently cloning amplified fragments into MunI and PvuI digested pKH-*apr-dsred2-katG* vector in a single HiFi DNA assembly reaction.

For the deletion of *mapC* (MAB_2800) gene in *M. abscessus* ATCC 19977 strain and Δbla mutant, a 1.5 kb fragment containing the 5' flanking sequence of *mapC* including the first 3 codons of the ORF was PCR amplified with primers 2800_UP_F (p171) and 2800_UP_R (p172) and a 1.5 kb fragment containing the 3' flanking sequence of *mapC* including the last 30 codons of the ORF was PCR amplified with primers 2800_DW_F (p173) and 2800_DW_R (p174) using *M. abscessus* ATCC 19977 genomic DNA as template. Subsequent joining of PCR fragments with the *MunI* and *PvuI* linearized pKH-*apr-dsred2-katG* vector fragment in a single reaction by HiFi DNA assembly yielded the knockout vector pKH- $\Delta mapC$.

To delete three adjacent genes *mps1* (MAB_4099c), *mps2* (MAB_4098c) and *gap* (MAB_4097c) of the *gpl* cluster in the *M. abscessus* ATCC 19977 strain and respective deletion mutants ($\Delta mapA$, $\Delta mapB$, Δbla , $\Delta bla \Delta mapA$ and $\Delta bla \Delta mapB$), the pKH- Δgpl vector was generated by amplifying a 1.3 kb PCR fragment containing the 5' flanking region of *mps1* including the first 6 codons of the ORF with primers 4097c-4099c_UP_F (p241) and 4097c-4099c_UP_R (p242) and a 1.4 kb PCR fragment containing the 3' flanking region of *gap* including the last 101 codons of the ORF with primers 4097c-4099c_DW_F (p243) and 4097c-4099c_DW_R (p244) using genomic DNA from *M. abscessus* ATCC 19977 strain as template and subsequently cloning amplified fragments into *MunI* and *PvuI* digested pKH-*apr-dsred2-katG* vector by following the same procedure described above.

Generation of gene deletion mutants in *M. abscessus* with knockout vectors

To generate unmarked gene deletions in *M. abscessus* by homologous recombination, the amplified flanking homology regions of the targeted locus were cloned in a single cloning step into the pKH-*apr-dsred2-katG* suicide vector as described above and the resulting knockout vector was propagated in *E. coli* and subsequently transformed into *M. abscessus* (ATCC 19977 type strain or respective deletion mutant) by electroporation. Approximately 1-2 μg of supercoiled plasmid DNA was mixed with 100 μl of electrocompetent cells, transferred to a pre-chilled electroporation cuvette with 4 mm gap and electroporated in a BioRad Gene pulser II using the following settings: 2.5 kV, 25 μF and 1000 Ohms. After electroporation, cells were resuspended in 900 μl of pre-warmed 7H9 medium (37 °C) and incubated for 5 h at 37 °C with constant shaking (1000 rpm). Appropriate dilutions were subsequently spread on LB-agar plates containing apramycin (50 mg/L) and colonies were obtained after 6 days of incubation at 37 °C. Single crossover transformants were selected on apramycin plates and distinguished from background growth by colony fluorescence of red fluorescent protein DsRed2, present on the vector backbone as a fusion gene with the apramycin resistance marker. The red

fluorescence of DsRed2 in single colonies was detected with an ImageQuant LAS 4000 instrument (GE Healthcare). Single red fluorescent colonies were picked, restreaked and screened for vector integration by PCR. Primer pairs were designed to anneal within the upstream and downstream flanking regions and yielded a PCR product corresponding to the target gene (or gene cluster) and another PCR product corresponding to the deleted region only upon plasmid integration in the genome. Positive clones were subjected to counterselection on agar plates containing isoniazid (32 mg/L) and plates were imaged to select single non-fluorescent colonies corresponding to clones in which the second recombination event had occurred. These clones were screened for gene deletion by PCR amplifying the deleted region (with the same primer pair used for identification of single crossover transformants) and the genotype was subsequently confirmed by Southern blot analysis⁴⁶.

In this way, a 0.6 kb region of the *mapA* gene was deleted from the genome in *M. abscessus* ATCC 19977 strain and Δbla mutant, respectively, and the deletion was verified by Southern blot analysis of BamHI digested genomic DNA with a 0.3 kb 5' *mapA* probe, PCR amplified with primers P_1080_F (p231) and P_1080_R (p232). Similarly, the deletion of a 0.6 kb region of the *mapB* gene from the genome in *M. abscessus* ATCC 19977 strain and Δbla mutant, respectively, was confirmed by Southern blot analysis of BamHI digested genomic DNA with a 0.3 kb 3' *mapB* probe, PCR amplified with P_1081_F (p233) and P_1081_R (p234) primers. Likewise, a 0.6 kb region of the *mapC* gene was deleted from the genome in *M. abscessus* ATCC 19977 strain and Δbla mutant, respectively, and the deletion was confirmed by Southern blot analysis of BamHI digested genomic DNA with a 0.3 kb 5' *mapC* probe, PCR amplified with primers P_2800_F (p235) and P_2800_R (p236). Finally, an 18.7 kb region encompassing three adjacent genes (*mps1*, *mps2* and *gap*) of the *gpl* locus, was deleted in the genome in *M. abscessus* ATCC 19977 strain and the following deletion mutants; $\Delta mapA$, $\Delta mapB$, Δbla , $\Delta bla \Delta mapA$ and $\Delta bla \Delta mapB$, respectively, to generate the corresponding rough variants and the deletion was verified by Southern blot analysis of Van91I digested genomic DNA with a 0.3 kb 5' *gpl* probe, PCR amplified with P_4097c-4099c_F (p270) and P_4097c-4099c_R (p271) primers. Probes used for Southern blot were PCR amplified with Q5 DNA polymerase using *M. abscessus* ATCC 19977 genomic DNA as template. Isolation of genomic DNA was performed by phenol/chloroform/isoamyl alcohol extraction as described previously⁵¹.

A 1 kb PCR fragment containing the *mapA* gene was amplified with primers C_1080_F (p208) and C_1080_R (p209) using the genomic DNA of *M. abscessus* ATCC 19977 as template and cloned into KpnI digested pMV361-*apr* vector, an integrative plasmid containing the

mycobacteriophage integrase *int* and *attP* site for chromosomal integration via *attP/attB* recombination, according to the HiFi DNA assembly protocol to form the complementation vector pMV361-*mapA*. The control vector pMV361-*apr* or the complementation vector pMV361-*mapA* was transformed into *M. abscessus* Δ *mapA* mutant and integrants were obtained by positive selection on apramycin plates. The presence of the *apr* or the *mapA* gene in the resulting strains was confirmed by colony PCR. To generate the complementation vector pOLYG-*bla*, a 2 kb PCR fragment containing the two adjacent genes, MAB_2874 and MAB_2875 (*bla*), (organized in an operon on the *M. abscessus* chromosome), was amplified from *M. abscessus* ATCC 19977 genomic DNA with C_2874-2875_F (p255) and C_2874-2875_R (p256) primers and cloned into HindIII digested pOLYG-*apr* vector, a replicating multicopy vector that contains a mycobacterial origin of replication (*oriM*), via HiFi DNA assembly. Following electroporation of pOLYG-*bla* complementation vector or pOLYG-*apr* control vector into *M. abscessus* Δ *bla* and Δ *bla* Δ *mapA* mutants, respectively, transformants were selected on agar plates containing apramycin and confirmed by colony PCR. Primers used for cloning of gene deletion and complementation constructs are listed in Supplementary Table S1.

MIC assays

MIC determination for *M. abscessus* strains was carried in a 96-well format by the microdilution method and according to the CLSI guidelines as described previously^{46,51}. β -Lactam antibiotics were purchased from Sigma-Aldrich, Switzerland and stock solutions were prepared by dissolving the antibiotics in H₂O (cefotaxime, imipenem, doripenem, biapenem, ertapenem and faropenem) or DMSO (meropenem) according to the manufacturer's recommendations and stored at -80 °C. One day prior to the conduction of a MIC assay, the stock solution for each antibiotic, was diluted in Cation-Adjusted Müller-Hinton Broth (CAMHB; pH 7.4) (Becton Dickinson, Switzerland) to prepare a working solution at a concentration corresponding to twice the desired final concentration (for example, a working solution of 2048 mg/L was prepared for ertapenem to achieve a maximal concentration of 1024 mg/L in the MIC experiment). Working solutions were stored at -80 °C. For a MIC test in a 96-well format, a 2-fold dilution series of freshly thawed working solutions was prepared using CAMHB to achieve 10 different drug concentrations per row of a sterile 96-well microtiter plate (Greiner Bio-One, Switzerland). A positive growth control lacking the antibiotic and a sterile negative control containing only CAMHB were included in each 96-well microtiter plate. The inoculum was prepared from *M. abscessus* strains grown on LB-agar plates, by

transferring 3-4 colonies of each strain into a glass tube containing 2 ml NaCl with a sterile cotton swab. Bacterial suspensions were adjusted to a McFarland standard of 0.5 (for *M. abscessus* displaying smooth colony morphotype) or 3.0 (for *M. abscessus* displaying rough colony morphotype) and subsequently diluted in CAMHB to obtain a final inoculum titer of $1-5 \times 10^5$ cfu/ml, respectively. For each inoculum, the correct titer was checked by cfu count enumeration on LB-agar plates. After addition of inoculum, yielding a final volume per well of 100 μ l, the plates were sealed with adhesive sealing covers and incubated at 37 °C and MIC values for *M. abscessus* strains were assessed by visual inspection after 3, 5, 7 and 12 days of incubation. For each MIC determination, three biological replicates were determined. MIC assays for all *M. abscessus* smooth variants were performed in triplicate while those for *M. abscessus* rough variants were conducted in duplicate.

Cloning of porin ORFs into mycobacterial expression vectors by fragment-exchange (FX) cloning

A PCR fragment containing the ORF coding for porin MapA fused to a C-terminal Strep-tag II was amplified using primers MapA-Strep II_F (p279) and MapA-Strep II_R (p280) and another PCR fragment containing the ORF coding for MapB porin was amplified using primers MapB_F (p281) and MapB_R (p282) using *M. abscessus* genomic DNA as template. Amplification was performed with Q5 DNA polymerase (NEB) and HiFi DNA assembly compatible primers designed with the NEBuilder assembly tool (nebuilder.neb.com). The ends of PCR amplicons contain homologous overlap regions that result in their insertion into a vector in the desired orientation. The two fragments were cloned into KpnI linearized pMV361-*apr* vector in a single reaction according to the HiFi DNA assembly protocol as described previously. Following transformation of a 1 μ l aliquot of the reaction mixture into electrocompetent *E. coli* XL1-Blue cells, aliquots were plated on LB-agar supplemented with 50 mg/L apramycin and colonies were obtained after overnight incubation at 37 °C. Clones carrying the correctly assembled construct resulting in the vector pMV361-MapA-MapB were selected by restriction digest analysis and ORFs were sequenced.

A fragment containing the ORF coding for MapA fused to a C-terminal Strep-tag II flanked by SapI sites was PCR amplified from pMV361-MapA-MapB using the forward primer INIT_MapA_F (p283) extended on its 5' end by 5'-atatatGCTCTTcAGT(...)-3' and the reverse primer INIT_MapA_R (p287) extended on its 5' end by 5'-tatatatGCTCTTCaAGG(...)-3', where (...) corresponds to the sequence that anneals on the template DNA. A fragment containing the ORF coding for MapB flanked by SapI sites was

PCR amplified from pMV361-MapA-MapB using the forward primer INIT_MapB_F (p289) extended on its 5' end by 5'-atatatGCTCTTCtCCTAGAAAAGGAGGTTAATAATG(...)-3' and the reverse primer INIT_MapB_R (p284) extended on its 5' end by 5'-tatataGCTCTTCaTGC(...)-3'. The forward primer used to amplify MapA ORF and the reverse primer used to amplify MapB ORF were standard FX cloning compatible primers designed with the FX primer tool (www.fxcloning.org). The SapI cleavage sites present in the INIT_MapA_R and INIT_MapB_F primers produce the CCT overhang at the 3' and 5' ends of *mapA* and *mapB* PCR fragments thereby creating a unique ligation site for joining the two fragments. Furthermore, the SapI recognition sites in the two primers are directed in a way so that they are lost after digestion leaving behind only the CCT sequence connecting the two PCR fragments. In addition, the INIT_MapB_F primer adds expression elements including a Shine-Dalgarno sequence (AAGGAGG) (underlined) flanking a start codon (ATG) (bold) to the 5' end of PCR amplified ORF coding for MapB devoid of its start codon and stop codon. A fragment containing the ORF coding for MspA flanked by SapI sites was PCR amplified from *M. smegmatis* genomic DNA using standard FX compatible primers INIT_MspA_F (p285) and INIT_MspA_R (p286).

The purified PCR amplicons were initially cloned into the pINIT-*cat* vector according to the FX protocol⁵⁰ and ORFs were sequenced. The selection of three different types of sequences (AGT, CCT and GCA) as terminal single-stranded overhangs resulting from SapI cleavage of PCR fragments facilitated insertion of ORFs coding for MapA and MapB into the pINIT-*cat* backbone in a fixed orientation. The short three base pair cloning related sequences AGT and GCA added to the 5' and 3' ends of the target ORF result in the addition of single amino acids serine and alanine at the N- and C-termini of the translated protein. For initial cloning of ORFs into the pINIT-*cat* vector, 50-100 ng of pINIT-*cat* vector and 5-fold molar excess of each PCR fragment were mixed with 1 µl of 10x buffer Tango (Thermo Scientific) and the reaction volume was adjusted to 9 µl with water. After addition of 1 µl of SapI (5U) (Thermo Scientific), the mixture was digested for 1 hour at 37 °C. Subsequently, the reaction was incubated at 65 °C for 20 min for heat inactivation of SapI and cooled to 25 °C. For ligation of fragments, 1.25 µl of 10 mM ATP and 1.25 µl of T4 ligase (5 U/µl) (Thermo Scientific) were added to the same reaction and the mixture was incubated for 1 hour at 25 °C. Following heat inactivation of T4 ligase by a 20 min incubation at 65 °C, the ligation mixture was diluted 1:2 with water and a 2 µl aliquot was transformed into 50 µl electrocompetent *E. coli* XL1-Blue cells. Aliquots were plated on LB-agar supplemented with 25 mg/L chloramphenicol and colonies were obtained

after overnight incubation at 37 °C. Subsequent subcloning of ORFs into the FX cloning compatible expression vector pACEC3GH-*apr* was performed according to the FX protocol. In brief, 50-100 ng of pACEC3GH-*apr* vector was mixed with the pINIT-*cat* vector containing the ORF(s) to a final molar ratio of 1:5 (expression vector:pINIT-ORF). The subsequent steps followed were identical to those described above including digestion with SapI followed by ligation and subsequent transformation into *E. coli* XL1-Blue cells. After transformation, aliquots were plated on LB-agar supplemented with 50 mg/L apramycin and colonies were obtained after overnight incubation at 37 °C. Positive clones carrying the pACEC3GH-*apr* construct containing the ORF(s) were selected by restriction digest analysis. In the resulting expression vectors pACE-MapA-MapB-C3GH and pACE-MspA-C3GH, a 3C protease cleavage site, a GFP reporter gene and a His₁₀-tag are fused to the C-termini of the cloned ORFs coding for MapB and MspA, respectively.

Finally, analogous expression constructs devoid of GFP were assembled using HiFi DNA assembly. For the generation of pACE-MapA-MapB, an insert fragment containing the *mapA* gene (fused to a C-terminal Strep-tag II) and the *mapB* gene (fused to a C-terminal 3C cleavage site) downstream of a single acetamide promoter was PCR amplified using primers pACE-MapA-MapB_F (p306) and pACE-MapA-MapB_R (p307) from pACE-MapA-MapB-C3GH vector. For the generation of pACE-MspA, an insert fragment containing the *mspA* gene (fused to a C-terminal 3C cleavage site) downstream of the acetamide promoter was PCR amplified from pACE-MspA-C3GH vector using primers pACE-MspA_F (p306) and pACE-MspA_R (p307). For both constructs, a second insert fragment containing the His₁₀-tag, the apramycin resistance gene and the *oriM* of pACEC3GH-*apr* vector was PCR amplified using His₁₀-Apr-Ori_F (p308) and His₁₀-Apr-Ori_R (p309) primers. The pACEC3GH-*apr* vector backbone was linearized by inverse PCR using pACE-B_F (p310) and pACE-B_R (p311) primers. Amplification was performed with Q5 DNA polymerase (NEB) and HiFi DNA assembly compatible primers designed with the NEBuilder assembly tool (nebuilder.neb.com). The PCR-generated vector and insert fragments share 15-25 nucleotide overlap regions between the adjacent fragments that are required for their assembly. All PCR products were gel-purified. The PCR fragment containing either the *mspA* gene or the *mapA* and *mapB* genes organized into an operon and the PCR fragment containing a His₁₀-tag, an apramycin resistance gene and an *oriM* were assembled into the PCR amplified pACEC3GH-*apr* vector backbone according to the HiFi DNA assembly protocol recommended for assembly of 2-3 fragments. In brief, 50-100 ng of pACEC3GH-*apr* vector fragment was mixed with the respective insert fragments to

a final molar ratio of 1:2 (vector:insert) and the reaction volume was adjusted to 10 μ l with water. The total amount of all DNA fragments in the assembly reaction was 0.03-0.2 pmols. After addition of 10 μ l of 2X NEBuilder HiFi DNA assembly master mix, the reaction mixture was incubated at 50 °C for 60 minutes. Following incubation, 1 μ l of assembled product was transformed into electrocompetent *E. coli* XL1-Blue cells and aliquots were plated on LB-agar supplemented with 50 mg/L apramycin. Positive clones carrying the correctly assembled expression construct were selected based on restriction digest analysis and confirmed by sequencing. In the resulting expression vectors pACE-MapA-MapB and pACE-MspA, the cloned ORFs coding for MapB and MspA, respectively, are fused to a C-terminal 3C cleavage site and a His₁₀-tag. Primers used for cloning of the expression constructs are listed in Supplementary Table S1. About 750 ng of the porin expression plasmid was electroporated into *M. smegmatis*. After electroporation, cells were resuspended in 7H9 medium, incubated for 3.5 h at 37 °C with constant shaking and subsequently spread on LB-agar plates containing appropriate antibiotics. Positive clones containing the expression plasmid were confirmed by colony PCR.

Expression and extraction of *M. abscessus* porins from *M. smegmatis*

The *mapA* gene fused to a C-terminal Strep-tag II and the *mapB* gene fused to a His₁₀-tag at its C-terminus, were expressed in *M. smegmatis* mc² 155 strain using the pACE-MapA-MapB vector. In addition, the wildtype *mspA* gene with a C-terminal His₁₀-tag was expressed in *M. smegmatis* using the pACE-MspA vector. *M. smegmatis* containing the respective expression plasmid was grown in 10 ml 7H9 medium supplemented with apramycin. Cultures were grown at 37 °C while shaking, until they reached an A_{600} of around 0.6. Protein expression was then induced by addition of 0.4% (w/v) acetamide and cells were grown at 37 °C overnight. To examine the expression of tagged porins in the outer membrane of *M. smegmatis*, a selective extraction procedure for Msp-type porins was used²⁹. Briefly, 4 ml of cells were harvested in 5 ml tubes and washed two times with 4 ml of ice-cold PBS buffer (100 mM NaH₂PO₄/Na₂HPO₄ pH 7, 150 mM NaCl, 0.1 mM Na₂EDTA, 0.05% (w/v) Tween 80). After washing with PBS, cells were resuspended in 100 mM NaH₂PO₄/Na₂HPO₄ pH 6.5, 150 mM NaCl, 0.1 mM Na₂EDTA, 0.5% (w/v) *N*-octyl-POE to obtain a cell density of 10 mg of cells (wet weight)/35 μ l, and heated to 100 °C while stirring in a water bath for 30 min. The suspension was cooled for 10 min on ice and spun 15 min at 4 °C at 14'000 rpm to pellet the cell debris. The supernatant containing extracted porins was used directly or was stored at -20 °C. For analysis, protein samples were mixed with loading buffer (140 mM Tris pH 7.5, 30% glycerol, 4% SDS

(w/v), 0.1% bromophenol blue (w/v)), incubated at room temperature for 10 min and 10 μ l of the samples were loaded on a 10% SDS-PAGE gel. Protein production was visualized by Western blotting using either an anti-His-tag antibody (MapB and MspA) or an anti-Strep-tag II antibody (MapA).

Western blotting

For detection of recombinant protein production in induced *M. smegmatis* pACE cultures, total protein from a small amount of cells was separated on a denaturing 10% polyacrylamide gel and transferred to a polyvinylidene fluoride (PVDF) membrane (Immobilon-PSQ, Merck). The protein gel was blotted onto the membrane in transfer buffer (5.8 g Tris, 2.9 g glycine, 0.1% SDS (w/v), 20% methanol (v/v) in 1L) at 12 V for 1 h using a Trans-Blot[®] SD Semi-Dry Electrophoretic Transfer Cell (BIO-RAD). The membrane was blocked in 20 mM Tris pH 7.6, 150 mM NaCl (TBS) containing 5% (w/v) milk powder and 0.1% (v/v) Tween 20 at room temperature for 1 h, followed by overnight incubation at 4 °C while rotating in blocking buffer with tag-specific antibody (anti-His-tag antibody (Abcam, ab15149) diluted 1:500 (v/v) or anti-Strep-tag II antibody (Abcam, ab180957) diluted 1:1'000 (v/v)). The membrane was washed three times with TBS buffer containing 0.1% (v/v) Tween 20 and incubated with the respective HRP conjugated secondary antibody (α -mouse-HRP antibody (Abcam, ab205719) diluted 1:2'000 (v/v) or α -rabbit-HRP antibody (Abcam, ab6721) diluted 1:3'000 (v/v)) in blocking buffer for 1 h at room temperature while shaking. After washing the membrane 3x with TBS buffer containing 0.1% (v/v) Tween 20, Immobilon Western Chemiluminescent HRP Substrate (Merck) was added and proteins were detected by measuring chemiluminescence with an ImageQuant LAS 4000 instrument (GE Healthcare)⁵⁰.

Porin production and purification in *M. smegmatis*

For purification of His-tagged MapB protein from *M. smegmatis* outer membrane, *M. smegmatis* containing the pACE-MapA-MapB expression vector was grown in 1-liter 7H9 medium supplemented with apramycin to an A_{600} of around 0.6 before 0.4% (w/v) acetamide was added to the cells to induce protein production. After induction of protein expression at 37 °C overnight, cells were harvested and washed 2x with ice-cold PBS buffer (100 mM $\text{NaH}_2\text{PO}_4/\text{Na}_2\text{HPO}_4$ pH 7, 150 mM NaCl, 0.1 mM Na_2EDTA , 0.05% (w/v) Tween 80). Extraction of *M. abscessus* porins from the outer membrane of *M. smegmatis* was performed using a method that yields predominantly Msp porins in the supernatant in wildtype *M. smegmatis*. Briefly, cells were resuspended in 100 mM $\text{NaH}_2\text{PO}_4/\text{Na}_2\text{HPO}_4$ pH 6.5, 150 mM NaCl, 0.1 mM Na_2EDTA , 0.5% (w/v) *N*-octyl-POE to a cell density of 10 mg/35 μ l, and heated

to 100 °C while stirring in a water bath for 30 min. The suspension was cooled for 10 min on ice and centrifuged for 15 min at 14'000 rpm at 4 °C to remove cell debris. For buffer exchange, the total protein in the supernatant was precipitated after adding an equal volume of acetone and 1 h incubation on ice. After centrifugation at 4 °C for 15 min at 14'000 rpm, the pellet was dissolved in binding buffer (50 mM NaH₂PO₄ pH 7.5, 300 mM NaCl, 20 mM Imidazole, 0.5% (w/v) *N*-octyl-POE) and filtered with a 5 µm-filter. The protein sample was loaded onto a Ni²⁺-NTA gravity flow column (Qiagen). The column was washed 2x with wash buffer (50 mM Imidazole pH 7.5, 300 mM NaCl, 0.5% (w/v) *N*-octyl-POE), and then eluted 2x with elution buffer (200 mM Imidazole pH 7.5, 300 mM NaCl, 0.5% (w/v) *N*-octyl-POE)^{29,50}.

SUPPLEMENTARY DATA

Table S1. Primers used in this study

Name	Description	Sequence
1080_UP_F (p161)	Forward primer for amplification of 5' flanking region of <i>mapA</i> (MAB_1080).	cacttcgcaatggccaagacTGCTGGAC GCCATCCAGAC
1080_UP_R (p162)	Reverse primer for amplification of 5' flanking region of <i>mapA</i> (MAB_1080).	cctacttcatCAGCTTCATTCTGTTC CTATCAGTCC
1080_DW_F (p163)	Forward primer for amplification of 3' flanking region of <i>mapA</i> (MAB_1080).	aatgaagctgATGAAGTAGGCAGG TATC
1080_DW_R (p164)	Reverse primer for amplification of 3' flanking region of <i>mapA</i> (MAB_1080).	ggcgtctgctaggaccgatGATTCAGA GATTTTCTGCTG
1081_UP_F (p165)	Forward primer for amplification of 5' flanking region of <i>mapB</i> (MAB_1081).	cacttcgcaatggccaagacCCATGCCTT CGCTGGGTC
1081_UP_R (p166)	Reverse primer for amplification of 5' flanking region of <i>mapB</i> (MAB_1081).	gccacttcatCGTTCTCATTGGT TCCCTCAATTC
1081_DW_F (p167)	Forward primer for amplification of 3' flanking region of <i>mapB</i> (MAB_1081).	aatgagaacgATGAAGTAGTGGCG GCAC
1081_DW_R (p168)	Reverse primer for amplification of 3' flanking region of <i>mapB</i> (MAB_1081).	ggcgtctgctaggaccgatAGAGTGCT AGTGGCGTTTC
1080-1081_ UP_F (p161)	Forward primer for amplification of 5' flanking region of <i>mapA</i> (MAB_1080) & <i>mapB</i> (MAB_1081). Primer sequence is identical to 1080_UP_F (p161).	cacttcgcaatggccaagacTGCTGGAC GCCATCCAGAC
1080-1081_ UP_R (p169)	Reverse primer for amplification of 5' flanking region of <i>mapA</i> (MAB_1080) & <i>mapB</i> (MAB_1081).	gccacttcatCAGCTTCATTCTGT TCCTATCAGTCC

CHAPTER 1

1080-1081_ DW_F (p170)	Forward primer for amplification of 3' flanking region of <i>mapA</i> (MAB_1080) & <i>mapB</i> (MAB_1081).	aatgaagctgATGAAGTAGTGGCG GCAC
1080-1081_ DW_R (p168)	Reverse primer for amplification of 3' flanking region of <i>mapA</i> (MAB_1080) & <i>mapB</i> (MAB_1081). Primer sequence is identical to 1081_DW_R (p168).	ggcgtctgctaggaccgatAGAGTGCT AGTGGCGTTTC
1080-Del 1081_UP_F (p161)	Forward primer for amplification of 5' flanking region of <i>mapA</i> (MAB_1080) in $\Delta mapB$ (Δ MAB_1081) mutant. Primer sequence is identical to 1080_UP_F (p161).	cacttcgcaatggccaagacTGCTGGAC GCCATCCAGAC
1080-Del 1081_UP_R (p162)	Reverse primer for amplification of 5' flanking region of <i>mapA</i> (MAB_1080) in $\Delta mapB$ (Δ MAB_1081) mutant. Primer sequence is identical to 1080_UP_R (p162).	cctacttcatCAGCTTCATTCTGTTC CTATCAGTCC
1080-Del 1081_DW_F (p237)	Forward primer for amplification of 3' flanking region of <i>mapA</i> (MAB_1080) in $\Delta mapB$ (Δ MAB_1081) mutant.	aatgaagctgATGAAGTAGGCAGG TATCCCTG
1080-Del 1081_DW_R (p238)	Reverse primer for amplification of 3' flanking region of <i>mapA</i> (MAB_1080) in $\Delta mapB$ (Δ MAB_1081) mutant.	ggcgtctgctaggaccgatACTGCACT GCAGCGCATATC
1081-Del 1080_UP_F (p239)	Forward primer for amplification of 5' flanking region of <i>mapB</i> (MAB_1081) in $\Delta mapA$ (Δ MAB_1080) mutant.	cacttcgcaatggccaagacAACGGTTA CGGTTGCTTC
1081-Del 1080_UP_R (p240)	Reverse primer for amplification of 5' flanking region of <i>mapB</i> (MAB_1081) in $\Delta mapA$ (Δ MAB_1080) mutant.	actacttcatCGTTCTCATTGTTTC CCTCAATTC
1081-Del 1080_DW_F (p167)	Forward primer for amplification of 3' flanking region of <i>mapB</i> (MAB_1081) in $\Delta mapA$ (Δ MAB_1080) mutant. Primer	aatgagaacgATGAAGTAGTGGCG GCAC

CHAPTER 1

	sequence is identical to 1081_DW_F (p167).	
1081-Del 1080_DW_R (p168)	Reverse primer for amplification of 3' flanking region of <i>mapB</i> (MAB_1081) in $\Delta mapA$ (Δ MAB_1080) mutant. Primer sequence is identical to 1081_DW_R (p168).	ggcgtctgctaggaccgatAGAGTGCT AGTGGCGTTTC
2800_UP_F (p171)	Forward primer for amplification of 5' flanking region of <i>mapC</i> (MAB_2800).	cacttcgcaatggccaagacACGCAACG CGGTCCGTCC
2800_UP_R (p172)	Reverse primer for amplification of 5' flanking region of <i>mapC</i> (MAB_2800).	gcaggaaggaGTCGTTTCATCTATC AGACGGCCTTGG
2800_DW_F (p173)	Forward primer for amplification of 3' flanking region of <i>mapC</i> (MAB_2800).	gatgaacgacTCCTTCCTGCGCTCC TAC
2800_DW_R (p174)	Reverse primer for amplification of 3' flanking region of <i>mapC</i> (MAB_2800).	ggcgtctgctaggaccgatCCTTGTACA TGGTGTCCATC
4097c-4099c _UP_F (p241)	Forward primer for amplification of 5' flanking region of <i>mps1</i> (MAB_4099c), <i>mps2</i> (MAB_4098c) & <i>gap</i> (MAB_4097c) genes of the <i>gpl</i> locus.	cacttcgcaatggccaagacCGGTCTTTG TCATGCTGATG
4097c-4099c _UP_R (p242)	Reverse primer for amplification of 5' flanking region of <i>mps1</i> (MAB_4099c), <i>mps2</i> (MAB_4098c) & <i>gap</i> (MAB_4097c) genes of the <i>gpl</i> locus.	ccagtgccacCGGTCCTCAGACTCC AAC
4097c-4099c _DW_F (p243)	Forward primer for amplification of 3' flanking region of <i>mps1</i> (MAB_4099c), <i>mps2</i> (MAB_4098c) & <i>gap</i> (MAB_4097c) genes of the <i>gpl</i> locus.	ctgaggaccgGTGGCACTGGTACT CGGAATC
4097c-4099c _DW_R (p244)	Reverse primer for amplification of 3' flanking region of <i>mps1</i> (MAB_4099c), <i>mps2</i>	ggcgtctgctaggaccgatGTTCCGTCC TCGTAGACG

CHAPTER 1

	(MAB_4098c) & <i>gap</i> (MAB_4097c) genes of the <i>gpl</i> locus.	
C_1080_F (p208)	Forward primer for amplification of <i>mapA</i> (MAB_1080) for cloning into pMV361 complementation vector.	aacgcgtgcggccgcgtacAGGTCGCC AATCACGGATAC
C_1080_R (p209)	Reverse primer for amplification of <i>mapA</i> (MAB_1080) for cloning into pMV361 complementation vector.	tctagaggatccccgggtacGTTGCGGC AGGGATACCTG
C_2874- 2875_F (p255)	Forward primer for amplification of MAB_2874 & MAB_2875 (<i>bla</i>) for cloning into pOLYG complementation vector.	cgaggtcgacgggtatcgataCCACGATA TAGCAGTTCG
C_2874- 2875_R (p256)	Reverse primer for amplification of MAB_2874 & MAB_2875 (<i>bla</i>) for cloning into pOLYG complementation vector.	actgcaggaattcgatatcaAGAACGTAG ATCTCGCGAG
P_1080_F (p231)	Forward primer for amplification of <i>mapA</i> (MAB_1080) hybridization probe.	GAGATTGTGACCTTCGCCAC
P_1080_R (p232)	Reverse primer for amplification of <i>mapA</i> (MAB_1080) hybridization probe.	ACGTCCGCAAGTTAACATCC
P_1081_F (p233)	Forward primer for amplification of <i>mapB</i> (MAB_1081) hybridization probe.	TGAAGTCCAGATACTGCCCG
P_1081_R (p234)	Reverse primer for amplification of <i>mapB</i> (MAB_1081) hybridization probe.	GAAAGGGTGGTAATGGTCGC
P_2800_F (p235)	Forward primer for amplification of <i>mapC</i> (MAB_2800) hybridization probe.	CCGTTGAAATTCGCCTGCTA
P_2800_R (p236)	Reverse primer for amplification of <i>mapC</i> (MAB_2800) hybridization probe.	CCAGAGCGCAAACAGTAGTC
P_4097c- 4099c_F (p270)	Forward primer for amplification of <i>gpl</i> (MAB_4097c-4099c) hybridization probe.	CAAATTTCACTCCACCGCCA

CHAPTER 1

P_4097c-4099c_R (p271)	Reverse primer for amplification of <i>gpl</i> (MAB_4097c-4099c) hybridization probe.	CGTAGCAGTTTGTACCACA
MapA-Strep II_F (p279)	Forward primer for amplification of <i>mapA</i> (MAB_1080) fused to a C-terminal Strep-tag II for cloning into pMV361 intermediate vector.	aacgcgtgcccgcggtacGAAATTCTCATGTTTCGCC
MapA-Strep II_R (p280)	Reverse primer for amplification of <i>mapA</i> (MAB_1080) fused to a C-terminal Strep-tag II for cloning into pMV361 intermediate vector.	ctgcgggtggtccaCTTCATGTCCCA GGTCTC
MapB_F (p281)	Forward primer for amplification of <i>mapB</i> (MAB_1081) for cloning into pMV361 intermediate vector.	ggacatgaagtggagccaccgcagttcgaaaa atagAGGTAGGCATTTGCCCTG
MapB_R (p282)	Reverse primer for amplification of <i>mapB</i> (MAB_1081) for cloning into pMV361 intermediate vector.	tctagaggatccccgggtacTTCTTCTGC TCGTGCCGC
INIT_MapA_F (p283)	Forward primer containing a SapI site for amplification of <i>mapA</i> (MAB_1080) fused to a C-terminal Strep-tag II for cloning into ORF sequencing vector pINIT.	atatatGCTCTTCtAGTaaactgttgggca aggtatcgggctgg
INIT_MapA_R (p287)	Reverse primer containing a SapI site for amplification of <i>mapA</i> (MAB_1080) fused to a C-terminal Strep-tag II for cloning into ORF sequencing vector pINIT.	tatatatGCTCTTCaAGGtgaacgccagg gcaaatgcctacct
INIT_MapB_F (p289)	Forward primer containing a SapI site for amplification of <i>mapB</i> (MAB_1081) for cloning into ORF sequencing vector pINIT. The primer also contains a consensus Shine-Dalgarno sequence flanking a start codon.	atatatGCTCTTCtCCTAGAAAGG <u>AGGTTAATAATG</u> gagaacggttgcat ccggcgggttg
INIT_MapB_R (p284)	Reverse primer containing a SapI site for amplification of <i>mapB</i> (MAB_1081) for cloning into ORF sequencing vector pINIT.	tatataGCTCTTCaTGCcttcatgtcccag gtctcggctaggt
INIT_MspA_F (p285)	Forward primer containing a SapI site for amplification of <i>mspA</i>	atatatGCTCTTCtAGTaaaggcaatcagt cgggtgctgatcgcg

	(MSMEG_0965) for cloning into ORF sequencing vector pINIT.	
INIT_MspA_R (p286)	Reverse primer containing a SapI site for amplification of <i>mspA</i> (MSMEG_0965) for cloning into ORF sequencing vector pINIT.	tatataGCTCTTCaTGCgttcatgttccag ggttcgccgtaggt
ACE_MapA-MapB_F (p306)	Forward primer for amplification of a fragment containing <i>mapA</i> (fused to a C-terminal Strep-tag II) and <i>mapB</i> genes downstream of a single acetamide promoter for construction of pACE-MapA-MapB expression vector.	acccttgacttttattttcaTCTGGATATAT TTCGGGTG
ACE_MapA-MapB_R (p307)	Reverse primer for amplification of a fragment containing <i>mapA</i> (fused to a C-terminal Strep-tag II) and <i>mapB</i> genes downstream of a single acetamide promoter for construction of pACE-MapA-MapB expression vector.	ggtgatgatgatgTGGACCTTGAAAC AAAAC
ACE_MspA_F (p306)	Forward primer for amplification of a fragment containing <i>mspA</i> gene downstream of an acetamide promoter for construction of pACE-MspA expression vector. Primer sequence is identical to ACE_MapA-MapB_F (p306).	acccttgacttttattttcaTCTGGATATAT TTCGGGTG
ACE_MspA_R (p307)	Reverse primer for amplification of a fragment containing <i>mspA</i> gene downstream of an acetamide promoter for construction of pACE-MspA expression vector. Primer sequence is identical to ACE_MapA-MapB_R (p307).	ggtgatgatgatgTGGACCTTGAAAC AAAAC
ACE_His ₁₀ -Apra-Ori_F (p308)	Forward primer for amplification of a fragment containing His ₁₀ -tag, apramycin resistance gene and mycobacterial origin of replication from pACE-C3GH expression vector.	tcaaggtccaCATCATCATCACCAT CATC
ACE_His ₁₀ -Apra-Ori_R (p309)	Reverse primer for amplification of a fragment containing His ₁₀ -tag, apramycin resistance gene and	gtatcagctcactcaaaggcGGTAATAC GGTTATCCAC

CHAPTER 1

	mycobacterial origin of replication from pACE-C3GH expression vector.	
ACE_B_F (p310)	Forward primer for amplification of a fragment containing the remaining backbone of pACE-C3GH expression vector.	GCCTTTGAGTGAGCTGATAC
ACE_B_R (p311)	Reverse primer for amplification of a fragment containing the remaining backbone of pACE-C3GH expression vector.	TGAAAATAAAAAGTCAAGGGT G

CHAPTER 1

Table S2. MIC determination of *M. abscessus* deletion and complemented mutants

Table S2. MIC determination of <i>M. abscessus</i> deletion and complemented mutants																												
Strains	<i>M. abscessus</i> ATCC 19977				$\Delta mapA$				$\Delta mapA$ pMV361- <i>mapA</i>				$\Delta mapA$ pMV361				$\Delta mapB$				$\Delta mapC$							
Day of MIC reading	3	5	7	12	3	5	7	12	3	5	7	12	3	5	7	12	3	5	7	12	3	5	7	12	3	5	7	12
Compound	MIC (mg/L)																											
Cefotaxime	16	32	128	256	16	32	64	256	Not determined				Not determined				16	32	64	256	16	32	64	256				
Imipenem	2	16	64	>256	4	64	256	>256	2	16	64	>256	4	64	256	>256	2	16	64	>256	2	16	64	>256				
Meropenem	16	32	64	256	32	64	128	256	16	32	64	256	16	64	128	256	16	32	64	256	8	32	64	256				
Doripenem	8	16	64	256	16	64	256	>256	8	16	32	256	16	64	128	>256	8	16	64	256	8	16	64	256				
Biapenem	16	64	128	256	32	128	256	>256	16	64	128	>256	32	128	256	>256	16	64	128	256	8	64	128	256				
Ertapenem	64	128	256	>512	64	512	>512	>512	64	128	256	>512	64	512	>512	>512	64	128	256	>512	64	128	256	>512				
Faropenem	16	32	64	128	16	32	32	128	Not determined				Not determined				16	32	32	128	8	32	32	64				

Strains	Δbla				Δbla pOLYG- <i>bla</i>				Δbla pOLYG				Δbla $\Delta mapA$				Δbla $\Delta mapA$ pOLYG- <i>bla</i>				Δbla $\Delta mapA$ pOLYG				Δbla $\Delta mapB$				Δbla $\Delta mapC$			
Day of MIC reading	3	5	7	12	3	5	7	12	3	5	7	12	3	5	7	12	3	5	7	12	3	5	7	12	3	5	7	12	3	5	7	12
Compound	MIC (mg/L)																															
Cefotaxime	8	16	32	64	64	128	256	>512	16	16	32	64	8	16	32	64	64	128	256	>512	16	16	32	64	8	16	32	64	8	16	32	64
Imipenem	1	4	32	>256	8	32	256	>512	1	8	64	>512	1	4	32	>256	32	256	>512	>512	2	8	64	>512	1	4	32	>256	1	4	32	>256
Meropenem	2	4	8	64	128	256	256	256	4	4	8	32	2	4	16	64	128	256	256	256	4	8	16	64	2	4	8	64	2	4	8	32
Doripenem	2	4	8	64	32	128	256	256	4	4	8	64	2	4	16	64	128	512	>512	>512	4	8	16	64	2	4	8	64	2	4	8	64
Biapenem	2	8	32	256	64	128	256	512	4	16	32	256	2	8	32	256	128	256	512	>512	4	16	32	256	2	8	32	256	2	8	32	256
Ertapenem	4	8	16	64	256	512	1024	>1024	8	16	32	128	8	32	64	256	512	1024	>1024	>1024	16	32	64	256	4	16	32	128	4	8	16	128
Faropenem	4	8	16	32	64	64	128	256	8	16	16	32	8	8	16	64	128	256	256	512	8	16	32	64	4	8	16	32	4	8	16	16

Strains	Δgpl				$\Delta mapA$ Δgpl				$\Delta mapB$ Δgpl				Δbla Δgpl				Δbla $\Delta mapA$ Δgpl				Δbla $\Delta mapB$ Δgpl							
Day of MIC reading	3	5	7	12	3	5	7	12	3	5	7	12	3	5	7	12	3	5	7	12	3	5	7	12				
Compound	MIC (mg/L)																											
Cefotaxime	64	128	256	512	256	512	1024	1024	128	256	512	1024	32	32	64	64	128	128	128	256	64	64	128	128				
Imipenem	4	16	64	>256	16	64	>256	>256	4	16	64	>256	4	8	32	>256	4	16	64	>256	4	8	32	>256				
Meropenem	16	32	64	256	64	128	256	256	32	64	128	256	8	8	8	64	8	8	16	64	8	8	8	64				
Doripenem	8	16	32	256	64	128	256	>256	16	32	64	>256	8	8	8	64	8	8	16	64	8	8	8	64				
Biapenem	16	64	128	>256	64	256	256	>256	32	128	256	>256	8	16	32	256	16	16	64	256	8	16	32	256				
Ertapenem	64	128	256	1024	256	512	1024	>1024	128	256	512	>1024	16	16	32	64	32	64	128	256	16	32	32	128				
Faropenem	32	64	64	128	128	256	256	>256	64	128	256	256	16	16	16	32	64	64	128	128	16	32	32	64				

References

1. Floto, R. A. et al. US Cystic Fibrosis Foundation and European Cystic Fibrosis Society consensus recommendations for the management of non-tuberculous mycobacteria in individuals with cystic fibrosis. *Thorax* **71**, i1–i22 (2016).
2. Bryant, J. M. et al. Emergence and spread of a human-transmissible multidrug-resistant nontuberculous mycobacterium. *Science* **354**, 751–757 (2016).
3. Esther, C. R., Esserman, D. A., Gilligan, P., Kerr, A. & Noone, P. G. Chronic *Mycobacterium abscessus* infection and lung function decline in cystic fibrosis. *J. Cyst. Fibros.* **9**, 117–123 (2010).
4. Jarand, J. et al. Clinical and microbiologic outcomes in patients receiving treatment for *Mycobacterium abscessus* pulmonary disease. *Clin. Infect. Dis.* **52**, 565–571 (2011).
5. Nessar, R., Cambau, E., Reyrat, J. M., Murray, A. & Gicquel, B. *Mycobacterium abscessus*: a new antibiotic nightmare. *J. Antimicrob. Chemother.* **67**, 810–818 (2012).
6. Kwak, N. et al. *Mycobacterium abscessus* pulmonary disease: individual patient data meta-analysis. *Eur. Resp. J.* <https://doi.org/10.1183/13993003.01991-2018> (2019).
7. Chiaradia, L. et al. Dissecting the mycobacterial cell envelope and defining the composition of the native mycomembrane. *Sci. Rep.* **7**, 12807 (2017).
8. Hoffmann, C., Leis, A., Niederweis, M., Plitzko, J. M. & Engelhardt, H. Disclosure of the mycobacterial outer membrane: cryo-electron tomography and vitreous sections reveal the lipid bilayer structure. *Proc. Natl Acad. Sci. USA* **105**, 3963–3967 (2008).
9. Zuber, B. et al. Direct visualization of the outer membrane of mycobacteria and corynebacteria in their native state. *J. Bacteriol.* **190**, 5672–5680 (2008).
10. Minnikin, D. E. et al. Pathophysiological implications of cell envelope structure in *Mycobacterium tuberculosis* and related taxa. in *Tuberculosis - Expanding Knowl.* (ed. Ribon, W.) (InTech, 2015). <https://doi.org/10.5772/59585>
11. Marrakchi, H., Lanéelle, M.-A. & Daffé, M. Mycolic acids: structures, biosynthesis, and beyond. *Chem. & Biol.* **21**, 67–85 (2014).
12. Dulberger, C. L., Rubin, E. J. & Boutte, C. C. The mycobacterial cell envelope — a moving target. *Nat. Rev. Microbiol.* **18**, 47–59 (2020).
13. Nikaido, H., Kim, S. H. & Rosenberg, E. Y. Physical organization of lipids in the cell wall of *Mycobacterium chelonae*. *Mol. Microbiol.* **8**, 1025–1030 (1993).
14. Liu, J., Rosenberg, E. Y. & Nikaido, H. Fluidity of the lipid domain of cell wall from *Mycobacterium chelonae*. *Proc. Natl Acad. Sci. USA* **92**, 11254–11258 (1995).

15. Liu, J., Barry, C. E., Besra, G. S. & Nikaido, H. Mycolic acid structure determines the fluidity of the mycobacterial cell wall. *J. Biol. Chem.* **271**, 29545–29551 (1996).
16. Jarlier, V. & Nikaido, H. Permeability barrier to hydrophilic solutes in *Mycobacterium chelonae*. *J. Bacteriol.* **172**, 1418–1423 (1990).
17. Nikaido, H. Molecular basis of bacterial outer membrane permeability revisited. *Microbiol. Mol. Biol. Rev.* **67**, 593–656 (2003).
18. Delcour, A. H. Solute uptake through general porins. *Front. Biosci.* **8**, D1055–D1071 (2003).
19. Schulz, G. E. The structure of bacterial outer membrane proteins. *Biochim. Biophys. Acta* **1565**, 308–317 (2002).
20. Nikaido, H. Prevention of drug access to bacterial targets: permeability barriers and active efflux. *Science* **264**, 382–388 (1994).
21. Niederweis, M. et al. Cloning of the *mspA* gene encoding a porin from *Mycobacterium smegmatis*. *Mol. Microbiol.* **33**, 933–945 (1999).
22. Stahl, C. et al. MspA provides the main hydrophilic pathway through the cell wall of *Mycobacterium smegmatis*. *Mol. Microbiol.* **40**, 451–464 (2001).
23. Faller, M., Niederweis, M. & Schulz, G. E. The Structure of a Mycobacterial Outer-Membrane Channel. *Science* **303**, 1189–1192 (2004).
24. Cowan, S. W. et al. Crystal structures explain functional properties of two *E. coli* porins. *Nature* **358**, 727–733 (1992).
25. Baslé, A., Rummel, G., Storici, P., Rosenbusch, J. P. & Schirmer, T. Crystal structure of osmoporin OmpC from *E. coli* at 2.0 Å. *J. Mol. Biol.* **362**, 933–942 (2006).
26. Paul, T. R. & Beveridge, T. J. Reevaluation of envelope profiles and cytoplasmic ultrastructure of mycobacteria processed by conventional embedding and freeze-substitution protocols. *J. Bacteriol.* **174**, 6508–6517 (1992).
27. Paul, T. R. & Beveridge, T. J. Ultrastructure of mycobacterial surfaces by freeze-substitution. *Zentbl. Bakteriologie* **279**, 450–457 (1993).
28. Paul, T. R. & Beveridge, T. J. Preservation of surface lipids and determination of ultrastructure of *Mycobacterium kansasii* by freeze-substitution. *Infect. Immun.* **62**, 1542–1550 (1994).
29. Mahfoud, M., Sukumaran, S., Hülsmann, P., Grieger, K. & Niederweis, M. Topology of the porin MspA in the outer membrane of *Mycobacterium smegmatis*. *J. Biol. Chem.* **281**, 5908–5915 (2006).

30. Bush, K. & Bradford, P. A. in *Antibiotics and Antibiotic Resistance* (eds Silver, L. L. & Bush, K.) 23–44 (Cold Spring Harbor Laboratory Press, 2016).
31. Kohanski, M. A., Dwyer, D. J. & Collins, J. J. How antibiotics kill bacteria: from targets to networks. *Nat. Rev. Microbiol.* **8**, 423–435 (2010).
32. Lavollay, M. et al. The peptidoglycan of *Mycobacterium abscessus* is predominantly cross-linked by L,D-transpeptidases. *J. Bacteriol.* **193**, 778–782 (2011).
33. Kaushik, A. et al. Carbapenems and Rifampin Exhibit Synergy against *Mycobacterium tuberculosis* and *Mycobacterium abscessus*. *Antimicrob. Agents Chemother.* **59**, 6561–6567 (2015).
34. Kumar, P. et al. Non-classical transpeptidases yield insight into new antibacterials. *Nat. Chem. Biol.* **13**, 54–61 (2017).
35. Lefebvre, A.-L. et al. Bactericidal and intracellular activity of β -lactams against *Mycobacterium abscessus*. *J. Antimicrob. Chemother.* **71**, 1556–1563 (2016).
36. Kumar, P. et al. *Mycobacterium abscessus* L,D-transpeptidases are susceptible to inactivation by carbapenems and cephalosporins but not penicillins. *Antimicrob. Agents Chemother.* <https://doi.org/10.1128/AAC.00866-17> (2017).
37. Soroka, D. et al. Characterization of broad-spectrum *Mycobacterium abscessus* class A β -lactamase. *J. Antimicrob. Chemother.* **69**, 691–696 (2014).
38. Luthra, S., Rominski, A. & Sander, P. The role of antibiotic-target-modifying and antibiotic-modifying enzymes in *Mycobacterium abscessus* drug resistance. *Front. Microbiol.* **9**, 1–13 (2018).
39. Soroka, D. et al. Inhibition of β -lactamases of mycobacteria by avibactam and clavulanate. *J. Antimicrob. Chemother.* **72**, 1081–1088 (2017).
40. Gutiérrez, A. V., Viljoen, A., Ghigo, E., Herrmann, J.-L. & Kremer, L. Glycopeptidolipids, a double-edged sword of the *Mycobacterium abscessus* complex. *Front. Microbiol.* **9**, 1145 (2018).
41. Johansen, M. D., Herrmann, J. L. & Kremer, L. Non-tuberculous mycobacteria and the rise of *Mycobacterium abscessus*. *Nat. Rev. Microbiol.* **18**, 392–407 (2020).
42. Billman-Jacobe, H., McConville, M. J., Haites, R. E., Kovacevic, S. & Coppel, R. L. Identification of a peptide synthetase involved in the biosynthesis of glycopeptidolipids of *Mycobacterium smegmatis*. *Mol. Microbiol.* **33**, 1244–1253 (1999).
43. Sondén, B. et al. Gap, a mycobacterial specific integral membrane protein, is required for glycolipid transport to the cell surface. *Mol. Microbiol.* **58**, 426–440 (2005).

44. Pawlik, A. et al. Identification and characterization of the genetic changes responsible for the characteristic smooth-to-rough morphotype alterations of clinically persistent *Mycobacterium abscessus*. *Mol. Microbiol.* **90**, 612–629 (2013).
45. Park, I. K. et al. Clonal diversification and changes in lipid traits and colony morphology in *Mycobacterium abscessus* clinical isolates. *J. Clin. Microbiol.* **53**, 3438–3447 (2015).
46. Rominski, A. et al. Elucidation of *Mycobacterium abscessus* aminoglycoside and capreomycin resistance by targeted deletion of three putative resistance genes. *J. Antimicrob. Chemother.* **72**, 2191–2200 (2017).
47. Noinaj, N., Gumbart, J. C. & Buchanan, S. K. The β -barrel assembly machinery in motion. *Nat. Rev. Microbiol.* **15**, 197–204 (2017).
48. Arunmanee, W. et al. Gram-negative trimeric porins have specific LPS binding sites that are essential for porin biogenesis. *Proc. Natl Acad. Sci. USA* **113**, E5034–E5043 (2016).
49. Pavlenok, M. & Niederweis, M. Hetero-oligomeric MspA pores in *Mycobacterium smegmatis*. *FEMS Microbiol. Lett.* <https://doi.org/10.1093/femsle/fnw046> (2016).
50. Arnold, F. M. et al. A uniform cloning platform for mycobacterial genetics and protein production. *Sci. Rep.* **8**, 9539 (2018).
51. Becker, K. et al. Lipoprotein glycosylation by protein-O-mannosyltransferase (MAB_1122c) contributes to low cell envelope permeability and antibiotic resistance of *Mycobacterium abscessus*. *Front. Microbiol.* <https://doi.org/10.3389/fmicb.2017.02123> (2017).
52. Pagès, J. M., James, C. E. & Winterhalter, M. The porin and the permeating antibiotic: a selective diffusion barrier in Gram-negative bacteria. *Nat. Rev. Microbiol.* **6**, 893–903 (2008).
53. Vergalli, J. et al. Porins and small-molecule translocation across the outer membrane of Gram-negative bacteria. *Nat. Rev. Microbiol.* **18**, 164–176 (2020).
54. Masi, M., Réfregiers, M., Pos, K. M. & Pagès, J.-M. Mechanisms of envelope permeability and antibiotic influx and efflux in Gram-negative bacteria. *Nat. Microbiol.* **2**, 17001 (2017).
55. Dupont, H. et al. Molecular characterization of carbapenem-nonsusceptible enterobacterial isolates collected during a prospective interregional survey in France and susceptibility to the novel ceftazidime-avibactam and aztreonam-avibactam combinations. *Antimicrob. Agents Chemother.* **60**, 215–221(2016).

56. Doumith, M., Ellington, M. J., Livermore, D. M. & Woodford, N. Molecular mechanisms disrupting porin expression in ertapenem-resistant *Klebsiella* and *Enterobacter* spp. clinical isolates from the UK. *J. Antimicrob. Chemother.* **63**, 659–667 (2009).
57. Wozniak, A. et al. Porin alterations present in non-carbapenemase-producing *Enterobacteriaceae* with high and intermediate levels of carbapenem resistance in Chile. *J. Med. Microbiol.* **61**, 1270–1279 (2012).
58. Yamaguchi, A., Nakashima, R. & Sakurai, K. Structural basis of RND-type multidrug exporters. *Front. Microbiol.* **6**, 327 (2015).
59. Bernut, A. et al. Insights into the smooth-to-rough transitioning in *Mycobacterium boletii* unravels a functional Tyr residue conserved in all mycobacterial MmpL family members. *Mol. Microbiol.* **99**, 866–883 (2016).
60. Deshayes, C. et al. MmpS4 promotes glycopeptidolipids biosynthesis and export in *Mycobacterium smegmatis*. *Mol. Microbiol.* **78**, 989–1003 (2010).
61. Richard, M. et al. Mutations in the MAB_2299c TetR regulator confer cross-resistance to clofazimine and bedaquiline in *Mycobacterium abscessus*. *Antimicrob. Agents Chemother.* **63**, e01316–e01318 (2019).
62. Gutiérrez, A. V., Richard, M., Roquet-Banères, F., Viljoen, A. & Kremer, L. The TetR-family transcription factor MAB_2299c regulates the expression of two distinct MmpS-MmpL efflux pumps involved in cross-resistance to clofazimine and bedaquiline in *Mycobacterium abscessus*. *Antimicrob. Agents Chemother.* **63**, e01000-19 (2019).
63. Halloum, I. et al. Resistance to thiacetazone derivatives active against *Mycobacterium abscessus* involves mutations in the MmpL5 transcriptional repressor MAB_4384. *Antimicrob. Agents Chemother.* **61**, 02509–02516 (2017).
64. Nikaido, H. Outer membrane barrier as a mechanism of antimicrobial resistance. *Antimicrob. Agents Chemother.* **33**, 1831–1836 (1989).
65. Ames, G. F., Spudich, E. N. & Nikaido, H. Protein composition of the outer membrane of *Salmonella typhimurium*: effect of lipopolysaccharide mutations. *J. Bacteriol.* **117**, 406–416 (1974).
66. Koplow, J. & Goldfine, H. Alterations in the outer membrane of the cell envelope of heptose-deficient mutants of *Escherichia coli*. *J. Bacteriol.* **117**, 527–543 (1974).
67. Roantree, R. J., Kuo, T. T. & MacPhee, D. G. The effect of defined lipopolysaccharide core defects upon antibiotic resistances of *Salmonella typhimurium*. *J. Gen. Microbiol.* **103**, 223–234 (1977).

68. Smit, J., Kamio, Y. & Nikaido, H. Outer membrane of *Salmonella typhimurium*: chemical analysis and freeze-fracture studies with lipopolysaccharide mutants. *J. Bacteriol.* **124**, 942–958 (1975).
69. Kamio, Y. & Nikaido, H. Outer membrane of *Salmonella typhimurium*: accessibility of phospholipid head groups to phospholipase c and cyanogen bromide activated dextran in the external medium. *Biochemistry* **15**, 2561–2570 (1976).
70. Takeuchi, Y. & Nikaido, H. Persistence of segregated phospholipid domains in phospholipid–lipopolysaccharide mixed bilayers: studies with spin-labeled phospholipids. *Biochemistry* **20**, 523–529 (1981).
71. Nikaido, H. & Vaara, M. Molecular basis of bacterial outer membrane permeability. *Microbiol. Rev.* **49**, 1–32 (1985).
72. Heinz, C., Engelhardt, H. & Niederweis, M. The core of the tetrameric mycobacterial porin MspA is an extremely stable beta-sheet domain. *J. Biol. Chem.* **278**, 8678–8685 (2003).

Funding

Research in the group of PS was supported by the Swiss National Science Foundation (#31003A_153349), Lungenliga Schweiz, the Institute of Medical Microbiology and the University of Zurich.

Acknowledgements

We thank M. Seeger for providing us with pINIT and pACE plasmids.

Personal contribution to chapter 1

As first author, my contribution to this manuscript (in preparation) was as follows:

1. Design of the study.
2. Cloning of all the plasmids used in this study (gene knockout plasmids, complementation vectors and porin expression constructs; listed in Table 2).
3. Generation of single, double and triple-gene knockouts in *M. abscessus* —
 - a. *M. abscessus* $\Delta mapA$, *M. abscessus* $\Delta mapB$ and *M. abscessus* $\Delta mapC$ strains.
 - b. *M. abscessus* $\Delta bla \Delta mapA$, *M. abscessus* $\Delta bla \Delta mapB$, *M. abscessus* $\Delta bla \Delta mapC$, *M. abscessus* $\Delta mapA \Delta gpl$ and *M. abscessus* $\Delta mapB \Delta gpl$ strains.
 - c. *M. abscessus* $\Delta bla \Delta mapA \Delta gpl$ and *M. abscessus* $\Delta bla \Delta mapB \Delta gpl$ strains.
4. Complementation of *mapA* into a *mapA*-null strain of *M. abscessus* — generation of
 - a. *M. abscessus* $\Delta mapA$ pMV361-*mapA* and *M. abscessus* $\Delta mapA$ pMV361 strains.
5. Overexpression of *bla* in β -lactamase-null *M. abscessus* strains that either exhibit normal expression of wildtype MapA (that is, *M. abscessus* Δbla) or show an altered porin phenotype (that is, *M. abscessus* $\Delta bla \Delta mapA$) — generation of
 - a. *M. abscessus* $\Delta bla \Delta mapA$ pOLYG-*bla* and *M. abscessus* $\Delta bla \Delta mapA$ pOLYG strains.
 - b. *M. abscessus* Δbla pOLYG-*bla* and *M. abscessus* Δbla pOLYG strains.
6. Determination of minimal inhibitory concentrations of antibiotics for all *M. abscessus* strains.
7. Porin production and purification in *M. smegmatis*.
8. Analysis of the data.
9. Preparation of the manuscript (abstract, introduction, results, discussion, methods and all figures).

The Role of Antibiotic-Target-Modifying and Antibiotic-Modifying Enzymes in *Mycobacterium abscessus* Drug Resistance

Sakshi Luthra, Anna Rominski and Peter Sander

Frontiers in Microbiology (published: 12th September 2018, doi: 10.3389/fmicb.2018.02179)

Abstract

The incidence and prevalence of non-tuberculous mycobacterial (NTM) infections have been increasing worldwide and lately led to an emerging public health problem. Among rapidly growing NTM, *Mycobacterium abscessus* is the most pathogenic and drug resistant opportunistic germ, responsible for disease manifestations ranging from “curable” skin infections to only “manageable” pulmonary disease. Challenges in *M. abscessus* treatment stem from the bacteria’s high-level innate resistance and comprise long, costly and non-standardized administration of antimicrobial agents, poor treatment outcomes often related to adverse effects and drug toxicities, and high relapse rates. Drug resistance in *M. abscessus* is conferred by an assortment of mechanisms. Clinically acquired drug resistance is normally conferred by mutations in the target genes. Intrinsic resistance is attributed to low permeability of *M. abscessus* cell envelope as well as to (multi)drug export systems. However, expression of numerous enzymes by *M. abscessus*, which can modify either the drug-target or the drug itself, is the key factor for the pathogen’s phenomenal resistance to most classes of antibiotics used for treatment of other moderate to severe infectious diseases, including macrolides, aminoglycosides, rifamycins, β -lactams, and tetracyclines. In 2009, when *M. abscessus* genome sequence became available, several research groups worldwide started studying *M. abscessus* antibiotic resistance mechanisms. At first, lack of tools for *M. abscessus* genetic manipulation severely delayed research endeavours. Nevertheless, the last 5 years, significant progress has been made towards the development of conditional expression and homologous recombination systems for *M. abscessus*. As a result of recent research efforts, an erythromycin ribosome methyltransferase, two aminoglycoside acetyltransferases, an aminoglycoside phosphotransferase, a rifamycin ADP-ribosyltransferase, a β -lactamase, and a monooxygenase were identified to frame the complex and multifaceted intrinsic resistome of *M. abscessus*, which clearly contributes to complications in treatment of this highly resistant pathogen. Better

knowledge of the underlying mechanisms of drug resistance in *M. abscessus* could improve selection of more effective chemotherapeutic regimen and promote development of novel antimicrobials which can overwhelm the existing resistance mechanisms. This article reviews the currently elucidated molecular mechanisms of antibiotic resistance in *M. abscessus*, with a focus on its drug-target-modifying and drug-modifying enzymes.

Keywords: non-tuberculous mycobacteria, *Mycobacterium abscessus*, antibiotic, drug resistance, resistance genes, antibiotic-target-modifying enzymes, antibiotic-modifying enzymes

Introduction

Non-tuberculous mycobacteria (NTM) encompass all species of mycobacteria that do not cause tuberculosis (TB) or leprosy (Lee et al., 2015). NTM are ubiquitous in the environment and occasionally infect humans with various predisposing conditions like cystic fibrosis, bronchiectasis or immunosuppression, causing a variety of pathological conditions including pulmonary, skin and soft tissue infections and disseminated diseases (Chan and Iseman, 2013). The last few decades saw an alarming increase in the incidence and prevalence of NTM-pulmonary disease throughout the globe. Importantly, more than 90% of all reported NTM-pulmonary disease cases involved infections with the *Mycobacterium avium* complex (comprising of *M. avium*, *Mycobacterium chimaera* and *Mycobacterium intracellulare*) or *Mycobacterium abscessus*, accentuating the medical importance of these emerging pathogens (Hoefsloot et al., 2013; Ryu et al., 2016; Wu et al., 2018). For a long while, it was believed that infections with genetically diverse NTM strains were exclusively acquired upon exposure to the environment. However, a recent whole genome analysis of more than 1000 *M. abscessus* clinical isolates from different geographical locations, revealed the presence of genetically clustered strains in patients. This suggests a human-to-human transmission of *M. abscessus*, presumably through indirect mechanisms like cough aerosols or surface contamination (Bryant et al., 2016).

Mycobacterium abscessus is an opportunistic pathogen, ubiquitous in the environment, that often causes infections in humans with compromised natural defences such as patients with cystic fibrosis or other chronic lung diseases (Sanguinetti et al., 2001; Brown-Elliott and Wallace, 2002; Howard, 2006; Griffith et al., 2007). A current taxonomic classification suggests separation of *M. abscessus* into three distinct subspecies: *M. abscessus* subsp. *abscessus*, *M. abscessus* subsp. *bolletii*, and *M. abscessus* subsp. *massiliense* (Tortoli et al.,

2016). Although a saprophyte in water and soil, following lung infection *M. abscessus* can swiftly grow and survive intra-cellularly within macrophages as well as in extra-cellular caseous lesions and airway mucus (Wu et al., 2018). Several factors contribute to the success of this rapidly growing mycobacterium. A plethora of intrinsic resistance mechanisms renders almost all clinically used antibiotics ineffective against *M. abscessus* (Nessar et al., 2012). In addition, the presence of a highly dynamic open pan-genome in *M. abscessus* might explain the ease with which the bacterium evolves and adapts to a wide-spectrum of stressful environmental conditions encountered in diverse habitats (Choo et al., 2014; Wu et al., 2018). Importantly, the respiratory habitat of *M. abscessus* brings it in close proximity to highly virulent pathogens (for example, *Pseudomonas aeruginosa* in cystic fibrosis lung) which can serve as donors of novel drug resistance or virulence genes (Ripoll et al., 2009).

Treatment of *M. abscessus* pulmonary infection is very difficult owing to the bacterium's high-level innate resistance towards most antibiotics commonly used for Gram-negative and Gram-positive bacterial infections, including majority of β -lactams, tetracyclines, aminoglycosides, and macrolides. In addition, anti-TB drugs including first-line drugs (such as rifampicin and isoniazid) as well as some second-line agents (such as capreomycin) are ineffective against this pathogen (Table 1). Thus, the term "incurable nightmare" is often used to describe *M. abscessus* (Brown-Elliott et al., 2012; Nessar et al., 2012). So far, no reliable antibiotic regimen has been established for *M. abscessus* pulmonary disease. Antibiotic administration is largely empirical and relies on *in vitro* antibiotic susceptibility testing and definitive subspecies identification (Griffith et al., 2007; Ryu et al., 2016). Treatment of *M. abscessus* pulmonary disease as recommended by the British Thoracic Society involves administration of a multi-drug regimen encompassing intravenous antibiotics - amikacin, tigecycline, and imipenem along with an oral macrolide (clarithromycin or azithromycin) for clinical isolates susceptible to macrolides, during the initial treatment phase. For the continuation phase of treatment, nebulised amikacin and an oral macrolide combined with one to three of the following oral antibiotics: linezolid, clofazimine, minocycline, co-trimoxazole, and moxifloxacin are generally recommended (Haworth et al., 2017). Standard of care calls for continuation of antibiotic therapy for a minimum of 12 months after culture conversion. However, microbiological eradication of *M. abscessus* bacilli from lung tissues, using recommended antibiotic regimens, is rare and recurrence is often after completion of a treatment course and successful symptom management (Jarand et al., 2011; Stout et al., 2016).

Table 1 | Drug susceptibility of *Mycobacterium abscessus* wild-type and isogenic mutants in comparison to screening concentrations for *M. tuberculosis* with decreased susceptibility.

Antimicrobial agent	<i>M. tuberculosis</i> * (mg/L)	<i>M. abscessus</i> MIC (mg/L)	<i>M. abscessus</i> mutant MIC (mg/L)	Reference
Isoniazid	0.1	>512	<i>katG</i> ⁺ (<i>M. tb</i>): 32	Pers. Communication
Rifampicin	1.0	128	Δarr : 0.25	Rominski et al., 2017a
Ethambutol	5.0	64 (polymorphism in target gene)	N.A.	Alcaide et al., 1997
Capreomycin	2.5	>256	$\Delta eis2$: 4	Rominski et al., 2017c
Clarithromycin	N.D.	64	Δerm : 0.5	Choi et al., 2012
Kanamycin B	N.D.	8	$\Delta aac(2')$: 0.125	Rominski et al., 2017c
Amikacin	1.0	4	$\Delta eis2$: 0.25	Rominski et al., 2017c
Streptomycin	1.0	32	$\Delta str(3'')$: 2	Dal Molin et al., 2017
Tetracycline	N.D.	60	$\Delta tetX$: 4	Rudra et al., 2018
Amoxicillin	N.D.	>256	Δbla : 8	Dubée et al., 2015
Ampicillin	N.D.	>256	Δbla : 4	Dubée et al., 2015

*Epidemiologic cutoff values (ECOFF; MGIT960) as defined by Cambau et al. (2015); MIC, minimal inhibitory concentration; N.A., Not available; N.D., Not determined.

As a result of extensive, repeated or inappropriate use of macrolides and aminoglycosides, which inhibit protein biosynthesis by binding to the large and small ribosomal subunits, respectively, *M. abscessus* strains with clinically acquired pan-macrolide and pan-aminoglycoside resistance have emerged, due to mutation(s) in the corresponding 23S (*rrl*) and 16S (*rrs*) rRNA genes (Wallace et al., 1996; Prammananan et al., 1998; Maurer et al., 2012; Nessar et al., 2012). Acquired resistance to macrolides and aminoglycosides severely limits the remaining treatment options and highlights the urgent need for new antimicrobial agents.

Mechanisms underpinning intrinsic drug resistance of *M. abscessus* are multi-fold and fall into two main groups: first, the presence of a highly impermeable cell envelope and/or multi-drug efflux pumps might reduce the effective concentration of antibiotics within the bacterial cells; second, the genome of *M. abscessus* encodes several putative enzymes which can inactivate antibiotics by modification and/or degradation or lower the affinity of the drug for its target by modifying the target (Ripoll et al., 2009; Nessar et al., 2012). For long, molecular investigations aimed at elucidating antibiotic resistance mechanisms of *M. abscessus* were limited, however, significant progress has been made in recent years owing to the development of efficient tools for genetic manipulation of this bacterium (Figure 1). In this article, we provide an up-to-date overview of the main molecular mechanisms of antibiotic resistance in *M. abscessus* with a focus on the drug-target-modifying or drug-modifying enzymes and discuss the potential impact on clinical treatment. We also discuss how this knowledge could facilitate the discovery and development of new improved antimicrobial agents or help rescue the function of currently available antibiotics against *M. abscessus* and provide an update on the latest research underway to combat multi-drug resistant *M. abscessus* infections.

Antibiotic-Target-Modifying Enzymes in *M. abscessus*

Macrolide Resistance: MAB_2297 [*erm(41)*] Encoded Erythromycin Ribosome Methylase

Macrolides are among the most successful antibiotics in the world and are highly prescribed for infections caused by non-tuberculous mycobacteria. A multidrug regimen recommended for *M. abscessus* infections almost always includes macrolides, particularly clarithromycin or azithromycin. Macrolides target the nascent polypeptide exit tunnel within the 50S ribosomal subunit, which accommodates the newly synthesized polypeptide chain as it emerges from the ribosome. Following macrolide binding, the elongation of the polypeptide chain continues up

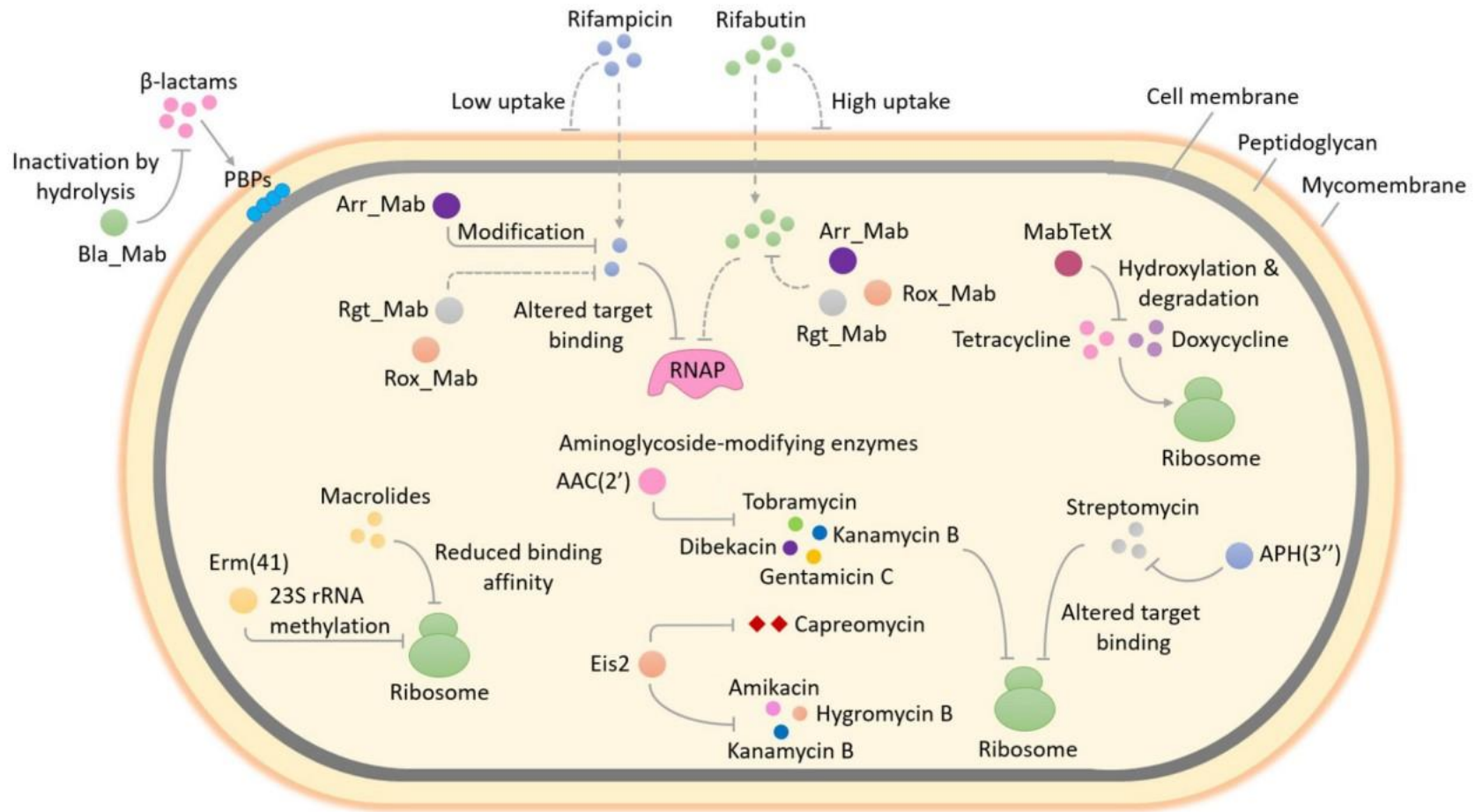


Figure 1 | **Enzyme-mediated antibiotic resistance in *Mycobacterium abscessus*.** *M. abscessus* is intrinsically resistant to a large and diverse array of antimicrobial agents. The occurrence of several enzymes that can modify and/or degrade antibiotics or alter their targets in *M. abscessus* enables it to resist the action of multiple classes of antibiotics. This figure provides an overview of the well-studied as well as some unexplored enzyme-mediated resistance mechanisms in *M. abscessus*. Methylation of 23S rRNA by Erm(41), an erythromycin ribosome methylase, lowers the binding affinity of macrolides for the ribosome exit tunnel and confers macrolide resistance. Expression of the *erm(41)* gene in *M. abscessus* is induced upon exposure to macrolides, therefore this type of resistance by target modification is known as inducible macrolide resistance. The addition of different chemical groups including acyl and phosphate

groups to vulnerable sites on the aminoglycoside molecule by *M. abscessus* enzymes can prevent the binding of aminoglycoside to its ribosomal target due to steric hindrance and result in resistance. A diverse group of enzymes that differ in the aminoglycosides that they can modify as well as in the region of the antibiotic that is modified, are found in *M. abscessus*. These include two putative acetyltransferases - AAC(2') and Eis2 and one putative phosphotransferase - APH(3''). The substrate aminoglycosides for each enzyme are shown. In addition to aminoglycosides, Eis2 can also modify other ribosome-targeting antibiotics like capreomycin. Resistance to rifampicin and other rifamycin antibiotics in *M. abscessus* involves covalent modification and drug inactivation by an ADP-ribosyltransferase, Arr_Mab. Apart from ADP-ribosylation, two additional group transfer mechanisms of rifampicin inactivation including glycosylation, phosphorylation as well as decomposition of rifampicin by monooxygenation, are widespread in environmental bacteria but have not been explored in mycobacteria. Being a saprophyte in soil, exposure to antibiotic producing actinomycetes that utilize a variety of rifamycin inactivating mechanisms in its natural habitat might have favoured the selection of an unknown reservoir of rifamycin resistance genes in *M. abscessus*, for example, those encoding a rifamycin glycosyltransferase (Rgt_Mab) and/or a rifamycin monooxygenase (Rox_Mab) (dashed lines). *M. abscessus* also produces a tetracycline-degrading flavin monooxygenase, MabTetX that activates molecular oxygen to hydroxylate and destabilize the antibiotic, which subsequently undergoes non-enzymatic decomposition, thereby conferring resistance. Resistance to β -lactams in *M. abscessus* is afforded by the production of a hydrolytic β -lactamase enzyme, Bla_Mab with the ability to degrade a broad range of β -lactams including extended-spectrum cephalosporins and carbapenems. RNAP, RNA polymerase; PBPs, penicillin-binding proteins; AAC(2'), 2'-N-acetyltransferase; Eis2, enhanced intracellular survival protein 2; APH(3''), aminoglycoside 3''-O-phosphotransferase.

to a few amino acids before the peptidyl-tRNA dissociates from the ribosome, thereby arresting protein synthesis (Wilson, 2014).

In bacteria, innate resistance towards macrolides is most often the result of increased efflux, ribosomal methyltransferases and GTP-dependent macrolide kinases (Pawlowski et al., 2018). A well-studied example of macrolide resistance by target modification in bacteria is the erythromycin ribosome methylase (Erm) enzyme, which specifically methylates A2058 nucleotide of 23S rRNA and lowers the macrolide affinity for the ribosome exit tunnel (Blair et al., 2015). An Erm methyltransferase is also responsible for inducible macrolide resistance in *M. abscessus* (Figure 1). Interestingly, the *erm(41)* gene, first described by Nash et al. (2009), is only functional in two out of three subspecies of the *M. abscessus* complex. The subspecies *M. massiliense* harbors deletions in its *erm(41)* gene copy, which render the Erm(41) enzyme inactive and the bacterium susceptible to macrolides. This may explain why patients with *M. massiliense* infections have better treatment outcomes than patients with *M. abscessus* or *M. bolletii* infections. To further complicate matters, a T/C polymorphism at position 28 of the *erm(41)* sequence determines the appearance of inducible macrolide resistance in *M. bolletii* and *M. abscessus* subspecies. Only those isolates that harbor a T28 *erm(41)* sequevar develop inducible macrolide resistance. Phenotypic detection of inducible macrolide resistance in the *M. abscessus* complex by drug susceptibility testing requires extended incubation (14 days rather than 3 days) in the presence of the drug (Nash et al., 2009; Kim et al., 2010).

A functional role of *erm(41)* in inducible resistance to macrolides has been confirmed by genetic studies. Deletion of *erm(41)* in *M. abscessus* lowered the minimal inhibitory concentration (MIC) of clarithromycin by 128-fold (Table 1), while introduction of a functional *M. abscessus erm(41)* gene into *M. massiliense* led to a 64-fold increase in the clarithromycin MIC on day 14 (Choi et al., 2012). Inducible Erm(41)-dependent rRNA methylation severely affects the efficacy of macrolides against *M. abscessus*. The long duration of partially effective macrolide therapy, eventually favours the emergence of isolates with high-level constitutive macrolide resistance. Mutations that alter the 23S rRNA nucleotides 2058 and 2059 within the peptidyl-transferase center (PTC), are a frequent cause of constitutive macrolide resistance in *M. abscessus* (Wallace et al., 1996; Bastian et al., 2011; Brown-Elliott et al., 2015).

Antibiotic-Modifying Enzymes in *M. abscessus*

Aminoglycoside Resistance: MAB_4395 [*aac(2')*] & MAB_4532c (*eis2*) Encoded Acetyltransferases; MAB_2385 Encoded 3''-*O*-Phosphotransferase

Aminoglycosides are among the broadest classes of antibiotics that interfere with specific steps in bacterial protein synthesis (Kohanski et al., 2010). All aminoglycosides primarily target the 16S rRNA component of 30S ribosomal subunit, however, their exact binding site and mode of action may differ slightly depending on their chemical structure. For example, 2-deoxystreptamine (2-DOS) aminoglycosides (such as kanamycin, amikacin, apramycin, arbekacin), which are chemically distinct from the non-DOS aminoglycosides (for example, streptomycin), specifically bind to the A-site region of small ribosomal subunit at the decoding center, encompassing conserved nucleotides A1492 and A1493 of 16S rRNA. 2-DOS aminoglycosides function by inhibiting the translocation of tRNA-mRNA complex through the ribosome. Additionally, several members of this class also induce protein mistranslation by promoting and stabilizing the interaction of non-cognate aminoacylated tRNAs with mRNA. In contrast, the non-DOS aminoglycoside streptomycin targets a different region of 16S rRNA in proximity of the decoding center and mainly interferes with the delivery of aminoacylated tRNA to the A-site (Wilson, 2014).

Bacterial resistance to aminoglycosides may occur due to low cell permeability/efflux, mutations or modification of 16S rRNA, mutations in ribosomal protein genes and enzymatic drug modification. Drug and target modification being the most extensively studied and clinically relevant aminoglycoside resistance mechanisms in pathogenic bacteria. Covalent modification of key amino or hydroxyl groups within the aminoglycoside molecule by bacterial enzymes markedly decreases the binding affinity for the ribosomal target and confers aminoglycoside resistance. Aminoglycoside-modifying enzymes in bacteria can be grouped into three main classes namely, acetyltransferases, nucleotidyltransferases, and phosphotransferases (D'Costa et al., 2011; Blair et al., 2015). A worrying discovery that the genome of emerging pathogen *M. abscessus* encodes several putative aminoglycoside-modifying enzymes which include members of all three classes, came in 2009 when Ripoll et al first sequenced the complete genome of *M. abscessus* (Ripoll et al., 2009). Some predictions were later substantiated by drug susceptibility testing and biochemical analysis (Maurer et al., 2015). More recently, direct genetic evidence for a functional role of some of these putative aminoglycoside-modifying enzymes in *M. abscessus* intrinsic resistance to this antibiotic class, was obtained.

Similar to all other mycobacteria that have been studied so far (Aínsa et al., 1997), *M. abscessus* also harbors a 2'-*N*-acetyltransferase [AAC(2')], encoded by MAB_4395 gene. This enzyme is capable of acetylating several aminoglycosides bearing a 2' amino group including gentamicin

C, dibekacin, tobramycin and kanamycin B (Figure 1). This was evident upon deletion of MAB_4395 in *M. abscessus* ATCC 19977 strain, which led to a 4-64-fold reduction in the MICs of these aminoglycosides (Table 1) (Rominski et al., 2017c). Interestingly, another *N*-acetyltransferase capable of conferring aminoglycoside resistance in *M. abscessus* is a homolog of *Anabaena variabilis* enhanced intracellular survival (Eis) protein (Figure 1). Eis proteins are widespread in mycobacteria as well as other Gram-positive bacteria. Eis protein in *Mycobacterium tuberculosis* has been shown to enhance intracellular survival within macrophages by acetylating and activating dual-specificity protein phosphatase 16/mitogen-activated protein kinase phosphatase-7 (DUSP16/MPK-7), a JNK-specific phosphatase that inhibits inflammation, autophagy and subsequent death of infected macrophages (Shin et al., 2010; Kim et al., 2012). Furthermore, upregulation of *eis* gene expression owing to mutations in its promoter was associated with kanamycin resistance in one-third of clinical isolates encompassing a large collection of *M. tuberculosis* strains from diverse geographical locations (Zaunbrecher et al., 2009). More recently, structural and biochemical characterization of *M. tuberculosis* Eis revealed its unprecedented ability to acetylate multiple amines of several aminoglycosides (Chen et al., 2011).

Analysis of *M. abscessus* genome revealed two genes, namely, MAB_4124 (*eis1*) and MAB_4532c (*eis2*), which show homology to *eis* from *M. tuberculosis* (Rv2416c) and *A. variabilis* (Ava_4977), respectively. Drug susceptibility testing could confirm a functional role for Eis2 but not Eis1, in intrinsic aminoglycoside resistance. Of note, deletion of MAB_4532c enhanced *M. abscessus* susceptibility towards a heterogeneous group of aminoglycosides including the cornerstone drug amikacin as well as a non-aminoglycoside antibiotic capreomycin (Table 1) (Rominski et al., 2017c). Furthermore, heterologous expression of *eis2* in *Mycobacterium smegmatis* decreased amikacin susceptibility (Hurst-Hess et al., 2017). Capreomycin is a cyclic peptide antibiotic that inhibits protein synthesis by blocking peptidyl-tRNA translocation. The drug is particularly active against *M. tuberculosis* and commonly used as a second-line agent for the treatment of TB (Stanley et al., 2010; Wilson, 2014). Although remarkable, the discovery that *M. abscessus* Eis2 exhibits a broad-spectrum acetyltransferase activity is not a real surprise. In fact, recent structural and functional studies on Eis enzymes from *M. tuberculosis* (Eis_Mtb), *M. smegmatis* (Eis_Msm), and *A. variabilis* (Eis_Ava) revealed the presence of an unusually large and complex active site unlike in other aminoglycoside acetyltransferases. The unique structure equips Eis with a regio-versatile multi-acetylating acetyltransferase activity towards a broad range of substrates (Chen et al.,

2012; Pricer et al., 2012; Jennings et al., 2013). However, there seems to be a notable difference between the acetylation activities of *M. abscessus* Eis2 and *M. tuberculosis* Eis especially towards capreomycin as the MIC of capreomycin in *M. abscessus* is about 100-fold higher than that in *M. tuberculosis* and this difference is almost completely abolished by the deletion of *eis2* gene (Table 1) (Rominski et al., 2017c).

Aminoglycoside acetyltransferases Eis2 and AAC(2') do not appear to modify streptomycin, an aminoglycoside which exhibits moderate *in vitro* activity against *M. abscessus* (MIC: 32 mg/L) (Rominski et al., 2017c). Instead, a MAB_2385 encoded putative aminoglycoside 3''-*O*-phosphotransferase is the main determinant for intrinsic streptomycin resistance in *M. abscessus* (Figure 1). Twelve putative aminoglycoside phosphotransferases are encoded in the genome of *M. abscessus* (Ripoll et al., 2009). Among them, MAB_2385 was found to be a close homolog of *aph(3'')-Ic*, an aminoglycoside 3''-*O*-phosphotransferase gene, which was previously shown to confer streptomycin resistance in *Mycobacterium fortuitum* (Ramón-García et al., 2006). Deletion of MAB_2385 enhanced the susceptibility of *M. abscessus* towards streptomycin by 16-fold (Table 1). Furthermore, MAB_2385 was able to confer streptomycin resistance when heterologously expressed in *M. smegmatis* (Dal Molin et al., 2017). To the best of our knowledge, other annotated aminoglycoside phosphotransferases (such as MAB_0163c, MAB_0313c, MAB_0327, MAB_0951, and MAB_1020) and aminoglycoside acetyltransferases (for example, MAB_0247c, MAB_0404c, MAB_0745, MAB_4235c, and MAB_4324c) have not been addressed experimentally, however, interesting regulatory features of drug resistance genes have been elucidated.

A WhiB7 like protein encoded by MAB_3508c was recently uncovered as a multi-drug inducible transcriptional regulator that modulates the expression of genes conferring aminoglycoside and macrolide resistance in *M. abscessus*. WhiB7, an autoregulatory transcriptional activator, is a determinant of innate antibiotic resistance in mycobacteria. In *M. tuberculosis*, genes conferring antibiotic resistance including *ermMT* (Rv1988), *eis* (Rv2416c) and *tap* (Rv1258c) are induced in a *whiB7*-dependent manner, upon exposure to antibiotics. Similarly, the *erm(41)* and *eis2* genes in *M. abscessus* are included in the *whiB7* regulon (Hurst-Hess et al., 2017). A recent study by Pryjma et al. (2017) demonstrated that exposure to sub-inhibitory levels of clarithromycin enhanced amikacin as well as clarithromycin resistance in *M. abscessus* in a *whiB7*-dependent manner. Of note, deletion of MAB_3508c rendered *M. abscessus* more susceptible to amikacin (fourfold) and clarithromycin (eightfold), while complementation with an intact gene copy restored resistance to these antibiotics, suggesting a

role of *whiB7* in *M. abscessus* amikacin and clarithromycin resistance. Interestingly, pre-exposure to clarithromycin, which is a potent inducer of *M. abscessus whiB7*, enhanced the resistance of *M. abscessus* wild-type strain towards amikacin by fourfold but had no effect on amikacin susceptibility of a $\Delta whiB7$ mutant. In addition, pre-treatment with clarithromycin markedly increased resistance to itself in the wild-type strain but did not alter clarithromycin sensitivity of a $\Delta whiB7$ mutant. Furthermore, a quantitative reverse transcription-PCR assay revealed a *whiB7*-dependent upregulation of *eis2* and *erm(41)* genes following pre-exposure to clarithromycin. These observations support the following conclusions: (i) in *M. abscessus*, *whiB7* (MAB_3508c) activates the expression of genes which confer amikacin and clarithromycin resistance, i.e., *eis2* and *erm(41)*, (ii) strong induction of *whiB7* following exposure to clarithromycin confers cross-resistance to amikacin in addition to activating inducible macrolide resistance (Pryjma et al., 2017). Thus, *in vitro* findings by Pryjma et al. (2017) suggest that front-line antibiotics, amikacin and clarithromycin may exhibit antagonistic effects when used in combination for the treatment of *M. abscessus* infections. This may at least partially explain the limited clinical efficacy of currently recommended multi-drug regimen for *M. abscessus* which almost always includes these two antibiotics.

Tetracycline Resistance: MAB_1496c Encoded Flavin Monooxygenase

Tetracyclines are a class of broad-spectrum natural product antibiotics that interfere with bacterial protein synthesis. These drugs bind with high affinity to the small ribosomal subunit and specifically interfere with the delivery of aminoacylated tRNA to the A-site (Kohanski et al., 2010; Wilson, 2014). While tetracyclines are an important class of ribosome-targeting antibiotics, their anthropogenic and prolific use in the clinic and agriculture has led to emergence of resistance among benign as well as pathogenic bacteria, thereby limiting their efficacy. Despite growing resistance, tetracyclines continue to remain one of the most successful and widely used chemotherapeutics against bacterial infections (Allen et al., 2010). Furthermore, a renaissance for tetracyclines is being fuelled by the development of next-generation derivatives such as tigecycline, approved for clinical use in 2005 and omadacycline and eravacycline, undergoing late-phase clinical trials (Kinch and Patridge, 2014). In fact, tigecycline is the only new antibiotic and the sole member of its class, which has been introduced in the treatment of recalcitrant *M. abscessus* lung disease with clinical evidence (Wallace et al., 2014).

Previously, resistance towards tetracyclines was thought to be exclusively mediated by two mechanisms namely, drug efflux and ribosome protection. However, evidence for enzymatic

inactivation of tetracyclines by a family of flavin adenine dinucleotide (FAD)-dependent monooxygenases in both benign and pathogenic bacteria has been recently documented. Few well characterized examples of such tetracycline-modifying enzymes include TetX from the obligate anaerobe *Bacteroides fragilis* and Tet(56) found in the human pathogen *Legionella longbeachae*, the causative agent of Legionnaires' disease and Pontiac fever (Yang et al., 2004; Park et al., 2017). Whether such a mechanism of tetracycline resistance existed in mycobacteria was not known until recently, when Rudra and colleagues demonstrated through elegant experiments, that high levels of intrinsic resistance towards tetracycline and second-generation derivative doxycycline in *M. abscessus* was mediated by a flavin monooxygenase, MabTetX (Figure 1). Deletion of MAB_1496c (encoding a putative FAD binding monooxygenase) enhanced the susceptibility of *M. abscessus* towards tetracycline and doxycycline by 15–20-fold (Table 1), while a complemented Δ MAB_1496c strain exhibited even higher levels of resistance towards both antibiotics compared to the wild-type strain, supporting the notion that MAB_1496c is a primary determinant for *M. abscessus* intrinsic tetracycline resistance. Furthermore, UV-Visible and mass spectrometry assays with purified MAB_1496c protein provided evidence for hydroxylation and subsequent degradation of tetracycline and doxycycline by MabTetX (Rudra et al., 2018). Interestingly, MAB_1496c is not a member of the *whiB7* regulon, even though tetracycline is a strong inducer of *whiB7* in *M. abscessus* (Hurst-Hess et al., 2017). In fact, MabTetX expression is regulated by a TetR family repressor, MabTetRx (encoded by the upstream gene MAB_1497c) which represses the MAB_1497c-MAB_1496c operon by binding to a 35bp operator sequence *tetO*. This repression is relieved in the presence of tetracycline and doxycycline which can bind the repressor protein, thereby preventing its interaction with the *tetO* operator (Rudra et al., 2018).

The glycolcylcine antibiotic tigecycline, specifically designed to evade resistance by ribosome protection and efflux, is not invulnerable to modification by *Bacteroides* TetX, which was recently also identified in numerous clinically relevant pathogens (Volkers et al., 2011; Leski et al., 2013). Although tigecycline was found to be a poor substrate of TetX, alarmingly, enzymatic activity of TetX was substantially improved upon acquisition of single amino acid substitutions to confer resistance at clinically relevant tigecycline concentrations when overexpressed in *Escherichia coli* (Linkevicius et al., 2016). Surprisingly, tigecycline resisted MabTetX-dependent degradation and did not induce its expression, which might contribute to its excellent *in vitro* activity and moderate clinical efficacy against *M. abscessus* (Rudra et al., 2018). However, selective pressure exerted by tigecycline will eventually favour the emergence

of *M. abscessus* isolates carrying extended-spectrum FAD-monoxygenases with the ability to modify glycolcyclines.

Another interesting feature is the ability of anhydrotetracycline (ATc), a degradation product of tetracycline with poor antibiotic activity, which was recently shown to be a competitive inhibitor of TetX and Tet(56) flavin monoxygenases, to rescue antibiotic activities of tetracycline and doxycycline against *M. abscessus* expressing MabTetX (Park et al., 2017; Rudra et al., 2018). However, ATc was also found to induce MabTetX expression by binding the MabTetRx repressor, a property at odds with its MabTetX inhibition activity. While this finding together with the severe side effects associated with ATc use, makes it an unattractive drug candidate, it nevertheless represents a flexible starting point for developing MabTetX inhibitors with improved activity, better tolerability and minimal binding affinity towards MabTetRx. Co-administration with a potent MabTetX monoxygenase inhibitor can potentially rescue the clinical efficacies of tetracycline and doxycycline which are currently inactive against the *M. abscessus* complex (Burgos et al., 2011; Rudra et al., 2018).

β-Lactam Resistance: MAB_2875 Encoded β-Lactamase

β-Lactams constitute an important class of antibiotics that function by inhibiting cell wall synthesis in bacteria. The β-lactam structure closely resembles the terminal D-alanyl-D-alanine dipeptide of peptidoglycan, a substrate of penicillin binding proteins (also known as D, D-transpeptidases) that catalyze the final cross-linking step of peptidoglycan synthesis. Penicilloylation of the D, D-transpeptidase active site following treatment with β-lactams disables the enzyme and prevents the formation of peptidoglycan cross-links, thereby interfering with cell wall biosynthesis (Kohanski et al., 2010). Despite being the cornerstones of antimicrobial chemotherapy and constituting one of the largest groups of antibiotics available today, only two members of the β-lactam class, namely, cefoxitin (a cephalosporin) and imipenem (a carbapenem), form a part of the antibiotic arsenal for *M. abscessus*. Furthermore, cefoxitin and imipenem have been shown to exhibit only moderate *in vitro* activity against *M. abscessus* with MICs of 32 and 4 mg/L, respectively (Lavollay et al., 2014). Majority of the other β-lactam antibiotics are not effective against this bacterium.

Several possible mechanisms may contribute to β-lactam resistance in *M. abscessus*. Low mycomembrane permeability and β-lactamase production may reduce the effective concentration of β-lactams at the site of action. Alternatively, modification of the transpeptidase profile of the cell by replacement of penicillin binding proteins (D, D-transpeptidases) with L,

D-transpeptidases for instance, may reduce the activity of penicillins and cephalosporins that have lower affinities for L, D-transpeptidases (Wivagg et al., 2014). However, most of the abovementioned resistance mechanisms are relatively unexplored in this organism except for one. Recently it was shown that the genome of *M. abscessus* encodes a strong, constitutive class A β -lactamase (Bla_Mab), which renders it highly resistant towards most β -lactams (Figure 1). The *M. abscessus* β -lactamase Bla_Mab, encoded by MAB_2875 is endowed with an exceptional broad-spectrum activity and can effectively hydrolyse several members of first- and second-generation cephalosporins, carbapenems, and penams (Soroka et al., 2014). The currently recommended β -lactams, namely, imipenem and ceftiofur, are substrates of Bla_Mab, however, they are hydrolysed at a very slow rate, which may contribute to their clinical efficacy. The instability of imipenem complicates drug susceptibility testing when generation times of test bacteria require incubation for several days as in the case of *M. abscessus* (Rominski et al., 2017b).

One strategy to overcome the hurdle of chromosomally encoded β -lactamase in *M. abscessus* is to co-administer a β -lactamase inhibitor with the failing β -lactam. Soroka and colleagues evaluated the *in vitro* efficacy of nitrocefin and meropenem in combination with approved β -lactamase inhibitors clavulanate, tazobactam, and sulbactam against Bla_Mab. Surprisingly, Bla_Mab inhibition was not detected for all the three inhibitor drugs (Soroka et al., 2014). This remarkable ability of Bla_Mab to resist inhibition even surpasses that of BlaC, a class A β -lactamase encoded by *M. tuberculosis*. Although BlaC is able to reverse inhibition caused by tazobactam and sulbactam, and return to its native functional form, clavulanate can slowly but irreversibly inhibit this enzyme (Sagar et al., 2017). In fact, a recent demonstration of *in vitro* synergy between meropenem and clavulanate in 13 extensively drug resistant (XDR) *M. tuberculosis* strains raised a renewed interest in β -lactams for use in TB therapy (Hugonnet et al., 2009). Fortunately, a surprising finding that *M. abscessus* Bla_Mab is effectively disabled by the newly approved β -lactamase inhibitor avibactam provides a new hope for old antibiotics. A study by Dub  e et al. (2015) showed that co-administering a small amount of avibactam (4 mg/L) with each of several representative antibiotics from three important β -lactam sub-classes (carbapenems, penams, and cephalosporins) lowered their MICs in *M. abscessus* CIP104536 strain to levels comparable to those observed in a β -lactamase deficient mutant. The authors also reported synergy between avibactam and amoxicillin within macrophages as well as in a zebrafish model of *M. abscessus* infection (Dub  e et al., 2015). More recently, an *in vitro* synergy screen of 110 β -lactam - β -lactamase inhibitor combinations against an *M. abscessus*

clinical isolate identified six potential hits. Five selected β -lactamase inhibitors encompassing both β -lactam-based (clavulanate, tazobactam, and sulbactam) as well as non- β -lactam-based inhibitors (avibactam and vaborbactam) were evaluated for synergistic effects with a large panel of β -lactams. Importantly, all observed synergy combinations exclusively involved non- β -lactam-based inhibitors, either avibactam or vaborbactam. Combinations of avibactam with each of the following drugs including ampicillin, amoxicillin, tebipenem, and panipenem displayed synergistic effects against *M. abscessus*. Furthermore, the carbapenems — tebipenem and panipenem — also exhibited synergy with a novel boronic acid β -lactamase inhibitor, vaborbactam (Aziz et al., 2018). Thus, non- β -lactam-based β -lactamase inhibitors such as avibactam and vaborbactam can potentially extend the spectrum of β -lactams employed for the treatment of largely incurable, chronic *M. abscessus* pulmonary infections.

Rifamycin Resistance: MAB_0591 Encoded ADP-Ribosyltransferase

Rifampicin, a rifamycin antibiotic commonly employed as a first-line agent in the treatment of *M. tuberculosis* infections, hardly exhibits any activity towards the *M. abscessus* complex (MIC: 128 mg/L) (Table 1). Since rifamycins inhibit transcription by binding with high affinity to *rpoB* encoded β -subunit of bacterial RNA polymerase, resistance towards this group of antibiotics is most commonly conferred by point mutations within the target gene *rpoB*, especially in *M. tuberculosis* (Campbell et al., 2001). However, additional rifamycin resistance mechanisms that involve enzymatic drug inactivation are also prevalent in other mycobacterial species. The presence of a rifamycin ADP-ribosyltransferase in *M. smegmatis* was known for quite a while (Quan et al., 1997), however, only recently, genetic studies involving gene knockout and heterologous expression unveiled the existence of a MAB_0591 encoded ADP-ribosyltransferase as the major determinant for high levels of innate rifamycin resistance in *M. abscessus* (Figure 1). Deletion of MAB_0591 enhanced the susceptibility of *M. abscessus* towards three tested rifamycins, including rifaximin, rifapentine and rifampicin by 64–512-fold, respectively (Rominski et al., 2017a).

Surprisingly, a rifampicin derivative, rifabutin showed up as an attractive hit (MIC: 2.5 mg/L), when a set of 2,700 FDA-approved drugs were screened against a clinical isolate of *M. abscessus*. Rifabutin exhibited approximately 10-fold higher potency *in vitro* relative to rifampicin and rifapentine against reference strains representative of all three subspecies of the *M. abscessus* complex as well as a collection of clinical isolates and its bactericidal activity was comparable to or better than that of clarithromycin, one of the cornerstone drugs for *M. abscessus* infections (Aziz et al., 2017). The higher efficacy of rifabutin relative to rifampicin

in *M. abscessus* as well as in *M. tuberculosis* (with no known rifamycin inactivating enzymes) suggests its increased accumulation within the bacterial cells. This may be due to differences in membrane penetration or specificity of efflux systems towards different rifamycins (Figure 1). Based on the findings reported by Aziz et al. (2017), rifampicin analog rifabutin, appears to be a potential candidate for repurposing and its clinical efficacy in patients with *M. abscessus* pulmonary disease should be further explored.

Clinical Relevance

Although the inherent ability of *M. abscessus* to exhibit resistance to a wide array of antibiotics has long been recognized, our knowledge of the prodigious diversity of mechanisms involved has improved immensely in recent years, owing to the development of tools for genetic manipulation of *M. abscessus*. A better understanding of the genetic basis of innate antibiotic resistance is a prerequisite for the discovery and development of synergistic drug combinations, where one agent serves to salvage the antibacterial activity of a failing antibiotic by inhibiting an intrinsic resistance mechanism. This is exemplified by the recent discovery that avibactam is a potent inhibitor of *M. abscessus* β -lactamase Bla_{Mab}. When used in combination, avibactam lowered the MICs of several β -lactams in *M. abscessus* by 4–32-fold (Dubée et al., 2015; Kaushik et al., 2017). Despite the success of β -lactamase inhibitors, the concept of designing drugs which target intrinsic resistance mechanisms in bacteria, has not gained substantial clinical exploitation beyond this antibiotic class (Brown, 2015). Recently, a repertoire of drug-modifying and target-modifying enzymes conferring innate resistance to aminoglycosides, tetracyclines, rifamycins, and macrolides in *M. abscessus* were delineated (Nash et al., 2009; Dal Molin et al., 2017; Rominski et al., 2017a,c; Rudra et al., 2018). Likewise, attempts to identify chemical entities, which could potentially rescue the function of one or more key members from each aforementioned antibiotic group, should be pursued in the near future.

Since the discovery that mutations within *eis* promoter are associated with kanamycin resistance in *M. tuberculosis*, vigorous attempts to identify Eis inhibitors that can potentially rescue kanamycin activity in this pathogen have been pursued with notable success. Recently, several structurally diverse competitive Eis inhibitors with 1,2,4-triazino[5,6*b*]indole-3-thioether-based, sulfonamide-based, pyrrolo[1,5-*a*]pyrazine-based and isothiazole S,S-dioxide heterocyclic scaffolds were identified by highthroughput screenings of large compound libraries. Importantly, few promising inhibitors could completely restore kanamycin

susceptibility in a kanamycin resistant *M. tuberculosis* strain *in vitro* at concentrations that were non-cytotoxic to mammalian cells (Green et al., 2012; Garzan et al., 2016, 2017; Willby et al., 2016; Ngo et al., 2018). Remarkably, inhibitors designed for *M. tuberculosis* Eis, were also found to be active against Eis homologs in *M. smegmatis* and *A. variabilis* (Chen et al., 2012; Pricer et al., 2012). These findings give rise to an intriguing possibility that Eis_Mtb inhibitors may be able to overcome Eis2 mediated resistance towards aminoglycoside and/or non-aminoglycoside antibiotics like capreomycin and restore their effectiveness against *M. abscessus*. Hence efforts to explore the activity of Eis_Mtb inhibitors against *M. abscessus* Eis2 enzyme should be undertaken. Alternatively, extending drug discovery efforts towards targeting WhiB7, could be a possible strategy to tackle intrinsic macrolide and aminoglycoside resistance in *M. abscessus*. WhiB7 is a conserved transcriptional regulator in mycobacteria that co-ordinates intrinsic resistance to a wide range of ribosome-targeting drugs (Burian et al., 2012). Recent evidence suggests that genes which contribute to intrinsic aminoglycoside and macrolide resistance in *M. abscessus*, i.e., *eis2* and *erm(41)*, are induced in a *whiB7*-dependent manner upon exposure to ribosomal antibiotics (Hurst-Hess et al., 2017). Thus, with the aim to kill two birds with one stone, compounds that prevent the induction of *eis2* and *erm(41)* resistance genes in *M. abscessus* by modulating the synthesis and/or activity of WhiB7, should be sought.

Since the discovery and development of compounds that can circumvent existing resistance mechanisms in *M. abscessus* is a daunting and time-consuming task, an immediate and relatively simple solution to improve treatment efficacy may involve repurposing and repositioning of currently available antibiotics. A number of candidate drugs suited for this purpose have been reviewed in detail elsewhere (Wu et al., 2018) and are therefore only briefly mentioned here. For example, a systematic screening of a collection of FDA-approved drugs revealed rifabutin, an analog of rifampicin, exhibiting potent *in vitro* activity against *M. abscessus* (MIC: 2.5 mg/L) (Aziz et al., 2017). Similarly, clofazimine, a leprosy drug currently repurposed for treatment of TB, was also found to be active against *M. abscessus*. In addition to promising *in vitro* activity (MIC \leq 1 mg/L), clofazimine displayed adequate clinical efficacy and safety when evaluated in patients with *M. abscessus* pulmonary infections (Yang et al., 2017). Likewise, a novel oxazolidinone LCB01-0371, presently in Phase II clinical development for TB, exhibited high potency against *M. abscessus* compared to linezolid, an FDA-approved drug of the same class (Kim et al., 2017). Moreover, some aminoglycosides such as kanamycin A, apramycin, isepamicin, and arbekacin were also found to exhibit potent

in vitro activities against *M. abscessus* (MICs \leq 1 mg/L) (Rominski et al., 2017c). Besides these, other compounds that have been extensively studied for their inhibitory effects against *M. abscessus* encompass anti-TB drug bedaquiline, some TB actives like indole-2-carboxamides and piperidinol-based compound 1 (PIPD1) as well as second-generation thiacetazone derivatives like D6, D15, and D17 (Dupont et al., 2016, 2017; Franz et al., 2017; Halloum et al., 2017; Kozikowski et al., 2017).

In addition, several recent studies have reported *in vitro* synergies between novel combinations of existing antibiotic classes. For example, vancomycin, an inhibitor of cell wall synthesis, exhibited synergy with clarithromycin, an inhibitor of protein synthesis, in *M. abscessus* (Mukherjee et al., 2017). Likewise, a combination of tigecycline (which inhibits protein synthesis) with teicoplanin (which disrupts peptidoglycan synthesis) displayed a strong synergistic effect against *M. abscessus* (Aziz et al., 2018). Since the mycobacterial cell envelope forms a major permeability barrier, drugs that perturb cell wall integrity, are likely to synergize with drugs having intracellular targets (Le Run et al., 2018). Such combinations based on mechanistic drug action should be further explored for synergistic effects against *M. abscessus*. For example, PIPD1 and indole-2-carboxamides, which disrupt mycolic acid synthesis by targeting MmpL3 transporter in mycobacteria (Dupont et al., 2016; Franz et al., 2017), may be able to potentiate the effects of other drugs modulating intracellular targets.

Taken together, a huge reservoir of intrinsic resistance genes combined with an unusually high evolutionary potential of its genome to acquire resistance renders almost all available antibiotics ineffective against *M. abscessus*. Therefore, in the long run, a better understanding of natural resistance mechanisms in *M. abscessus* will help jump start drug discovery projects for (i) compounds that can rescue current antibiotics by neutralizing intrinsic resistance (termed antibiotic resistance breakers), (ii) new drugs with one or more improved properties like ability to resist enzymatic modification and/or degradation, high affinity for modified or mutated targets, better solubility/uptake and low propensity for efflux (Brown, 2015). In the short run, available knowledge from studies seeking synergy between antibiotics together with those investigating potential candidates for repurposing, will aid in the development of dosing regimens that display adequate clinical efficacy and resistance to which will only emerge slowly.

Outlook and Perspectives

Molecular genetic tools that allow investigators to systematically probe gene function in mycobacteria by generation of unmarked gene deletions and functional complementation, have proven extremely useful in dissecting the intrinsic resistome of *M. abscessus* while genetic investigations in other NTM species are still lagging behind. Using the available genetic ‘toolkit,’ 7 orthologs of known resistance gene families have been discovered so far in *M. abscessus* that provide resistance or ‘immunity’ against antibiotics targeting major cellular pathways including cell wall synthesis (β -lactams), RNA synthesis (rifamycins) and protein synthesis (macrolides, aminoglycosides, and tetracyclines). The impressive resistance diversity shown by *M. abscessus* is expected given its natural habitat is shared by many antibiotic producers, primarily the soil dwelling actinomycetes which are also reservoirs of extensively diverse resistance elements (Pawlowski et al., 2016; Crofts et al., 2017; Koteva et al., 2018). Exposure to a variety of noxious antimicrobial molecules in the soil might have favoured selection of specialized and diverse resistance mechanisms in *M. abscessus* as well as in other NTM species.

Till now, the approach that researchers used to systematically probe the intrinsic resistome of *M. abscessus* involved analysis of few selected genes identified based on homology to known resistance determinants from other bacteria. As a result, this approach mainly revealed genes within *M. abscessus* that were involved in previously known resistance mechanisms and disguised the presence of potential determinants of entirely new resistance mechanisms that lack characterized homologs in other bacteria. To capture the remarkable resistance diversity of *M. abscessus* as well as other environmental NTM with unprecedented depth, future studies in this field should incorporate next-generation approaches that provide a comprehensive genome-wide definition of loci required for antibiotic resistance, using cutting-edge technologies. One such technique which can efficiently mine resistance determinants with novel sequences as well as assign resistance functions to known genes that were not previously shown to be involved in drug resistance, is the most recent incarnation of insertional mutagenesis, called transposon insertion sequencing (TIS) (Chao et al., 2016).

The utility of TIS in elucidating novel antibiotic resistance functions is highlighted by its recent application to the discovery of a repertoire of previously unknown intrinsic factors impacting resistance to antibiotics of different classes, including oxazolidinones, fluoroquinolones, and aminoglycosides in pathogens of high clinical concern such as *Staphylococcus aureus*, *P.*

aeruginosa and *E. coli* (Gallagher et al., 2011; Shan et al., 2015; Rajagopal et al., 2016). Screening large collections of transposon insertion mutants for antibiotic susceptibility using TIS approach, has identified promising novel targets for drugs that can restore or enhance susceptibility to existing antibiotics. For example, analysis of insertion mutants spanning all non-essential *S. aureus* genes for fitness defects resulting from exposure to antibiotics identified pathways/genes, including *graRS* and *vraFG* (*graRS/vraFG*), *fntA*, *mprF*, *SAOUHSC_01025*, and *SAOUHSC_01050*, which if inhibited, can greatly improve the efficacy of existing antibiotics, including daptomycin, vancomycin, gentamicin, ciprofloxacin, oxacillin, and linezolid and extend their utility for treating *S. aureus* infections (Rajagopal et al., 2016).

In the coming years, high-throughput next-generation strategies like TIS will undoubtedly rise to prominence in the NTM drug resistance field and radically advance our understanding of resistance mechanisms in *M. abscessus* and other emerging NTM pathogens. Such breakthrough technologies will greatly impact the kinds of questions which can be addressed in this field, for example, which resistance elements unique to *M. abscessus* render it unusually more drug resistant than other NTM species? or does *M. abscessus* already carry genes which confer resistance to novel NTM drugs in development?

Funding

Research in the group of PS was supported by the Swiss National Science Foundation (#31003A_153349), Lungenliga Schweiz, the Institute of Medical Microbiology and the University of Zurich.

Acknowledgements

We acknowledge the members of the research group for stimulating discussions and support.

References

1. Allen, H. K., Donato, J., Wang, H. H., Cloud-Hansen, K. A., Davies, J., and Handelsman, J. (2010). Call of the wild: antibiotic resistance genes in natural environments. *Nat. Rev. Microbiol.* 8, 251–259. doi: 10.1038/nrmicro2312
2. Aziz, D. B., Low, J. L., Wu, M.-L., Gengenbacher, M., Teo, J. W. P., Dartois, V., et al. (2017). Rifabutin is active against *Mycobacterium abscessus* complex. *Antimicrob. Agents Chemother.* 61:e00155-17. doi: 10.1128/AAC.00155-17
3. Aziz, D. B., Teo, J. W. P., Dartois, V., and Dick, T. (2018). Teicoplanin - tigecycline combination shows synergy against *Mycobacterium abscessus*. *Front. Microbiol.* 9:932. doi: 10.3389/fmicb.2018.00932
4. Bastian, S., Veziris, N., Roux, A.-L., Brossier, F., Gaillard, J.-L., Jarlier, V., et al. (2011). Assessment of Clarithromycin Susceptibility in Strains Belonging to the *Mycobacterium abscessus* Group by *erm*(41) and *rrl* Sequencing. *Antimicrob. Agents Chemother.* 55, 775–781. doi: 10.1128/AAC.00861-10
5. Blair, J. M. A., Webber, M. A., Baylay, A. J., Ogbolu, D. O., and Piddock, L. J. V. (2015). Molecular mechanisms of antibiotic resistance. *Nat. Rev. Microbiol.* 13, 42–51. doi: 10.1038/nrmicro3380
6. Brown, D. (2015). Antibiotic resistance breakers: can repurposed drugs fill the antibiotic discovery void? *Nat. Rev. Drug Discov.* 14, 821–832. doi: 10.1038/nrd4675
7. Brown-Elliott, B. A., Nash, K. A., and Wallace, R. J. (2012). Antimicrobial susceptibility testing, drug resistance mechanisms, and therapy of infections with nontuberculous mycobacteria. *Clin. Microbiol. Rev.* 25, 545–582. doi: 10.1128/CMR.05030-11
8. Brown-Elliott, B. A., Vasireddy, S., Vasireddy, R., Iakhiaeva, E., Howard, S. T., Nash, K., et al. (2015). Utility of sequencing the *erm*(41) gene in isolates of *Mycobacterium abscessus* subsp. *abscessus* with low and intermediate clarithromycin MICs. *J. Clin. Microbiol.* 53, 1211–1215. doi: 10.1128/JCM.02950-14
9. Brown-Elliott, B. A., and Wallace, R. J. (2002). Clinical and Taxonomic Status of Pathogenic Nonpigmented or Late-Pigmenting Rapidly Growing Mycobacteria. *Clin. Microbiol. Rev.* 15, 716–746. doi: 10.1128/CMR.15.4.716-746.2002
10. Bryant, J. M., Grogono, D. M., Rodriguez-Rincon, D., Everall, I., Brown, K. P., Moreno, P., et al. (2016). Population-level genomics identifies the emergence and

- global spread of a human transmissible multidrug-resistant nontuberculous mycobacterium. *Science* 354, 751–757. doi: 10.1126/science.aaf8156
11. Burgos, M. I., Fernández, R. A., Celej, M. S., Rossi, L. I., Fidelio, G. D., and Dassie, S. A. (2011). Binding of the Highly Toxic Tetracycline Derivative, Anhydrotetracycline, to Bovine Serum Albumin. *Biol. Pharm. Bull.* 34, 1301–1306. doi: 10.1248/bpb.34.1301
 12. Burian, J., Ramón-García, S., Howes, C. G., and Thompson, C. J. (2012). WhiB7, a transcriptional activator that coordinates physiology with intrinsic drug resistance in *Mycobacterium tuberculosis*. *Expert Rev. Anti Infect. Ther.* 10, 1037–1047. doi: 10.1586/eri.12.90
 13. Cambau, E., Viveiros, M., Machado, D., Raskine, L., Ritter, C., Tortoli, E., et al. (2015). Revisiting susceptibility testing in MDR-TB by a standardized quantitative phenotypic assessment in a European multicentre study. *J. Antimicrob. Chemother.* 70, 686–696. doi: 10.1093/jac/dku438
 14. Campbell, E. A., Korzheva, N., Mustaev, A., Murakami, K., Nair, S., Goldfarb, A., et al. (2001). Structural mechanism for rifampicin inhibition of bacterial RNA polymerase. *Cell* 104, 901–912. doi: 10.1016/S0092-8674(01)00286-0
 15. Chan, E., and Iseman, M. (2013). Underlying Host Risk Factors for Nontuberculous Mycobacterial Lung Disease. *Semin. Respir. Crit. Care Med.* 34, 110–123. doi: 10.1055/s-0033-1333573
 16. Chao, M. C., Abel, S., Davis, B. M., and Waldor, M. K. (2016). The design and analysis of transposon insertion sequencing experiments. *Nat. Rev. Microbiol.* 14, 119–128. doi: 10.1038/nrmicro.2015.7
 17. Chen, W., Biswas, T., Porter, V. R., Tsodikov, O. V., and Garneau-Tsodikova, S. (2011). Unusual regioversatility of acetyltransferase Eis, a cause of drug resistance in XDR-TB. *Proc. Natl. Acad. Sci.* 108, 9804–9808. doi: 10.1073/pnas.1105379108
 18. Chen, W., Green, K. D., Tsodikov, O. V., and Garneau-Tsodikova, S. (2012). The aminoglycoside multi-acetylating activity of the enhanced intracellular survival (Eis) protein from *Mycobacterium smegmatis* and its inhibition. *Biochemistry* 51, 4959–4967. doi: 10.1021/bi3004473
 19. Choi, G.-E., Shin, S. J., Won, C.-J., Min, K.-N., Oh, T., Hahn, M.-Y., et al. (2012). Macrolide treatment for *Mycobacterium abscessus* and *Mycobacterium massiliense* infection and inducible resistance. *Am. J. Respir. Crit. Care Med.* 186, 917–925. doi: 10.1164/rccm.201111-2005OC

20. Choo, S. W., Wee, W. Y., Ngeow, Y. F., Mitchell, W., Tan, J. L., Wong, G. J., et al. (2014). Genomic reconnaissance of clinical isolates of emerging human pathogen *Mycobacterium abscessus* reveals high evolutionary potential. *Sci. Rep.* 4:4061. doi: 10.1038/srep04061
21. Crofts, T. S., Gasparrini, A. J., and Dantas, G. (2017). Next-generation approaches to understand and combat the antibiotic resistome. *Nat. Rev. Microbiol.* 15, 422–434. doi: 10.1038/nrmicro.2017.28
22. Dal Molin, M., Gut, M., Rominski, A., Haldimann, K., Becker, K., and Sander, P. (2017). Molecular mechanisms of intrinsic streptomycin resistance in *Mycobacterium abscessus*. *Antimicrob. Agents Chemother.* 62:e01427-17. doi: 10.1128/AAC.01427-17
23. D’Costa, V. M., King, C. E., Kalan, L., Morar, M., Sung, W. W. L., Schwarz, C., et al. (2011). Antibiotic resistance is ancient. *Nature* 477, 457–461. doi: 10.1038/nature10388
24. Dubée, V., Bernut, A., Cortes, M., Lesne, T., Dorchene, D., Lefebvre, A.-L., et al. (2015). β -Lactamase inhibition by avibactam in *Mycobacterium abscessus*. *J. Antimicrob. Chemother.* 70, 1051–1058. doi: 10.1093/jac/dku510
25. Dupont, C., Viljoen, A., Dubar, F., Blaise, M., Bernut, A., Pawlik, A., et al. (2016). A new piperidinol derivative targeting mycolic acid transport in *Mycobacterium abscessus*. *Mol. Microbiol.* 101, 515–529. doi: 10.1111/mmi.13406
26. Dupont, C., Viljoen, A., Thomas, S., Roquet-Banères, F., Herrmann, J.-L., Pethe, K., et al. (2017). Bedaquiline inhibits the ATP synthase in *Mycobacterium abscessus* and is effective in infected zebrafish. *Antimicrob. Agents Chemother.* 61, 1–15. doi: 10.1128/AAC.01225-17
27. Franz, N. D., Belardinelli, J. M., Kaminski, M. A., Dunn, L. C., Calado Nogueira de Moura, V., Blaha, M. A., et al. (2017). Design, synthesis and evaluation of indole-2-carboxamides with pan anti-mycobacterial activity. *Bioorg. Med. Chem.* 25, 3746–3755. doi: 10.1016/j.bmc.2017.05.015
28. Gallagher, L. A., Shendure, J., and Manoil, C. (2011). Genome-scale identification of resistance functions in *Pseudomonas aeruginosa* using Tn-seq. *mBio* 2:e00315-10. doi: 10.1128/mBio.00315-10
29. Garzan, A., Willby, M. J., Green, K. D., Gajadeera, C. S., Hou, C., Tsodikov, O. V., et al. (2016). Sulfonamide-based inhibitors of aminoglycoside acetyltransferase Eis abolish resistance to kanamycin in *Mycobacterium tuberculosis*. *J. Med. Chem.* 59, 10619–10628. doi: 10.1021/acs.jmedchem.6b01161

30. Garzan, A., Willby, M. J., Ngo, H. X., Gajadeera, C. S., Green, K. D., Holbrook, S. Y. L., et al. (2017). Combating Enhanced Intracellular Survival (Eis)-Mediated Kanamycin Resistance of *Mycobacterium tuberculosis* by Novel Pyrrolo[1,5-*a*]pyrazine-Based Eis Inhibitors. *ACS Infect. Dis.* 3, 302–309. doi: 10.1021/acsinfecdis.6b00193
31. Green, K. D., Chen, W., and Garneau-Tsodikova, S. (2012). Identification and characterization of inhibitors of the aminoglycoside resistance acetyltransferase Eis from *Mycobacterium tuberculosis*. *ChemMedChem.* 7, 73–77. doi: 10.1002/cmdc.201100332
32. Griffith, D. E., Aksamit, T., Brown-Elliott, B. A., Catanzaro, A., Daley, C., Gordin, F., et al. (2007). An official ATS/IDSA statement: diagnosis, treatment, and prevention of nontuberculous mycobacterial diseases. *Am. J. Respir. Crit. Care Med.* 175, 367–416. doi: 10.1164/rccm.200604-571ST
33. Halloum, I., Viljoen, A., Khanna, V., Craig, D., Bouchier, C., Brosch, R., et al. (2017). Resistance to thiacetazone derivatives active against *Mycobacterium abscessus* involves mutations in the MmpL5 transcriptional repressor MAB_4384. *Antimicrob. Agents Chemother.* 61, e02509-16. doi: 10.1128/AAC.02509-16
34. Haworth, C. S., Banks, J., Capstick, T., Fisher, A. J., Gorsuch, T., Laurenson, I. F., et al. (2017). British thoracic society guideline for the management of nontuberculous mycobacterial pulmonary disease (NTM-PD). *BMJ Open Respir. Res.* 4:e000242. doi: 10.1136/bmjresp-2017-000242
35. Hoefsloot, W., van Ingen, J., Andrejak, C., Ängeby, K., Bauriaud, R., Bemer, P., et al. (2013). The geographic diversity of nontuberculous mycobacteria isolated from pulmonary samples: an NTM-NET collaborative study. *Eur. Respir. J.* 42, 1604–1613. doi: 10.1183/09031936.00149212
36. Howard, S. T. (2006). Spontaneous reversion of *Mycobacterium abscessus* from a smooth to a rough morphotype is associated with reduced expression of glycopeptidolipid and reacquisition of an invasive phenotype. *Microbiology* 152, 1581–1590. doi: 10.1099/mic.0.28625-0
37. Hugonnet, J., Tremblay, L. W., Boshoff, H. I., Barry, C. E., and Blanchard, J. S. (2009). Meropenem-Clavulanate Is Effective Against Extensively Drug-Resistant *Mycobacterium tuberculosis*. *Science* 323, 1215–1218. doi: 10.1126/science.1167498

38. Hurst-Hess, K., Rudra, P., and Ghosh, P. (2017). *Mycobacterium abscessus* WhiB7 regulates a species-specific repertoire of genes to confer extreme antibiotic resistance. *Antimicrob. Agents Chemother.* 61, e01347-17. doi: 10.1128/AAC.01347-17
39. Jarand, J., Levin, A., Zhang, L., Huitt, G., Mitchell, J. D., and Daley, C. L. (2011). Clinical and microbiologic outcomes in patients receiving treatment for *Mycobacterium abscessus* pulmonary disease. *Clin. Infect. Dis.* 52, 565–571. doi: 10.1093/cid/ciq237
40. Jennings, B. C., Labby, K. J., Green, K. D., and Garneau-Tsodikova, S. (2013). Redesign of substrate specificity and identification of aminoglycoside binding residues of Eis from *Mycobacterium tuberculosis*. *Biochemistry* 52, 5125–5132. doi: 10.1021/bi4002985
41. Kaushik, A., Gupta, C., Fisher, S., Story-Roller, E., Galanis, C., Parrish, N., et al. (2017). Combinations of avibactam and carbapenems exhibit enhanced potencies against drug-resistant *Mycobacterium abscessus*. *Future Microbiol.* 12, 473–480. doi: 10.2217/fmb-2016-0234
42. Kim, H.-Y., Kim, B. J., Kook, Y., Yun, Y.-J., Shin, J. H., Kim, B.-J., et al. (2010). *Mycobacterium massiliense* is differentiated from *Mycobacterium abscessus* and *Mycobacterium bolletii* by erythromycin ribosome methyltransferase gene (*erm*) and clarithromycin susceptibility patterns. *Microbiol. Immunol.* 54, 347–353. doi: 10.1111/j.1348-0421.2010.00221
43. Kim, K. H., An, D. R., Song, J., Yoon, J. Y., Kim, H. S., Yoon, H. J., et al. (2012). *Mycobacterium tuberculosis* Eis protein initiates suppression of host immune responses by acetylation of DUSP16/MKP-7. *Proc. Natl. Acad. Sci.* 109, 7729–7734. doi: 10.1073/pnas.1120251109
44. Kim, T. S., Choe, J. H., Kim, Y. J., Yang, C., Kwon, H., Jeong, J., et al. (2017). Activity of LCB01-0371, a novel oxazolidinone, against *Mycobacterium abscessus*. *Antimicrob. Agents Chemother.* 61, e02752-16. doi: 10.1128/AAC.02752-16
45. Kinch, M. S., and Patridge, E. (2014). An analysis of FDA-approved drugs for infectious disease: antibacterial agents. *Drug Discov. Today* 19, 1510–1513. doi: 10.1016/j.drudis.2014.05.012
46. Kohanski, M. A., Dwyer, D. J., and Collins, J. J. (2010). How antibiotics kill bacteria: from targets to networks. *Nat. Rev. Microbiol.* 8, 423–435. doi: 10.1038/nrmicro2333
47. Koteva, K., Cox, G., Kelso, J. K., Surette, M. D., Zubyk, H. L., Ejim, L., et al. (2018). Rox, a rifamycin resistance enzyme with an unprecedented mechanism of action. *Cell Chem. Biol.* 25, 403–412. doi: 10.1016/j.chembiol.2018.01.009

48. Kozikowski, A. P., Onajole, O. K., Stec, J., Dupont, C., Viljoen, A., Richard, M., et al. (2017). Targeting mycolic acid transport by indole-2-carboxamides for the treatment of *Mycobacterium abscessus* infections. *J. Med. Chem.* 60, 5876–5888. doi: 10.1021/acs.jmedchem.7b00582
49. Lavollay, M., Dubée, V., Heym, B., Herrmann, J.-L., Gaillard, J.-L., Gutmann, L., et al. (2014). *In vitro* activity of cefoxitin and imipenem against *Mycobacterium abscessus* complex. *Clin. Microbiol. Infect.* 20, O297–O300. doi: 10.1111/1469-0691.12405
50. Le Run, E., Arthur, M., and Mainardi, J.-L. (2018). *In vitro* and intracellular activity of imipenem combined to rifabutin and avibactam against *Mycobacterium abscessus*. *Antimicrob. Agents Chemother.* 62:e00623-18. doi: 10.1128/AAC.00623-18
51. Lee, M.-R., Sheng, W.-H., Hung, C.-C., Yu, C.-J., Lee, L.-N., and Hsueh, P.-R. (2015). *Mycobacterium abscessus* complex infections in humans. *Emerg. Infect. Dis.* 21, 1638–1646. doi: 10.3201/2109.141634
52. Leski, T. A., Bangura, U., Jimmy, D. H., Ansumana, R., Lizewski, S. E., Stenger, D. A., et al. (2013). Multidrug-resistant tet(X)-containing hospital isolates in Sierra Leone. *Int. J. Antimicrob. Agents* 42, 83–86. doi: 10.1016/j.ijantimicag.2013.04.014
53. Linkevicius, M., Sandegren, L., and Andersson, D. I. (2016). Potential of tetracycline resistance proteins to evolve tigecycline resistance. *Antimicrob. Agents Chemother.* 60, 789–796. doi: 10.1128/AAC.02465-15
54. Maurer, F. P., Bruderer, V. L., Castelberg, C., Ritter, C., Scherbakov, D., Bloemberg, G. V., et al. (2015). Aminoglycoside-modifying enzymes determine the innate susceptibility to aminoglycoside antibiotics in rapidly growing mycobacteria. *J. Antimicrob. Chemother.* 70, 1412–1419. doi: 10.1093/jac/dku550
55. Maurer, F. P., Ruegger, V., Ritter, C., Bloemberg, G. V., and Bottger, E. C. (2012). Acquisition of clarithromycin resistance mutations in the 23S rRNA gene of *Mycobacterium abscessus* in the presence of inducible *erm(41)*. *J. Antimicrob. Chemother.* 67, 2606–2611. doi: 10.1093/jac/dks279
56. Mukherjee, D., Wu, M.-L., Teo, J. W. P., and Dick, T. (2017). Vancomycin and clarithromycin show synergy against *Mycobacterium abscessus in vitro*. *Antimicrob. Agents Chemother.* 61, e01298-17. doi: 10.1128/AAC.01298-17
57. Nash, K. A., Brown-Elliott, A. B., and Wallace, R. J. (2009). A novel gene, *erm(41)*, confers inducible macrolide resistance to clinical isolates of *Mycobacterium abscessus* but is absent from *Mycobacterium chelonae*. *Antimicrob. Agents Chemother.* 53, 1367–1376. doi: 10.1128/AAC.01275-08

58. Nessar, R., Cambau, E., Reyrat, J. M., Murray, A., and Gicquel, B. (2012). *Mycobacterium abscessus*: a new antibiotic nightmare. *J. Antimicrob. Chemother.* 67, 810–818. doi: 10.1093/jac/dkr578
59. Ngo, H. X., Green, K. D., Gajadeera, C. S., Willby, M. J., Holbrook, S. Y. L., Hou, C., et al. (2018). Potent 1,2,4-Triazino[5,6*b*]indole-3-thioether Inhibitors of the Kanamycin Resistance Enzyme Eis from *Mycobacterium tuberculosis*. *ACS Infect. Dis.* 4, 1030–1040. doi: 10.1021/acsinfecdis.8b00074
60. Park, J., Gasparri, A. J., Reck, M. R., Symister, C. T., Elliott, J. L., Vogel, J. P., et al. (2017). Plasticity, dynamics, and inhibition of emerging tetracycline resistance enzymes. *Nat. Chem. Biol.* 13, 730–736. doi: 10.1038/nchembio.2376
61. Pawlowski, A. C., Stogios, P. J., Koteva, K., Skarina, T., Evdokimova, E., Savchenko, A., et al. (2018). The evolution of substrate discrimination in macrolide antibiotic resistance enzymes. *Nat. Commun.* 9:112. doi: 10.1038/s41467-017-02680-0
62. Pawlowski, A. C., Wang, W., Koteva, K., Barton, H. A., McArthur, A. G., and Wright, G. D. (2016). A diverse intrinsic antibiotic resistome from a cave bacterium. *Nat. Commun.* 7:13803. doi: 10.1038/ncomms13803
63. Prammananan, T., Sander, P., Brown, B. A., Frischkorn, K., Onyi, G. O., Zhang, Y., et al. (1998). A single 16S ribosomal RNA substitution is responsible for resistance to amikacin and other 2-deoxystreptamine aminoglycosides in *Mycobacterium abscessus* and *Mycobacterium chelonae*. *J. Infect. Dis.* 177, 1573–1581. doi: 10.1086/515328
64. Pricer, R. E., Houghton, J. L., Green, K. D., Mayhoub, A. S., and GarneauTsodikova, S. (2012). Biochemical and structural analysis of aminoglycoside acetyltransferase Eis from *Anabaena variabilis*. *Mol. Biosyst.* 8, 3305–3313. doi: 10.1039/c2mb25341k
65. Pryjma, M., Burian, J., Kuchinski, K., and Thompson, C. J. (2017). Antagonism between front-line antibiotics clarithromycin and amikacin in the treatment of *Mycobacterium abscessus* infections is mediated by the *whiB7* gene. *Antimicrob. Agents Chemother.* 61, e01353-17. doi: 10.1128/AAC.01353-17
66. Quan, S., Venter, H., and Dabbs, E. R. (1997). Ribosylative inactivation of rifampin by *Mycobacterium smegmatis* is a principal contributor to its low susceptibility to this antibiotic. *Antimicrob. Agents Chemother.* 41, 2456–2460.
67. Rajagopal, M., Martin, M. J., Santiago, M., Lee, W., Kos, V. N., Meredith, T., et al. (2016). Multidrug intrinsic resistance factors in *Staphylococcus aureus* identified by profiling fitness within high-diversity transposon libraries. *mBio* 7:e00950-16. doi: 10.1128/mBio.00950-16

68. Ramón-García, S., Otal, I., Martín, C., Gomez-Lus, R., and Ainsa, J. A. (2006). Novel streptomycin resistance gene from *Mycobacterium fortuitum*. *Antimicrob. Agents Chemother.* 50, 3920–3922. doi: 10.1128/AAC.00223-06
69. Ripoll, F., Pasek, S., Schenowitz, C., Dossat, C., Barbe, V., Rottman, M., et al. (2009). Non Mycobacterial Virulence Genes in the Genome of the Emerging Pathogen *Mycobacterium abscessus*. *PLoS One* 4:e5660. doi: 10.1371/journal.pone.0005660
70. Rominski, A., Roditscheff, A., Selchow, P., Böttger, E. C., and Sander, P. (2017a). Intrinsic rifamycin resistance of *Mycobacterium abscessus* is mediated by ADP-ribosyltransferase MAB_0591. *J. Antimicrob. Chemother.* 72, 376–384. doi: 10.1093/jac/dkw466
71. Rominski, A., Schulthess, B., Müller, D. M., Keller, P. M., and Sander, P. (2017b). Effect of β -lactamase production and β -lactam instability on MIC testing results for *Mycobacterium abscessus*. *J. Antimicrob. Chemother.* 72, 3070–3078. doi: 10.1093/jac/dkx284
72. Rominski, A., Selchow, P., Becker, K., Brülle, J. K., Dal Molin, M., and Sander, P. (2017c). Elucidation of *Mycobacterium abscessus* aminoglycoside and capreomycin resistance by targeted deletion of three putative resistance genes. *J. Antimicrob. Chemother.* 72, 2191–2200. doi: 10.1093/jac/dkx125
73. Rudra, P., Hurst-Hess, K., Lappierre, P., and Ghosh, P. (2018). High levels of intrinsic tetracycline resistance in *Mycobacterium abscessus* are conferred by a tetracycline-modifying monooxygenase. *Antimicrob. Agents Chemother.* 62:e00119-18. doi: 10.1128/AAC.00119-18

Personal contribution to chapter 2

As first author, the following sections of this article were my contribution;

1. Introduction
2. Antibiotic-target-modifying enzymes in *M. abscessus*:
 - Macrolide resistance: MAB_2297 [*erm*(41)] encoded erythromycin ribosome methylase
3. Antibiotic-modifying enzymes in *M. abscessus*:
 - Aminoglycoside resistance: MAB_4395 [*aac*(2')] & MAB_4532c (*eis*2) encoded acetyltransferases; MAB_2385 encoded 3"-*O*-phosphotransferase
 - Tetracycline resistance: MAB_1496c encoded flavin monooxygenase
 - β -Lactam resistance: MAB_2875 encoded β -lactamase
 - Rifamycin resistance: MAB_0591 encoded ADP-ribosyltransferase
4. Clinical relevance
5. Outlook and perspectives
6. Preparation of table 1
7. Preparation of figure 1 with legend

CONCLUSION & OUTLOOK

Concluding remarks

The genetic approach that we used in this study, was useful to identify different types of factors related to drug molecule influx or degradation that influence β -lactam susceptibility of *M. abscessus* and to show how sets of genes act in concert, rather than in isolation, to elicit bacterial resistance to antibiotics. Through a better understanding of how the alteration of mycomembrane permeability elicits bacterial resistance, we might be able to develop new means to overcome the ‘impermeability’ resistance mechanism in an effort to fight highly resistant *M. abscessus* infections.

Future directions

The use of the MIC assay with different porin mutants was useful to show that the drug resistance characteristics of *M. abscessus* rely on specific outer membrane porins. However, this method has limitations; first, it is not sensitive enough to detect reduced influx (or increased efflux), and second, the presence of other resistance mechanisms can distort the results. Progress in our understanding of the correlation between drug transport and susceptibility in bacteria and the influence of chemical properties of antibiotic molecules on influx or efflux will require more advanced experimental methods, such as electrophysiology¹⁻³, mass spectrometry⁴⁻⁶ and deep UV (DUV) fluorescent imaging or DUV microspectrofluorimetry⁷⁻⁹ that allow precise quantitative measurements of several influx and efflux parameters. By means of these technologies, it is possible to define the precise contribution of different bacterial factors (efflux pumps or porins) to intracellular antibiotic accumulation, measure the internal concentration and the critical inhibitory internal concentration of drugs and determine the effect of different chemical structures within a class of drugs on drug efflux or uptake.

The quantification of drug accumulation in a population of bacterial cells (both Gram-negative bacteria and mycobacteria) can be accomplished by mass spectrometry⁴⁻⁶. Methods that use DUV photons from synchrotron radiation have proven to be valuable tools to quantify the accumulation of antibiotics in individual bacteria. For example, the analysis of the time-course accumulation of fluorescent antibiotics in single bacterial cells using the microfluorospectrometry technique⁷⁻⁹ revealed a correlation between the activity of the AcrAB–TolC efflux system and the accumulation rate of fluoroquinolones. This approach could be applied to obtain information on the function of different adjuvants to enhance the intracellular accumulation of specific drugs in resistant strains that exhibit modified cell envelope permeability. Furthermore, applying a single-cell approach to visualize the

accumulation of different quinolones revealed differences in steady-state concentrations and kinetics of accumulation of the antibiotics⁸, which allowed the introduction of the ‘Structure Intracellular Concentration Activity Relationship’ (SICAR) concept. Relating antibiotic uptake efficiency and the resulting concentration inside bacterial cells to the chemical properties of drug molecules using SICAR can help dissect chemical structures that have a role in influx or retention of antibiotic within bacteria. These data could permit the design of antibacterial molecules that are less vulnerable to efflux and more permeant to defeat the resistance elicited by the permeability barrier of bacteria.

The generation and characterization of single and combinatorial isogenic mutants in the widespread *M. abscessus* type strain elucidated a role of porin loss in β -lactam resistance levels. It will be interesting to investigate the impact of altered membrane permeability on susceptibility to other hydrophilic antibiotics. Furthermore, characterization of clinical isolates by quantitative drug susceptibility testing and whole-genome sequencing techniques will provide insights if a corresponding β -lactam resistance mechanism is also selected for during (long-term) treatment in complex pathogen-host-drug interaction.

References

1. Danelon, C., Nestrovich, E. M., Winterhalter, M., Ceccarelli, M. & Bezrukov, S. M. Interaction of zwitterionic penicillins with the OmpF channel facilitates their translocation. *Biophys. J.* **90**, 1617–1627 (2006).
2. Nestorovich, E. M., Danelon, C., Winterhalter, M. & Bezrukov, S. M. Designed to penetrate: time-resolved interaction of single antibiotic molecules with bacterial pores. *Proc. Natl Acad. Sci. USA* **99**, 9789–9794 (2002).
3. Danelon, C., Brando, T. & Winterhalter, M. Probing the orientation of reconstituted maltoporin channels at the single-protein level. *J. Biol. Chem.* **278**, 35542–35551 (2003).
4. Cai, H., Rose, K., Liang, L.-H., Dunham, S. & Stover, C. Development of a liquid chromatography/mass spectrometry-based drug accumulation assay in *Pseudomonas aeruginosa*. *Anal. Biochem.* **385**, 321–325 (2009).
5. Zhou, Y. et al. Thinking outside the “bug”: a unique assay to measure intracellular drug penetration in Gram-negative bacteria. *Anal. Chem.* **87**, 3579–3584 (2015).
6. Davis, T. D., Gerry, C. J. & Tan, D. S. General platform for systematic quantitative evaluation of small-molecule permeability in bacteria. *ACS Chem. Biol.* **9**, 2535–2544 (2014).

CONCLUSION & OUTLOOK

7. Kaščáková, S., Maigre, L., Chevalier, J., Réfrégiers, M. & Pagès, J.-M. Antibiotic transport in resistant bacteria: synchrotron UV fluorescence microscopy to determine antibiotic accumulation with single cell resolution. *PLoS ONE* **7**, e38624 (2012).
8. Cinquin, B. et al. Microspectrometric insights on the uptake of antibiotics at the single bacterial cell level. *Sci. Rep.* **5**, 17968 (2015).
9. Pu, Y. et al. Enhanced efflux activity facilitates drug tolerance in dormant bacterial cells. *Mol. Cells* **62**, 284–294 (2016).

2018

Luthra, S., Rominski, A. & Sander, P. The role of antibiotic-target-modifying and antibiotic-modifying enzymes in *Mycobacterium abscessus* drug resistance. *Front. Microbiol.* **9**, 1–13 (2018).

CURRICULUM VITAE

PERSONAL DATA

Name: Sakshi Luthra
Date of Birth: March 29th 1995
Place of Birth: Mumbai, India
Nationality: Indian



EDUCATION AND RESEARCH ACTIVITIES

2018-2023 **Ph.D. studies** in Microbiology and Immunology, Institute of Medical Microbiology, University of Zurich, Switzerland

Antibiotic resistance characteristics of *Mycobacterium abscessus* rely on specific outer membrane porins and surface-associated glycopeptidolipids

2016-2017 **Master of Science** in Molecular Genetics and Diagnostics (With Distinction), School of Life Sciences, University of Nottingham, United Kingdom

Virulence traits of *Pseudomonas aeruginosa*

2013-2016 **Bachelor of Science** (Biotechnology) (With Distinction), Manipal University, India

Genetic variations in microRNA and microRNA target genes of cardiovascular diseases and clopidogrel drug response

